

Electronic Supplementary Information

Synthetic Glycosidase for Precise Hydrolysis of Oligosaccharides and Polysaccharides

Xiaowei Li and Yan Zhao*

Department of Chemistry, Iowa State University, Ames, Iowa 50011-3111, USA

zhaoy@iastate.edu

Table of Contents

General	4
Synthesis & Characterization.....	4
Synthesis of templates <i>o-5a</i> , <i>m-5a</i> and <i>p-5a</i>	5
<i>Scheme S1</i>	5
Synthesis of <i>o-5a</i>	5
Synthesis of <i>m-5a</i>	6
Synthesis of <i>p-5a</i>	7
Synthesis of template <i>p-5b</i>	8
<i>Scheme S2</i>	8
Synthesis of <i>p-5b</i>	8
Synthesis of template <i>p-5c</i>	10
<i>Scheme S3</i>	10
Synthesis of <i>p-5c</i>	10
¹ H NMR comparison of imine-templates <i>p-5a</i> , <i>p-5b</i> and <i>p-5c</i>	12
<i>Figure S1</i>	12
<i>Figure S2</i>	12
<i>Figure S3</i>	13
<i>Figure S4</i>	13
<i>Figure S5</i>	14
<i>Figure S6</i>	15
<i>Figure S7</i>	16

Dynamic Light Scattering	17
<i>Figure S8</i>	18
<i>Figure S9</i>	19
<i>Figure S10</i>	20
ITC Binding Studies.....	21
<i>Figure S11</i>	22
<i>Figure S12</i>	22
<i>Figure S13</i>	23
<i>Figure S14</i>	23
<i>Table S1</i>	24
<i>Figure S15</i>	24
<i>Figure S16</i>	25
<i>Figure S17</i>	25
<i>Figure S18</i>	26
<i>Figure S19</i>	26
<i>Figure S20</i>	27
<i>Figure S21</i>	27
<i>Figure S22</i>	28
<i>Figure S23</i>	28
<i>Figure S24</i>	29
Catalytic Hydrolysis of Oligosaccharide by MINPs	30
<i>Figure S25</i>	30
<i>Figure S26</i>	31
<i>Figure S27</i>	31
<i>Figure S28</i>	32
<i>Figure S29</i>	32
<i>Figure S30</i>	33
<i>Figure S31</i>	33
<i>Figure S32</i>	34
pH Effect of Maltohexaose Hydrolysis.....	35
<i>Table S2</i>	35
Full Characterization of the Hydrolyzed Products in the Maltohexaose (G6) Hydrolysis	36
<i>Table S3</i>	36
<i>Table S4</i>	36
Michaelis–Menten Kinetics	38
<i>Figure S33</i>	38
<i>Figure S34</i>	38
<i>Figure S35</i>	39

<i>Figure S36</i>	39
Product Inhibition Study	40
<i>Figure S37</i>	40
<i>Figure S38</i>	40
Substrate Selectivity Study of MINP Catalysts	41
<i>Figure S39</i>	41
<i>Figure S40</i>	41
<i>Figure S41</i>	42
<i>Figure S42</i>	42
<i>Figure S43</i>	43
<i>Figure S44</i>	43
<i>Figure S45</i>	44
<i>Figure S46</i>	44
<i>Figure S47</i>	45
<i>Figure S48</i>	45
^1H & ^{13}C NMR Spectra.....	46
ESI-MS Spectra.....	59
References	66

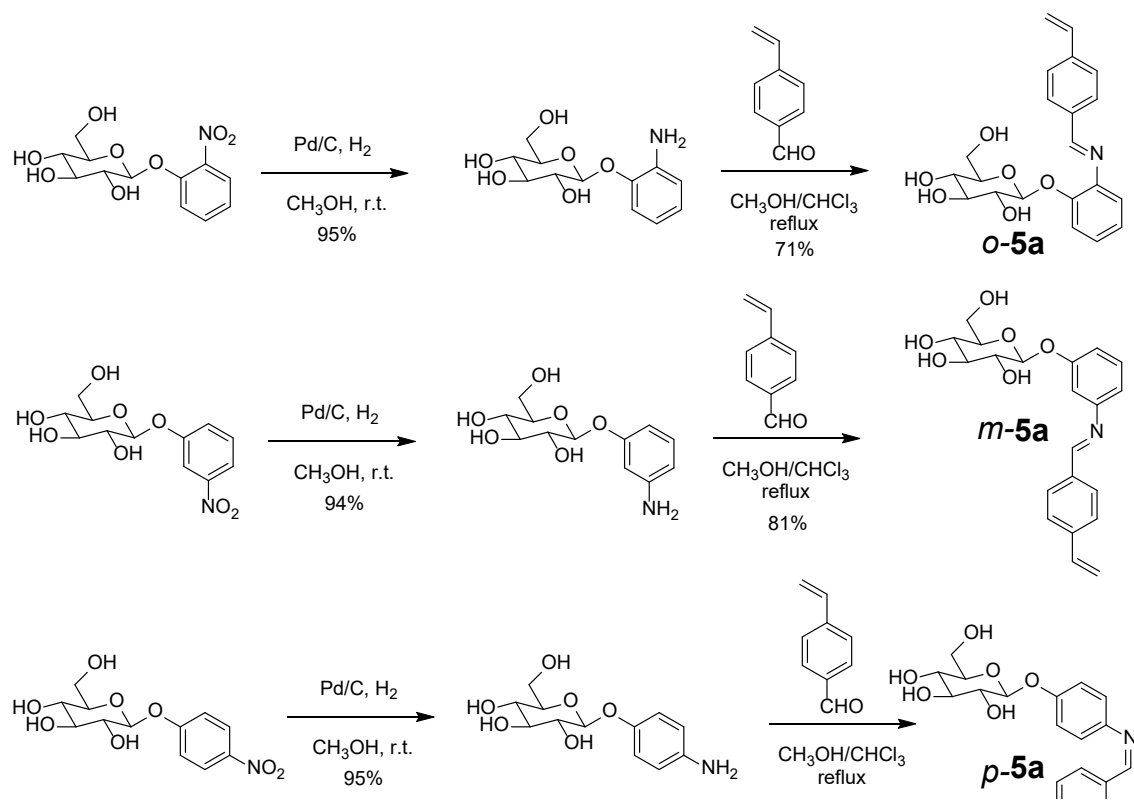
General

All organic solvents and reagents were of ACS-certified grade or higher grade, and were purchased from Fisher Scientific. Ultrapure water (18.2 MU; Millipore Co., USA) was used throughout the experiment to prepare buffers and nanoparticles. Flash column chromatography was performed on SiliFlash P60 silica gel (40-63 μm , 60 \AA). ^1H and ^{13}C NMR spectra were recorded on a Bruker DRX-400, Bruker AV III 600 or Varian VXR-400 spectrometer. Chemicals shifts are reported in ppm relative to residual solvent peaks ($\text{CDCl}_3 = 7.26 \text{ ppm}$ for ^1H NMR and 77.16 ppm for ^{13}C NMR, $\text{CD}_3\text{OD} = 3.31 \text{ ppm}$ for ^1H NMR and 49.00 ppm for ^{13}C NMR). Coupling constants are reported in hertz. High resolution mass spectra (HRMS) were recorded on Agilent QTOF 6540 mass spectrometer with a QTOF detector. Dynamic light scattering (DLS) was performed on a Malvern Zetasizer Nano ZS. Isothermal titration calorimetry (ITC) was performed using a MicroCal VP-ITC Microcalorimeter with Origin 7 software and VPViewer2000 (GE Healthcare, Northampton, MA). LC-MS analysis was performed with a Thermo Scientific HILIC-LC column (4.6 mm, 150 mm) coupled to an Agilent 1200 Series Binary VWD system with an Agilent 6540 UHD Accurate Mass Q-TOF mass spectrometry detector.

Synthesis & Characterization

Syntheses of compounds **1a**,¹ **1b**,² **2**,³ **3**,¹ and **4**³ were reported previously.

Synthesis of templates *o*-5a, *m*-5a and *p*-5a



Scheme S1. Syntheses of templates *o*-5a, *m*-5a and *p*-5a

Synthesis of *o*-5a

2-Aminophenyl- β -D-glucopyranoside. 2-Nitrophenyl- β -D-glucopyranoside (200 mg, 0.66 mmol) was hydrogenated in methanol (10 mL) with Pd/C (40 mg). After 12 h, the catalyst was removed by filtration, and methanol was removed in vacuo. The residue was crystallized from ethanol to a white crystal (171 mg, 95%). ^1H NMR (400 MHz, 298 K, CD_3OD) δ 7.36 (d, $J = 4.8$ Hz, 2H), 7.32 (t, $J = 4.8$ Hz, 1H), 7.14 (m, 1H), 5.01 (d, $J = 7.6$ Hz, 1H), 3.90-3.88 (m, 1H), 3.74-3.69 (m, 1H), 3.57-3.46 (m, 2H), 3.44-3.39 (m, 1H), 3.30-3.29 (m, 1H). HRMS (ESI $^+$ /QTOF): Calcd for $\text{C}_{12}\text{H}_{17}\text{NO}_6$ m/z: [M+H] $^+$ 272.1129; Found 272.1137.

Compound *o*-5a. A solution of 2-Aminophenyl- β -D-glucopyranoside (100 mg, 0.369 mmol) and 4-vinylbenzaldehyde (73 mg, 0.553 mmol) in CHCl_3 (0.5 mL) and ethanol (3 mL) was heated to reflux overnight. After the reaction mixture was cooled to room temperature, diethyl ether (30 mL) was added

slowly. The precipitate formed was collected by filtration and washed with cold diethyl ether to yield a white powder (101 mg, 71%). ^1H NMR (400 MHz, 298 K, DMSO- d_6) δ 8.65 (s, 1H), 7.92 (d, J = 8.4 Hz, 2H), 7.62 (d, J = 8.4 Hz, 2H), 7.23 (dd, J_1 = 8.0 Hz, J_2 = 0.8 Hz, 1H), 7.18-7.12 (m, 2H), 7.07-7.03 (m, 1H), 6.81 (dd, J_1 = 18.0 Hz, J_2 = 11.2 Hz, 1H), 5.98 (d, J = 18.0 Hz, 1H), 5.39 (d, J = 11.2 Hz, 1H), 5.30 (d, J = 4.8 Hz, 1H), 5.06 (d, J = 4.8 Hz, 1H), 5.02 (d, J = 4.8 Hz, 1H), 4.94-4.92 (m, 1H), 4.58-4.49 (m, 1H), 4.36 (t, J = 5.2 Hz, 1H), 3.70-3.66 (m, 1H), 3.49-3.38 (m, 2H), 3.26-3.23 (m, 1H), 3.13-3.11 (m, 1H). ^{13}C NMR (100 MHz, 298 K, DMSO- d_6) δ 162.37, 149.79, 142.14, 140.40, 136.57, 136.15, 129.48, 126.91, 123.18, 122.09, 117.83, 109.99, 103.27, 101.78, 77.61, 77.09, 73.86, 70.08, 61.17. HRMS (ESI $^+$ /QTOF): Calcd for $\text{C}_{21}\text{H}_{23}\text{NO}_6$ m/z: [M+H] $^+$ 386.1598; Found 386.1600.

Synthesis of *m*-5a

3-Aminophenyl- β -D-glucopyranoside. The same procedure for 2-aminophenyl- β -D-glucopyranoside was followed, using 3-nitrophenyl- β -D-glucopyranoside (200 mg, 0.66 mmol) to afford 3-aminophenyl- β -D-glucopyranoside as a white crystal (169 mg, 94%). ^1H NMR (400 MHz, 298 K, CD₃OD) δ 7.45 (t, J = 8.4 Hz, 1H), 7.20 (dd, J_1 = 8.4 Hz, J_2 = 2.8 Hz, 1H), 7.15 (t, J = 2.0 Hz, 1H), 7.05 (dd, J_1 = 8.0 Hz, J_2 = 2.0 Hz, 1H), 4.95 (d, J = 7.6 Hz, 1H), 3.92 (dd, J_1 = 12.0 Hz, J_2 = 2.0 Hz, 1H), 3.72-3.67 (m, 1H), 3.51-3.46 (m, 2H), 3.41-3.39 (m, 1H), 3.31-3.29 (m, 1H). HRMS (ESI $^+$ /QTOF) Calcd for $\text{C}_{12}\text{H}_{17}\text{NO}_6$ m/z: [M+H] $^+$ 272.1129; Found 272.1148.

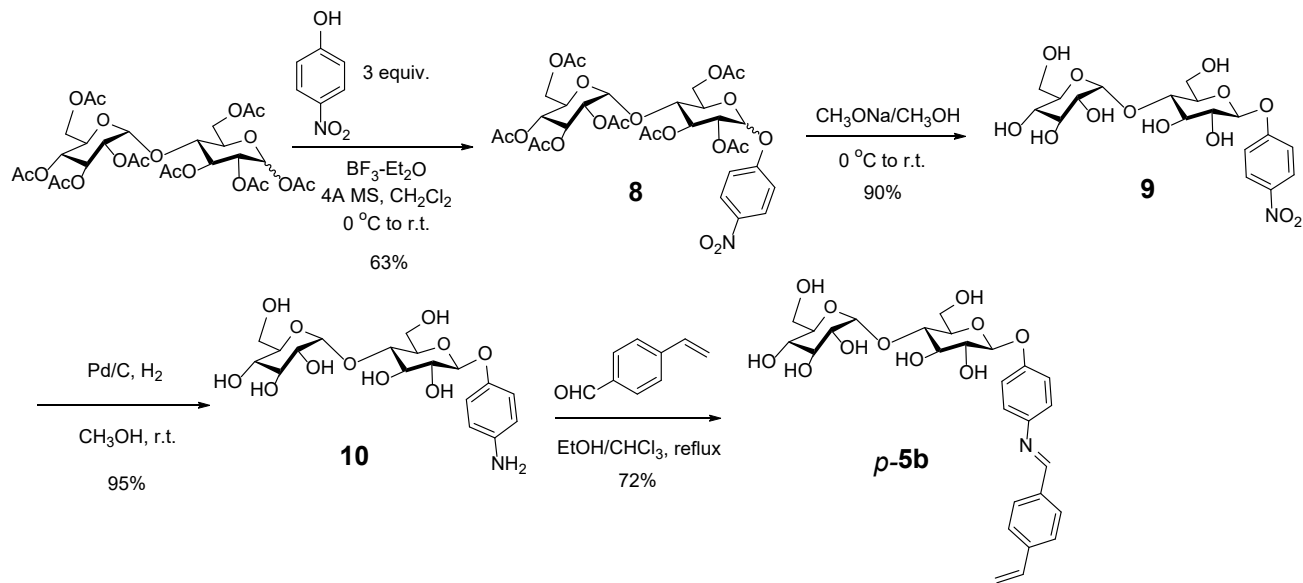
Compound ***m*-5a**. The same procedure for *o*-5a was followed, using 3-aminophenyl- β -D-glucopyranoside (100 mg, 0.369 mmol) to afford ***m*-5a** as a white powder (115 mg, 81%). ^1H NMR (400 MHz, 298 K, DMSO- d_6) δ 8.61 (s, 1H), 7.90 (d, J = 8.4 Hz, 2H), 7.62 (d, J = 8.4 Hz, 2H), 7.32 (t, J = 8.0 Hz, 1H), 6.95 (t, J = 2.0 Hz, 1H), 6.90 (dd, J_1 = 8.0 Hz, J_2 = 2.0 Hz, 2H), 6.81 (dd, J_1 = 18.0 Hz, J_2 = 10.8 Hz, 1H), 5.98 (d, J = 18.0 Hz, 1H), 5.39 (d, J = 10.8 Hz, 1H), 5.33 (d, J = 4.8 Hz, 1H), 5.11 (d, J = 4.4 Hz, 1H), 5.04 (d, J = 5.2 Hz, 1H), 4.92 (d, J = 7.6 Hz, 1H), 4.64 (t, J = 2.4 Hz, 1H), 3.73-3.69 (m, 1H), 3.38-3.58 (m, 1H), 3.29-3.24 (m, 2H), 3.17-3.11 (m, 1H). ^{13}C NMR (100 MHz, 298 K, DMSO- d_6) δ 160.91, 158.63, 153.08, 140.50, 136.54, 135.86, 130.28, 129.51, 126.99, 116.73, 115.54, 114.45, 108.86, 100.83, 77.56, 77.08, 73.71, 70.26, 61.21. HRMS (ESI $^+$ /QTOF): Calcd for $\text{C}_{21}\text{H}_{23}\text{NO}_6$ [M+H] $^+$ m/z 386.1598, found: m/z 386.1608. HRMS (ESI $^+$ /QTOF) Calcd for $\text{C}_{12}\text{H}_{17}\text{NO}_6$ m/z: [M+H] $^+$ 272.1129; Found 272.1148.

Synthesis of *p*-**5a**

4-Aminophenyl- β -D-glucopyranoside. The same procedure for 2-aminophenyl- β -D-glucopyranoside was followed, using 4-nitrophenyl- β -D-glucopyranoside (200 mg, 0.66 mmol) to afford 3-aminophenyl- β -D-glucopyranoside as a white crystal (171 mg, 95%). ^1H NMR (400 MHz, 298 K, CD₃OD) δ 6.95 (d, *J* = 8.8 Hz, 2H), 6.68 (d, *J* = 8.8 Hz, 2H), 5.27 (d, *J* = 4.0 Hz, 1H), 3.85-3.80 (m, 1H), 3.77-3.71 (m, 3H), 3.54-3.51 (m, 1H), 3.44-3.34 (m, 1H). ^{13}C NMR (100 MHz, 298 K, CD₃OD) δ 150.28, 142.05, 118.37, 116.44, 99.13, 73.59, 72.75, 72.01, 61.00. HRMS (ESI⁺/QTOF) Calcd for C₁₂H₁₇NO₆ m/z: [M+H]⁺ 272.1129; Found 272.1162.

Compound *p*-5a**.** The same procedure for *o*-**5a** was followed, using 4-aminophenyl- β -D-glucopyranoside (100 mg, 0.369 mmol) to afford *p*-**5a** as a white powder (111 mg, 78%). ^1H NMR (400 MHz, 298 K, DMSO-*d*₆) δ 8.63 (s, 1H), 7.89 (d, *J* = 8.4 Hz, 2H), 7.61 (d, *J* = 8.4 Hz, 2H), 7.28 (d, *J* = 8.8 Hz, 2H), 7.13 (d, *J* = 8.8 Hz, 2H), 6.81 (m, 1H), 5.97 (m, 1H), 5.39-5.36 (m, 3H), 5.07 (d, *J* = 6.4 Hz, 1H), 4.99 (d, *J* = 5.6 Hz, 1H), 4.95 (d, *J* = 5.6 Hz, 1H) 4.50 (m, 1H), 3.65-3.63 (m, 2H), 3.48-3.46 (m, 2H), 3.39-3.37 (m, 1H), 3.22-3.16 (m, 1H). ^{13}C NMR (100 MHz, 298 K, DMSO-*d*₆) δ 158.85, 156.25, 145.76, 140.14, 136.57, 136.17, 135.46, 129.22, 128.71, 126.97, 122.69, 118.05, 116.49, 98.66, 74.20, 73.51, 72.05, 70.38, 61.14. HRMS (ESI⁺/QTOF) Calcd for C₂₁H₂₃NO₆ m/z: [M+H]⁺ 386.1598; Found 386.1620. HRMS (ESI⁻/QTOF) Calcd for C₂₁H₂₃NO₆ m/z: [M+HCOO]⁻ 430.1507; Found 430.1493.

Synthesis of template *p*-5b



Scheme S2. Synthesis of maltose-imine template *p*-5b

Synthesis of *p*-5b

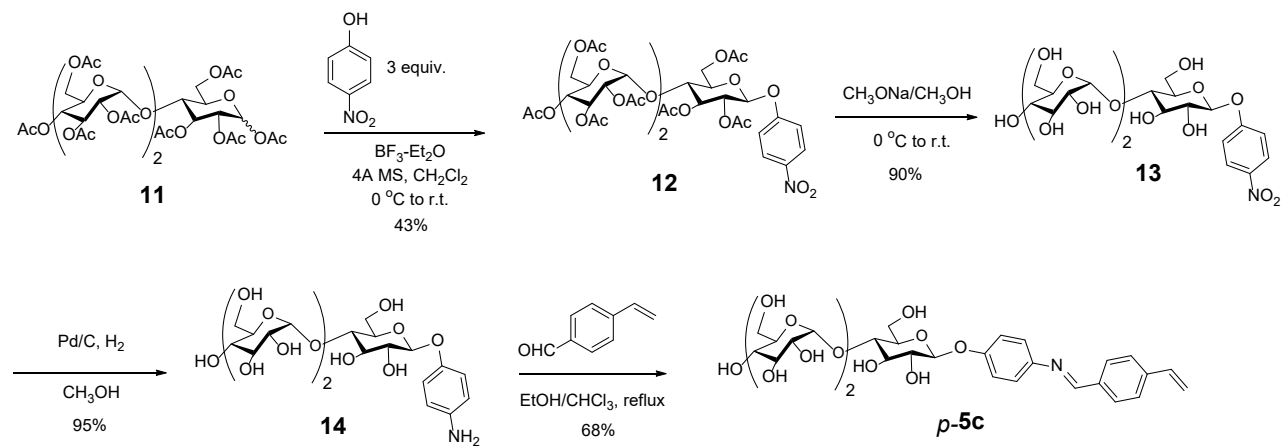
Compound 8.⁴ To a stirred solution of D-maltose octaacetate (500 mg, 0.74 mmol) and 4-nitrophenol (308 mg, 2.21 mmol) in anhydrous CH_2Cl_2 (5 mL) with activated 4 Å molecular sieves at 0 °C was added $\text{BF}_3\text{-OEt}_2$ (525 mg, 457 μL , 3.70 mmol). The mixture was warmed to room temperature and stirred for 24 h. A solution of saturated NaHCO_3 (20 mL) was added. The aqueous layer was extracted with CH_2Cl_2 (20 mL). The combined organic solution was washed with 1 M NaOH (3×20 mL) and H_2O (20 mL), dried over Na_2SO_4 , and concentrated in vacuo. The residue was crystallized from EtOAc/Hexane and the crude product was purified by column chromatography over silica gel to afford a colorless syrup (353 mg, 63%). ^1H NMR (600 MHz, 298 K, CDCl_3) δ 8.15 (d, $J = 9.0$ Hz, 2H), 7.02 (d, $J = 9.0$ Hz, 2H), 5.39-5.28 (m, 2H), 5.23 (d, $J = 7.2$ Hz, 1H), 5.11-5.07 (m, 1H), 5.02-4.98 (m, 1H), 4.83-4.80 (m, 1H), 4.46-4.43 (m, 1H), 4.23-4.18 (m, 2H), 4.07-4.00 (m, 3H), 3.93-3.91 (m, 2H), 2.05 (s, 3H), 2.04 (s, 3H), 2.03 (s, 3H), 2.01 (s, 3H), 1.99 (s, 3H), 1.98 (s, 3H), 1.96 (s, 3H). ^{13}C NMR (125 MHz, 298 K, CDCl_3) δ 170.41, 170.16, 170.14, 170.06, 169.88, 169.43, 169.32, 161.06, 143.17, 125.74, 116.57, 97.43, 95.73, 74.95, 74.93, 72.61, 72.58, 71.63, 69.99, 69.19, 68.64, 67.99, 62.63, 61.54, 20.95, 20.83, 20.81, 20.62, 20.53, 20.51, 20.50. HRMS (ESI $^+$ /QTOF) Calcd for $\text{C}_{32}\text{H}_{39}\text{NO}_{20}$ m/z: $[\text{M}+\text{NH}_2]^+$ 775.2404; Found 775.2359. HRMS (ESI $^-$ /QTOF) Calcd for $\text{C}_{32}\text{H}_{39}\text{NO}_{20}$ m/z: $[\text{M}+\text{HCOO}]^-$ 802.2047; Found 802.2105.

Compound 9. A solution of compound **8** (500 mg, 0.66 mmol) in methanol (10 mL) with a catalytic amount of sodium methoxide was stirred at room temperature for 3 h. The solution was neutralized with Amberlite® IR-120 (H^+) ion-exchange resin, filtered, and concentrated in vacuo. The residue was purified by column chromatography over silica gel to afford compound **9** as a white powder (297 mg, 90%). 1H NMR (400 MHz, 298 K, CD₃OD) δ 8.21 (d, J = 9.6 Hz, 2H), 7.23 (d, J = 9.6 Hz, 2H), 5.21 (d, J = 3.6 Hz, 1H), 5.11 (d, J = 7.6 Hz, 1H), 3.93-3.90 (m, 1H), 3.87-3.82 (m, 2H), 3.79-3.63 (m, 13H), 3.58-3.54 (m, 1H), 3.49-3.45 (m, 1H), 3.31-3.29 (m, 2H). ^{13}C NMR (100 MHz, 298 K, CD₃OD) δ 162.36, 142.47, 125.19, 116.29, 101.52, 100.03, 79.26, 76.12, 75.51, 73.62, 73.44, 72.86, 72.70, 70.11, 61.32, 60.42. HRMS (ESI/QTOF) Calcd for C₁₈H₂₅NO₁₃ m/z: [M-H]⁻ 462.1253; Found 462.1261, [M+Cl]⁻ 498.1020; Found: m/z 498.1036, [M+HCOO]⁻ 508.1308; Found 508.1321.

Compound 10. The same procedure for 2-aminophenyl- β -D-glucopyranoside was followed, using compound **9** (400 mg, 0.86 mmol) to afford compound **10** as a white crystal (354 mg, 95%). 1H NMR (400 MHz, 298 K, CD₃OD) δ 6.93 (d, J = 8.4 Hz, 2H), 6.70 (d, J = 8.4 Hz, 2H), 5.20 (d, J = 2.4 Hz, 1H), 4.78 (d, J = 7.6 Hz, 1H), 4.50 (br, s, 2H), 3.89-3.80 (m, 3H), 3.75-3.65 (m, 6H), 3.54-3.43 (m, 4H), 3.33-3.28 (m, 1H), 3.49-3.45 (m, 1H), 3.31-3.29 (m, 4H). ^{13}C NMR (100 MHz, 298 K, CD₃OD) δ 150.63, 142.11, 117.87, 116.60, 101.95, 101.57, 79.56, 76.12, 75.02, 73.53, 73.39, 73.10, 72.59, 70.23, 61.24, 60.48. HRMS (ESI/QTOF) Calcd for C₁₈H₂₇NO₁₁ m/z: [M+Cl]⁻ 468.1278; Found: m/z 468.1290, [M+HCOO]⁻ 478.1566; Found: m/z 478.1569.

Compound *p*-5b. The same procedure for *o*-**5a** was followed, using compound **10** (150 mg, 0.35 mmol) and 4-vinylbenzaldehyde (55 mg, 0.42 mmol) to afford **p**-**5b** as a white powder (136 mg, 72%). 1H NMR (600 MHz, 298 K, CD₃OD) δ 8.57 (s, 1H), 7.90 (d, J = 7.8 Hz, 2H), 7.58 (d, J = 7.8 Hz, 2H), 7.28 (d, J = 8.4 Hz, 2H), 7.18 (d, J = 8.4 Hz, 2H), 6.83 (m, 1H), 5.94 (m, 1H), 5.37 (m, 1H), 5.24 (m, 1H), 4.98 (d, J = 7.8 Hz, 1H), 3.96-3.93 (m, 1H), 3.90-3.86 (m, 4H), 3.80-3.75 (m, 2H), 3.71-3.64 (m, 4H), 3.62-3.54 (m, 2H), 3.51-3.49 (m, 1H), 3.32-3.29 (m, 5H). ^{13}C NMR (150 MHz, 298 K, CD₃OD) δ 159.62, 156.38, 145.94, 140.62, 136.08, 135.78, 135.46, 129.69, 128.71, 126.44, 126.24, 121.80, 117.89, 117.11, 116.50, 116.28, 114.70, 101.54, 100.93, 79.50, 76.25, 75.32, 73.64, 73.42, 73.09, 72.73, 70.14, 61.33, 60.53. HRMS (ESI/QTOF) Calcd for C₂₇H₃₃NO₁₁ m/z: [M-H]⁻ 546.1981; Found 546.2021, [M+Cl]⁻ 582.1748; Found 582.1802, [M+HCOO]⁻ 592.2036; Found: m/z 592.2088.

Synthesis of template *p*-5c



Scheme S3. Synthesis of template *p*-5c

Synthesis of *p*-5c

Compound 12. The same procedure for **8** was followed, using D-maltotriose acetate (600 mg, 0.62 mmol) and 4-nitrophenol (259 mg, 1.86 mmol) to afford **12** as a colorless syrup (201 mg, 43%). ¹H NMR (600 MHz, 298 K, CDCl₃) δ 8.15 (d, *J* = 9.0 Hz, 2H), 7.02 (d, *J* = 9.0 Hz, 2H), 5.39-5.28 (m, 2H), 5.23 (d, *J* = 7.2 Hz, 1H), 5.11-5.07 (m, 1H), 5.02-4.98 (m, 1H), 4.83-4.80 (m, 1H), 4.46-4.43 (m, 1H), 4.23-4.18 (m, 2H), 4.07-4.00 (m, 3H), 3.93-3.91 (m, 2H), 2.05 (s, 3H), 2.04 (s, 3H), 2.03 (s, 3H), 2.01 (s, 3H), 1.99 (s, 3H), 1.98 (s, 3H), 1.96 (s, 3H). ¹³C NMR (125 MHz, 298 K, CDCl₃) δ 170.41, 170.16, 170.14, 170.06, 169.88, 169.43, 169.32, 161.06, 143.17, 125.74, 116.57, 97.43, 95.73, 74.95, 74.93, 72.61, 72.58, 71.63, 69.99, 69.19, 68.64, 67.99, 62.63, 61.54, 20.95, 20.83, 20.81, 20.62, 20.53, 20.51, 20.50. HRMS (ESI⁺/QTOF) Calcd for C₄₄H₅₅NO₂₈ m/z: [M+NH₂]⁺ 1063.3249; Found 1063.3253.

Compound 13. The same procedure for **9** was followed, using compound **12** (500 mg, 0.48 mmol) to afford **13** as a white powder (282 mg, 90%). ¹H NMR (400 MHz, 298 K, CD₃OD) δ 8.21 (d, *J* = 9.2 Hz, 2H), 7.24 (d, *J* = 9.2 Hz, 2H), 5.21 (d, *J* = 3.6 Hz, 1H), 5.11 (d, *J* = 5.2 Hz, 1H), 4.49 (d, *J* = 8.0 Hz, 1H), 3.88-3.80 (m, 8H), 3.78-3.69 (m, 8H), 3.54-3.49 (m, 15H), 3.34-3.30 (m, 3H). ¹³C NMR (100 MHz, 298 K, CD₃OD) δ 162.37, 142.49, 125.21, 116.31, 101.48, 101.25, 96.72, 92.42, 80.40, 79.88, 79.82, 79.23, 76.11, 75.50, 73.66, 73.57, 73.52, 73.36, 72.80, 72.32, 72.04, 71.98, 70.07, 61.30,

60.76, 60.49. HRMS (ESI/QTOF) Calcd for $C_{24}H_{35}NO_{18}$ m/z: $[M+HCOO]^-$ 670.1836; Found: m/z 670.1857.

Compound 14. The same procedure for **10** was followed, using compound **13** (400 mg, 0.64 mmol) to afford **14** as a white powder (354 mg, 95%). 1H NMR (400 MHz, 298 K, CD_3OD) δ 6.91 (d, J = 8.8 Hz, 2H), 6.68 (d, J = 8.8 Hz, 2H), 5.20-5.15 (m, 1H), 4.74 (d, J = 7.6 Hz, 1H), 4.48 (d, J = 7.6 Hz, 1H), 3.89-3.70 (m, 15H), 3.68-3.58 (m, 5H), 3.52-3.34 (m, 5H), 3.30-3.26 (m, 5H). ^{13}C NMR (100 MHz, 298 K, CD_3OD) δ 150.72, 142.16, 117.89, 116.26, 102.13, 101.41, 96.74, 92.42, 80.42, 79.90, 79.86, 79.57, 76.27, 75.24, 75.19, 73.66, 73.34, 73.23, 73.16, 72.82, 72.35, 72.04, 71.93, 71.87, 70.22, 70.05, 61.03, 60.72. HRMS (ESI/QTOF) Calcd for $C_{24}H_{37}NO_{16}$ m/z: $[M+Cl]^-$ 630.1806; Found 630.1847, $[M+HCOO]^-$ 640.2094; Found 640.2134.

Compound *p*-5c. The same procedure for *o*-**5a** was followed, using compound **14** (100 mg, 0.17 mmol) and 4-vinylbenzaldehyde (27 mg, 0.20 mmol) to afford *p*-**5c** as a white powder (81 mg, 68%). 1H NMR (600 MHz, 298 K, CD_3OD) δ 8.54 (s, 1H), 7.86 (d, J = 8.4 Hz, 2H), 7.55 (d, J = 8.4 Hz, 2H), 7.25 (d, J = 9.2 Hz, 2H), 7.15 (d, J = 9.2 Hz, 2H), 6.79 (m, 1H), 5.90 (m, 1H), 5.34 (m, 1H), 5.24 (m, 1H), 5.22 (d, J = 3.6 Hz, 1H), 5.16-5.14 (m, 4H), 5.10 (d, J = 3.6 Hz, 1H), 4.95 (d, J = 8.0 Hz, 1H), 4.49 (d, J = 8.0 Hz, 1H), 3.90-3.68 (m, 8H), 3.68-3.59 (m, 5H), 55-3.45 (m, 5H), 3.34-3.30 (m, 4H), 3.19-3.15 (m, 1H). ^{13}C NMR (150 MHz, 298 K, CD_3OD) δ 159.66, 156.40, 145.95, 140.64, 136.09, 135.48, 128.70, 126.24, 121.79, 117.12, 114.68, 101.48, 101.45, 101.41, 101.26, 100.91, 96.73, 92.42, 80.41, 80.01, 79.85, 75.23, 74.43, 73.66, 73.57, 73.52, 73.33, 73.32, 72.94, 72.50, 72.35, 72.03, 71.89, 70.23, 70.06, 61.31, 60.76. HRMS (ESI/QTOF) Calcd for $C_{33}H_{43}NO_{16}$ m/z: $[M-H]^-$ 708.2509; Found 708.2484, $[M+Cl]^-$ 744.2276; Found 744.2247, $[M+HCOO]^-$ 754.2564; Found 754.2578.

¹H NMR comparison of imine-templates p-5a, p-5b and p-5c

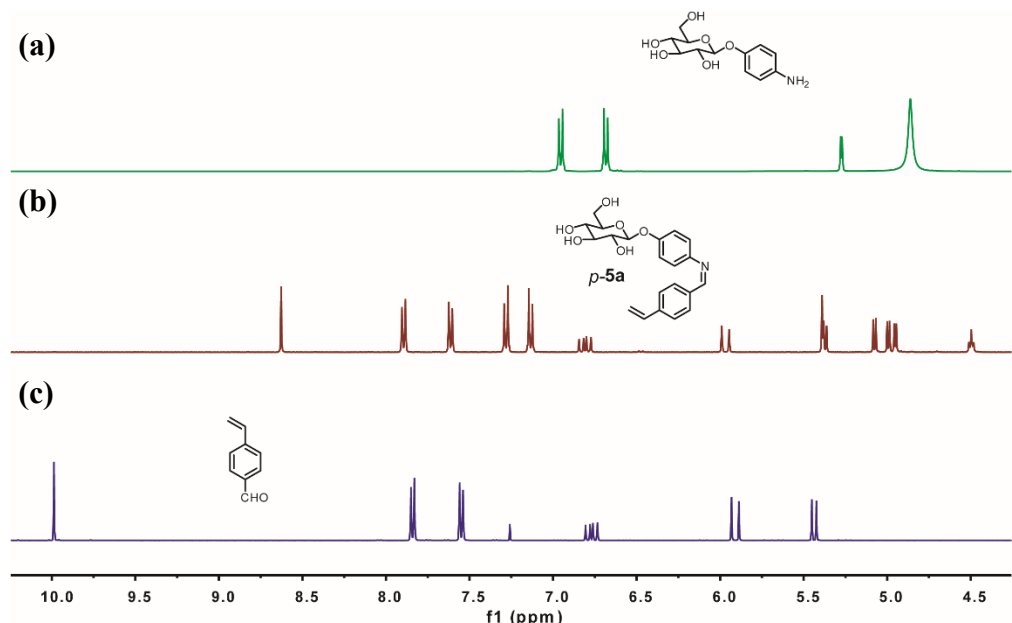


Figure S1. Partial stacked ¹H NMR spectra of (a) 4-aminophenyl- β -D-glucopyranoside in CD₃OD, (b) imine template p-5a in DMSO-*d*₆ and (c) 4-vinylbenzaldehyde in CDCl₃.

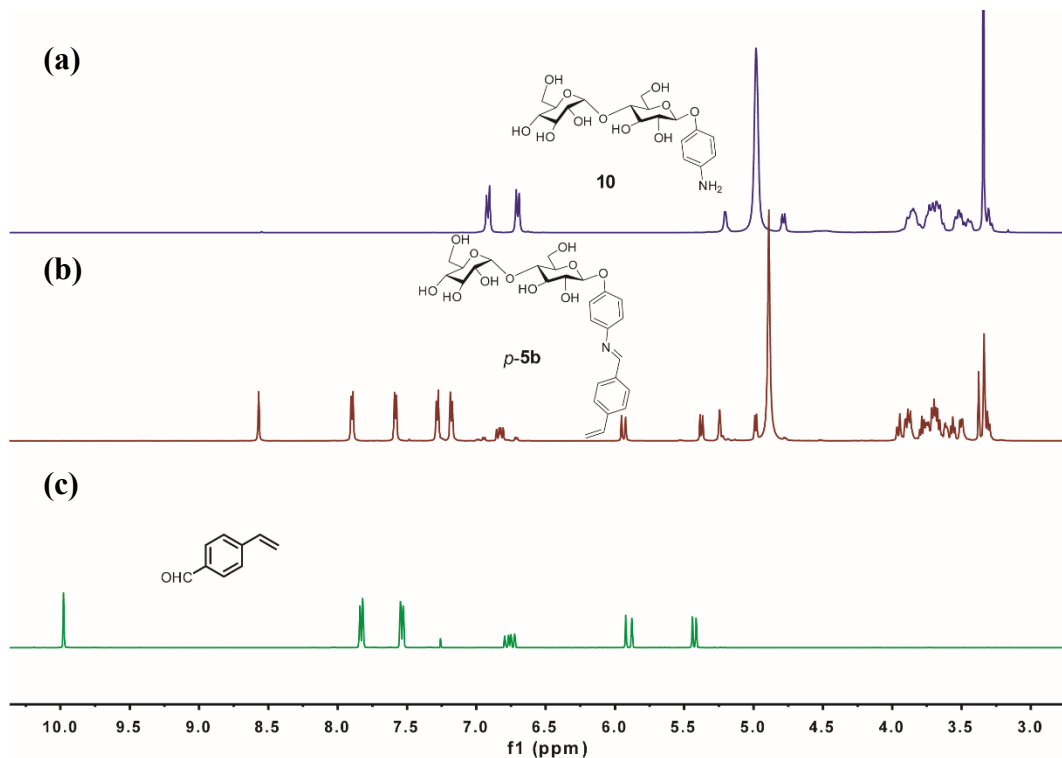


Figure S2. Partial stacked ¹H NMR spectra of (a) compound 10 in CD₃OD, (b) imine template p-5b in CD₃OD and 4-vinylbenzaldehyde in CDCl₃.

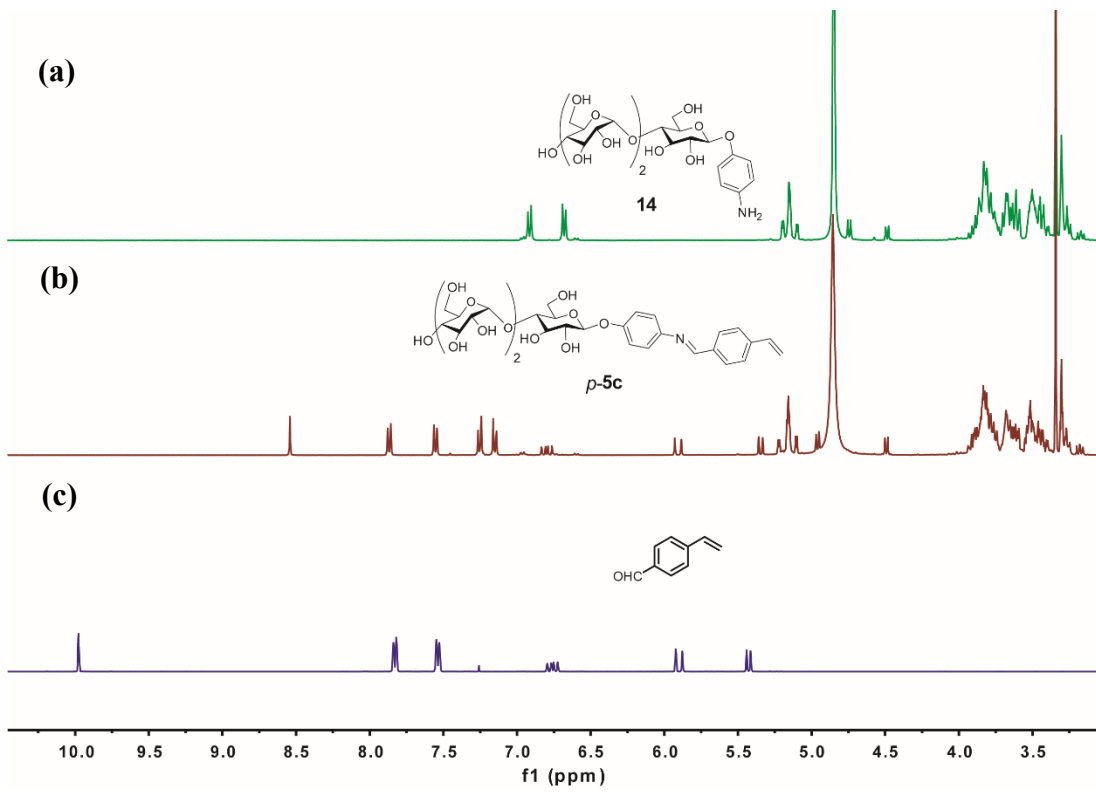


Figure S3. Partial stacked ^1H NMR spectra of (a) compound **14** in CD_3OD , (b) imine template *p*-**5c** in CD_3OD and (c) 4-vinylbenzaldehyde in CDCl_3 .

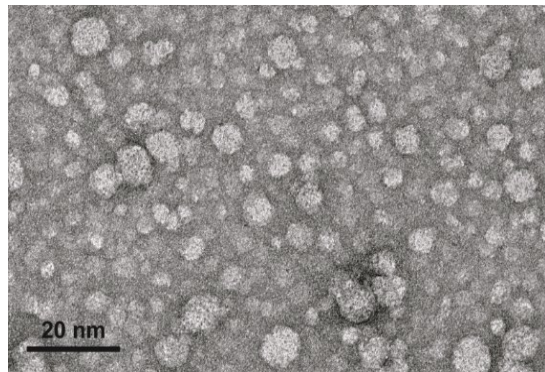


Figure S4. TEM image of typical MINPs (with some particles in the aggregated form caused by the negative staining).

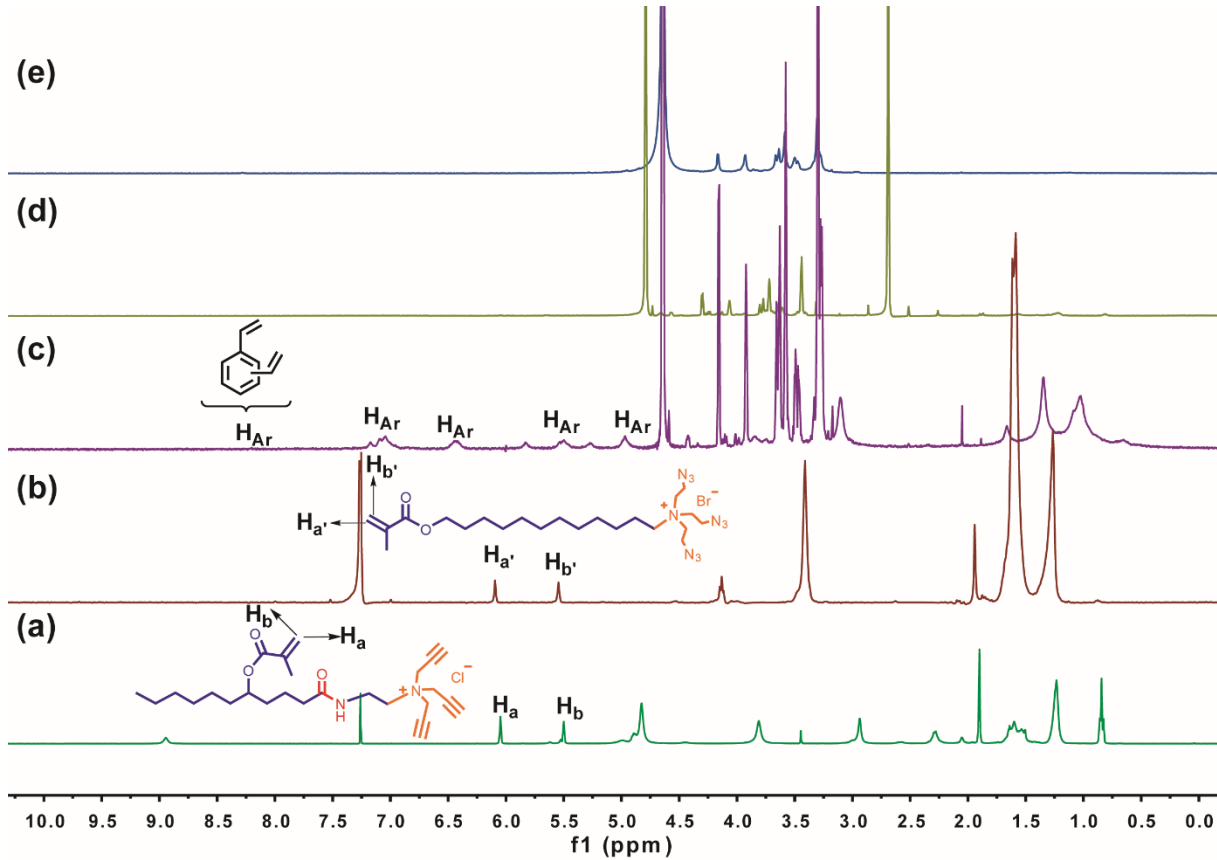


Figure S5. ^1H NMR spectra of (a) surfactant **1b** in CDCl_3 , (b) surfactant **2** in CDCl_3 (c) alkynyl-SCM in D_2O , (d) MINP-CHO(*p*-G1) in D_2O before solvent washing and (e) final MINP(*p*-G1+**7h**) in D_2O after post-modification and purification.

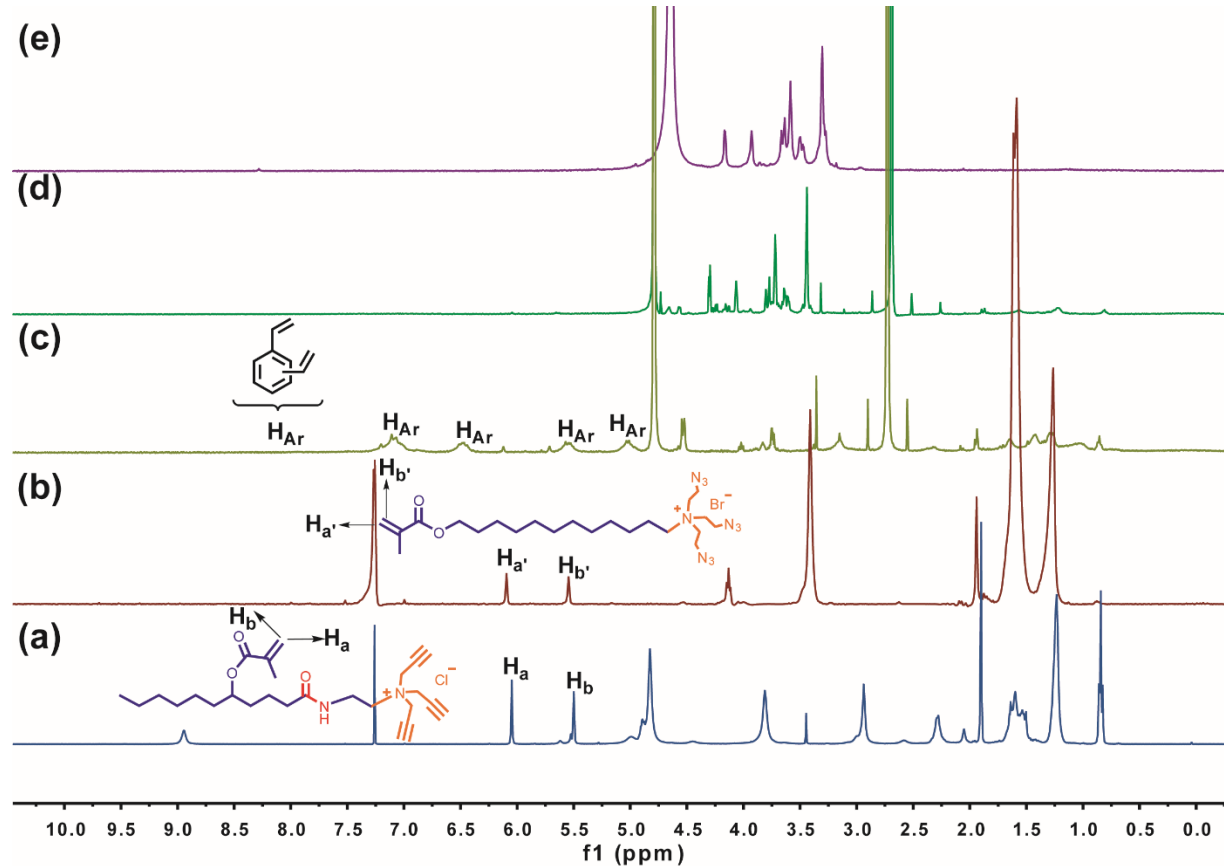


Figure S6. ^1H NMR spectra of (a) surfactant **1b** in CDCl_3 , (b) surfactant **2** in CDCl_3 (c) alkynyl-SCM in D_2O , (d) MINP-CHO(*p*-G2) in D_2O before solvent washing and (e) final MINP(*p*-G2+**7h**) in D_2O after post-modification and purification.

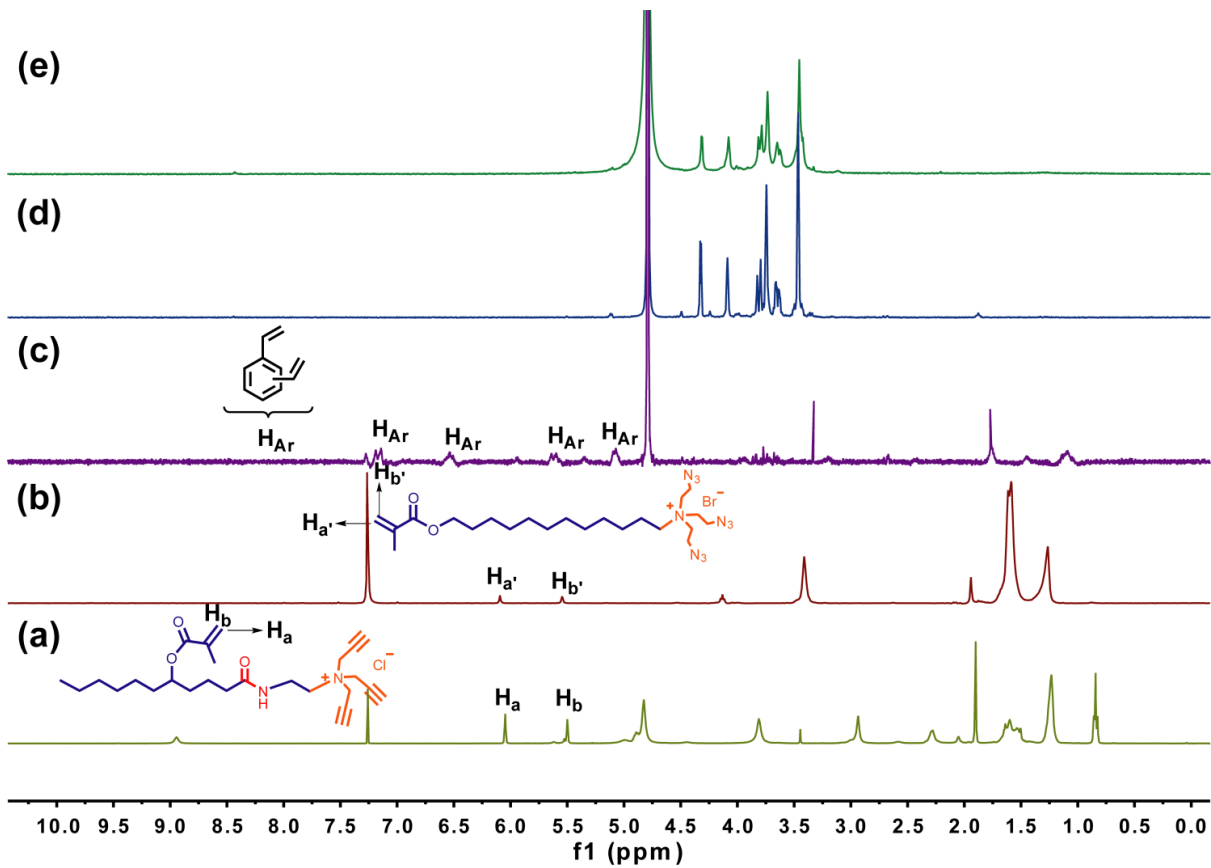


Figure S7. ^1H NMR spectra of (a) surfactant **1b** in CDCl_3 , (b) surfactant **2** in CDCl_3 (c) alkynyl-SCM in D_2O , (d) MINP-CHO(*p*-G3) in D_2O before solvent washing and (e) final MINP(*p*-G3+7h) in D_2O after post-modification and purification.

Dynamic Light Scattering

Particle size of MINP was determined on a Malvern Zetasizer Nano ZS using the Zetasizer software according to the Stokes-Einstein equation (1). The volume of a spherical nanoparticle (V_{D_h}) was calculated from equation (2). Assuming a density of 1.37 g/cm³ (the density of protein), the molecular weight of the particle can be calculated using equation (3).⁵ A nanoparticle with hydrodynamic diameter of 4.87 nm has a calculated molecular weight of 50 kDa.

$$D_h = \frac{k_B T}{6\pi\eta D_t} \quad (1)$$

in which D_h is the hydrodynamic diameter, D_t the translational diffusion coefficient measured by dynamic light scattering, T the temperature, k_B the Boltzmann's constant, and η is dynamic viscosity of water (0.890 cP at 298 K).

$$V_{D_h} = \frac{4\pi}{3} \left(\frac{D_h}{2}\right)^3 \quad (2)$$

$$\text{Mw in dalton} = \left(\frac{D_h}{0.132}\right)^3 \quad (3)$$

in which D_h is the hydrodynamic diameter in nm.

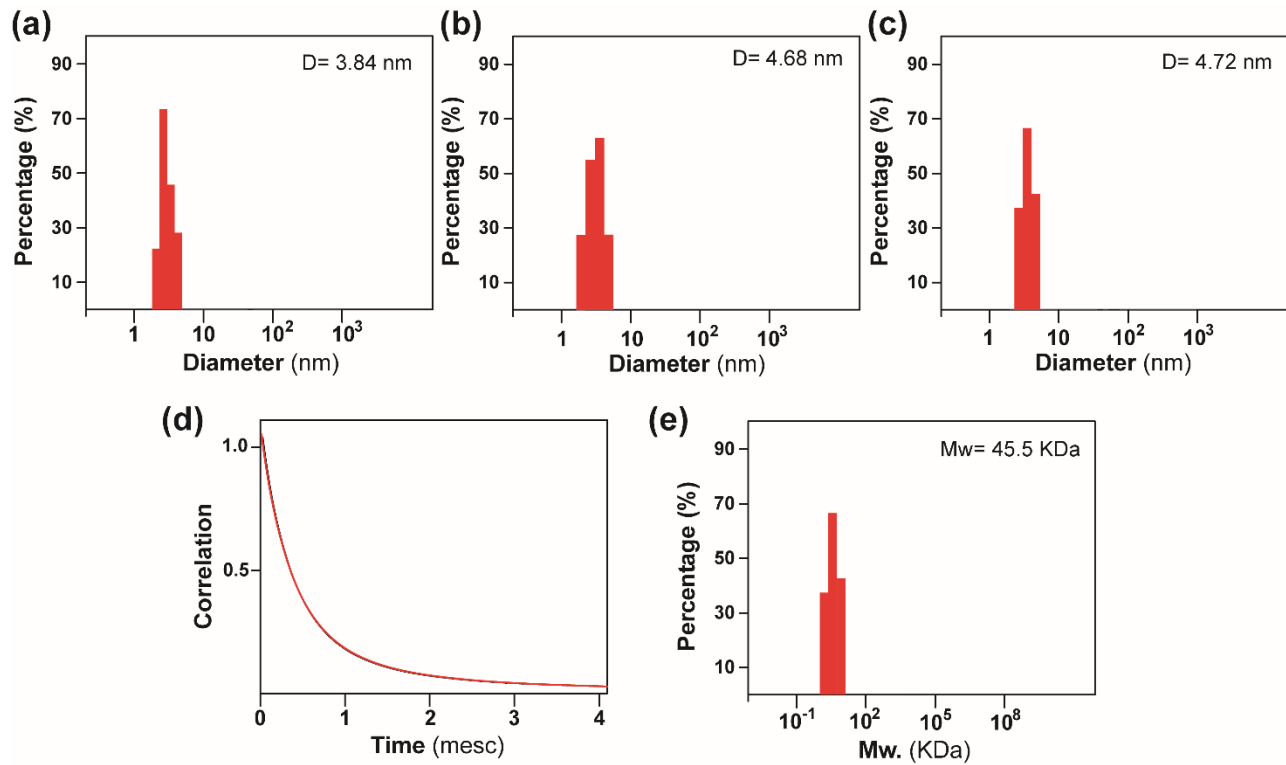


Figure S8. Distribution of the hydrodynamic diameters of the nanoparticles in water at 298 K as determined by DLS for (a) alkynyl-SCM, (b) MINP-CHO(*p*-**G1**) before post-modification and (c) final MINP(*p*-**G1+7h**) in H₂O after post-modification and purification (d) The correlation curve and (e) the corresponding molecular weight of the final MINP(*p*-**G1+7h**) based on the DLS size. If each unit of building block for the MINP is assumed to contain 0.6 molecules of compound **1b** ($M_w = 508$ g/mol), 0.4 molecules of compound **2** ($M_w = 558$ g/mol), one molecule of DVB ($M_w = 130$ g/mol) and 0.6 molecules of ligand **3** ($M_w = 264$ g/mol), 0.02 molecules of 6-vinylbenzoxaborole ($M_w = 160$ g/mol), and 0.02 molecules of compound **7h** ($M_w = 139$ g/mol) the molecular weight of the MINP(*p*-**G1+7h**) translates to 55 [$= 45500 / (0.6 \times 508 + 0.4 \times 558 + 0.6 \times 264 + 1.0 \times 130 + 0.02 \times 160 + 0.02 \times 139)$] of such units.

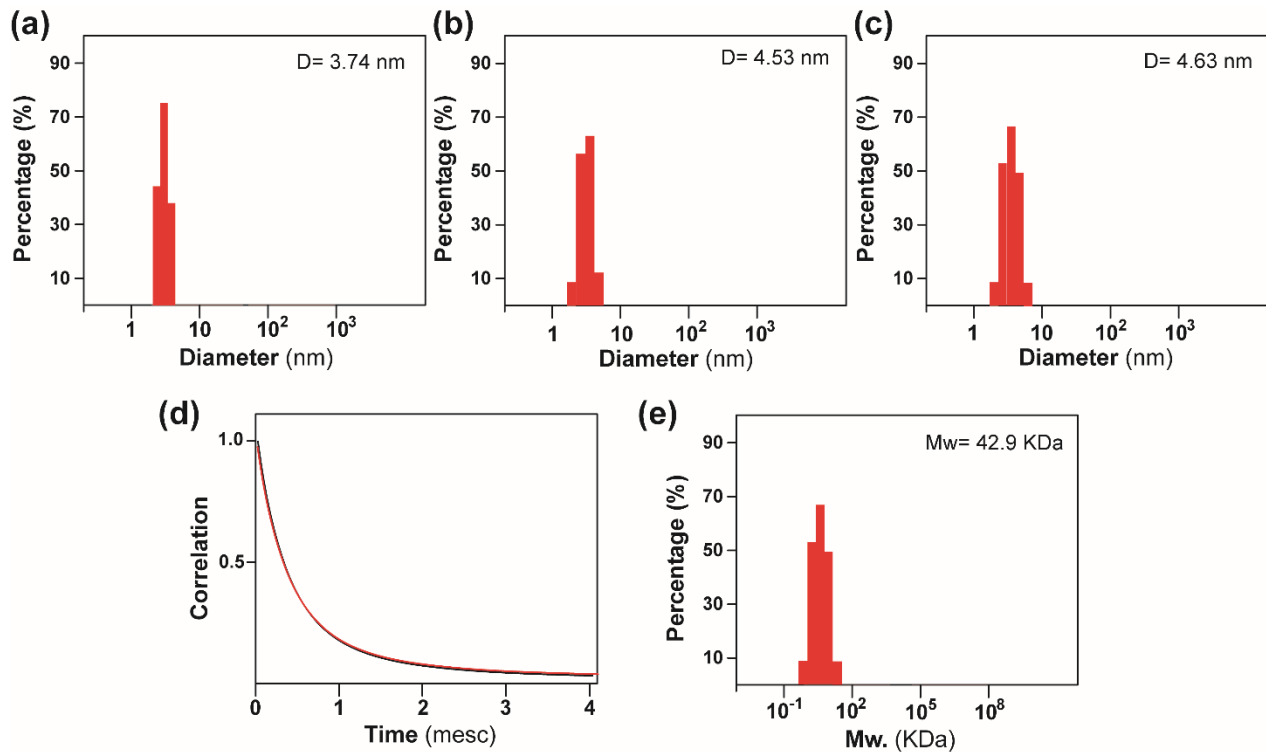


Figure S9. Distribution of the hydrodynamic diameters of the nanoparticles in water at 298 K as determined by DLS for (a) alkynyl-SCM, (b) MINP-CHO(*p*-G2) before post-modification and (c) final MINP(*p*-G2+7h) in H₂O after post-modification and purification (d) The correlation curve and (e) the corresponding molecular weight of the final MINP(*p*-G2+7h) based on the DLS size. If each unit of building block for the MINP is assumed to contain 0.6 molecules of compound **1b** ($M_w = 508$ g/mol), 0.4 molecules of compound **2** ($M_w = 558$ g/mol), one molecule of DVB ($M_w = 130$ g/mol) and 0.6 molecules of ligand **3** ($M_w = 264$ g/mol), 0.02 molecules of 6-vinylbenzoxaborole ($M_w = 160$ g/mol), and 0.02 molecules of compound **7h** ($M_w = 139$ g/mol) the molecular weight of the MINP(*p*-G2+7h) translates to 52 [$= 42900 / (0.6 \times 508 + 0.4 \times 558 + 0.6 \times 264 + 1.0 \times 130 + 0.02 \times 160 + 0.02 \times 139)$] of such units.

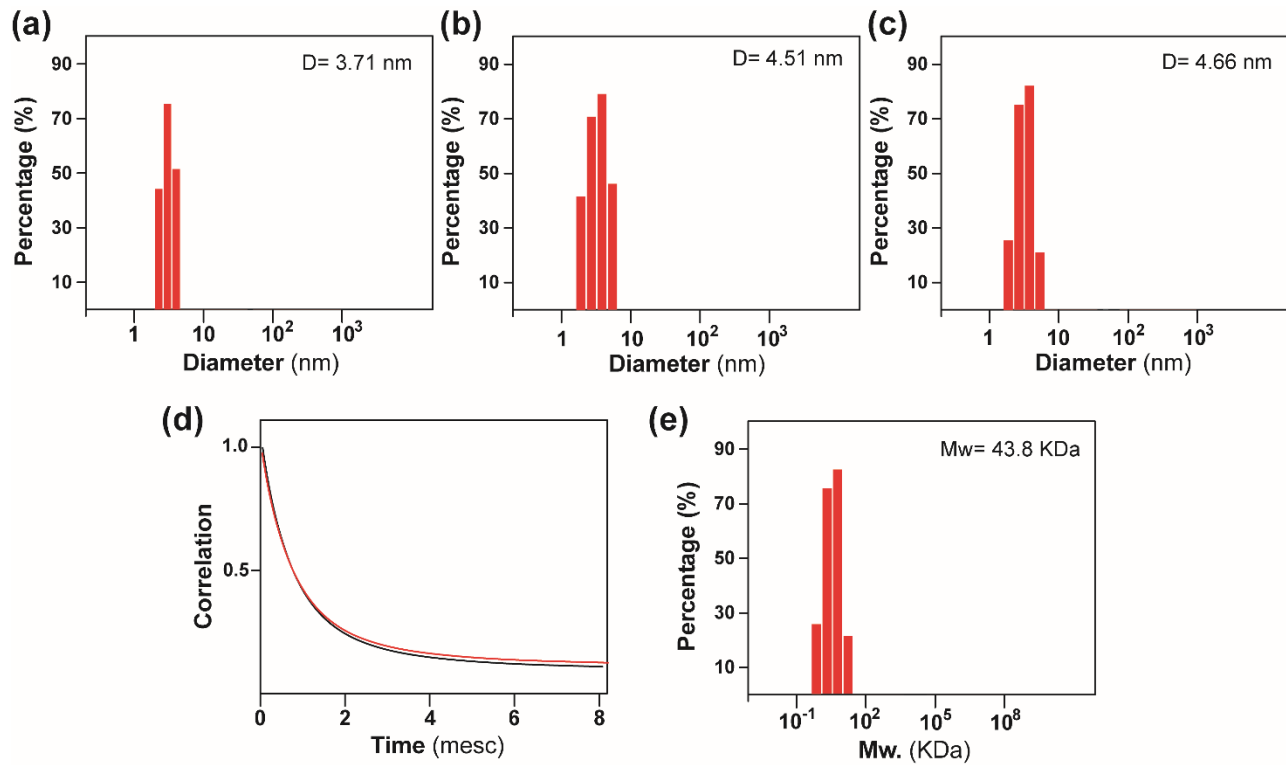
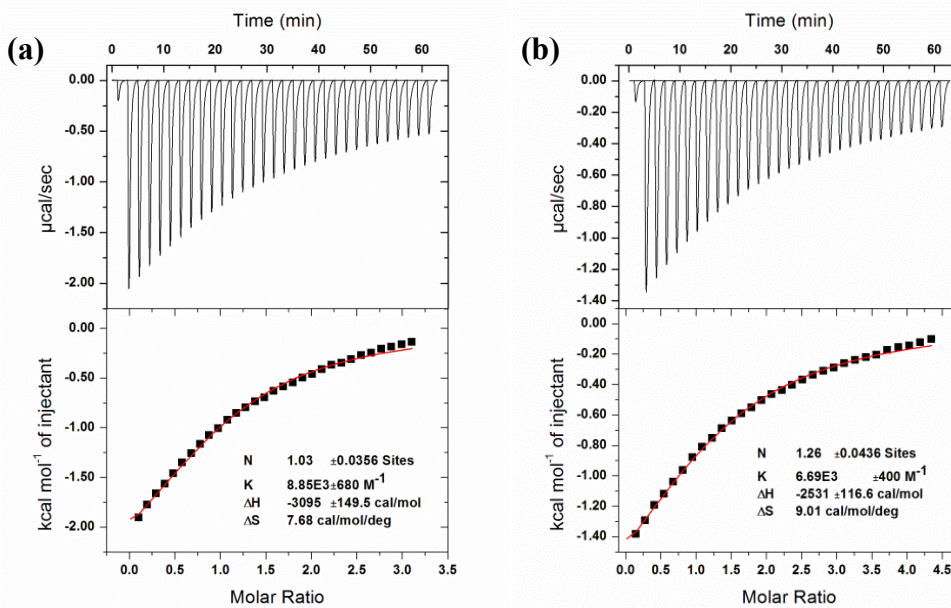


Figure S10. Distribution of the hydrodynamic diameters of the nanoparticles in water at 298 K as determined by DLS for (a) alkynyl-SCM, (b) MINP-CHO(*p*-G3) before post-modification and (c) final MINP(*p*-G3+7h) in H₂O after post-modification and purification (d) The correlation curve and (e) the corresponding molecular weight of the final MINP(*p*-G3+7h) based on the DLS size. If each unit of building block for the MINP is assumed to contain 0.6 molecules of compound **1b** ($M_w = 508$ g/mol), 0.4 molecules of compound **2** ($M_w = 558$ g/mol), one molecule of DVB ($M_w = 130$ g/mol) and 0.6 molecules of ligand **3** ($M_w = 264$ g/mol), 0.02 molecules of 6-vinylbenzoxaborole ($M_w = 160$ g/mol), and 0.02 molecules of compound **7h** ($M_w = 139$ g/mol) the molecular weight of the MINP(*p*-G3+7h) translates to 53 [$= 43800 / (0.6 \times 508 + 0.4 \times 558 + 0.6 \times 264 + 1.0 \times 130 + 0.02 \times 160 + 0.02 \times 139)$] of such units.

ITC Binding Studies

Procedure: The determination of binding constants by ITC followed standard procedures at 298.15 K.⁶⁻⁸ In general, a solution of an appropriate sugar in 10 mM HEPES buffer (pH 7.4) was injected in equal steps into 1.43 mL of the corresponding MINP in the same solution. The top panel shows the raw calorimetric data. The area under each peak represents the amount of heat generated at each ejection and is plotted against the molar ratio of the MINP to the guest. The smooth solid line is the best fit of the experimental data to the sequential binding of N binding site on the MINP. The heat of dilution for the guest, obtained by titration carried out beyond the saturation point, was subtracted from the heat released during the binding. Binding parameters were auto-generated after curve fitting using Microcal Origin 7.

ITC titration curves:



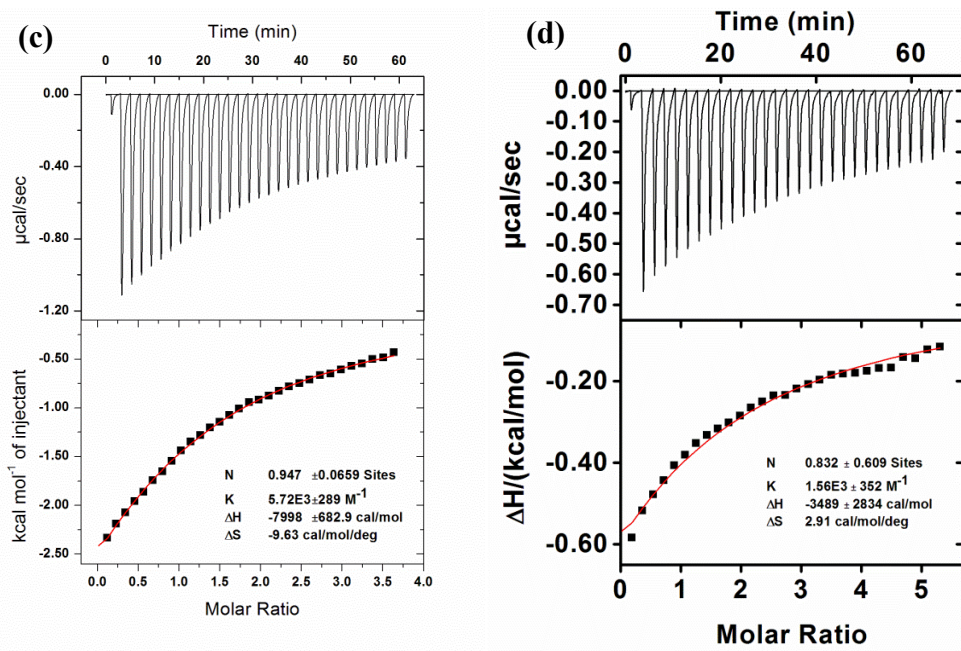


Figure S11. ITC curves obtained at 298 K from titration of MINP-CHO(*p*-G1) with (a) glucose, (b) maltose, (c) maltotriose and (d) maltohexaose in HEPEs buffer (10 mM, pH 7.4). The data correspond to entries 1-4 in Table 1, respectively.

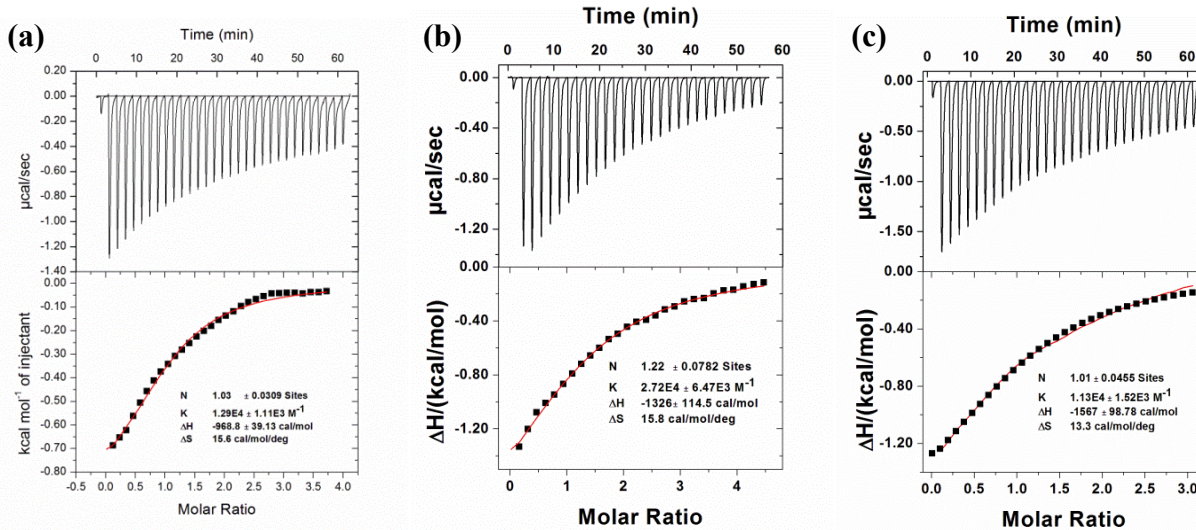


Figure S12. ITC curves obtained at 298 K from titration of MINP-CHO(*p*-G2) with (a) glucose, (b) maltose and (c) maltotriose in HEPEs buffer (10 mM, pH 7.4). The data correspond to entries 5-7 in Table 1, respectively.

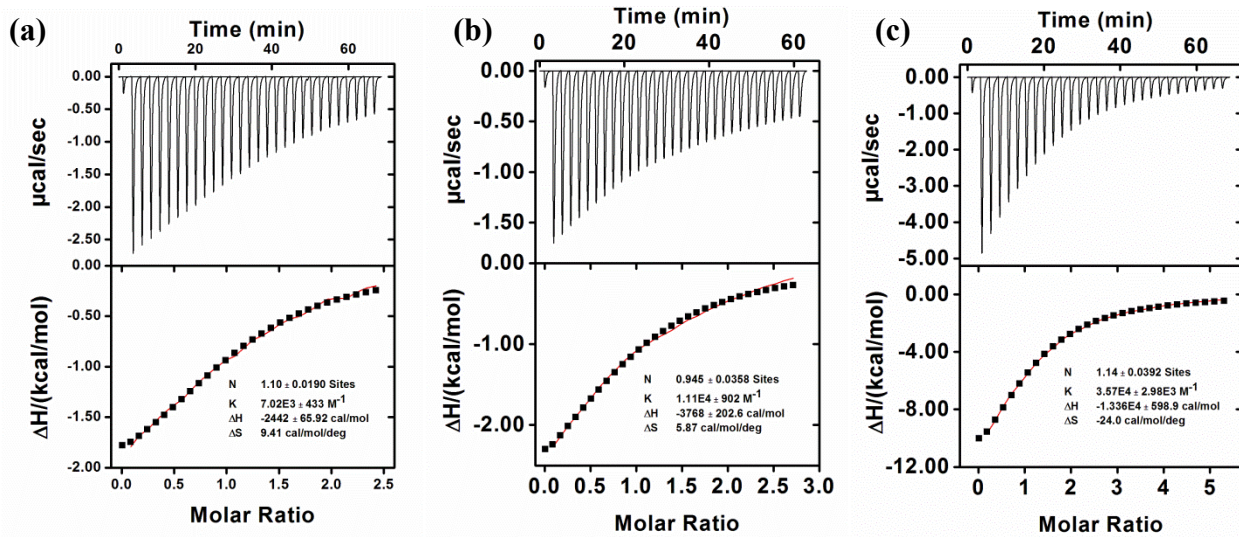


Figure S13. ITC curves obtained at 298 K from titration of MINP-CHO(*p*-G3) with (a) glucose, (b) maltose and (c) maltotriose in HEPES buffer (10 mM, pH 7.4). The data correspond to entries 8-10 in Table 1, respectively.

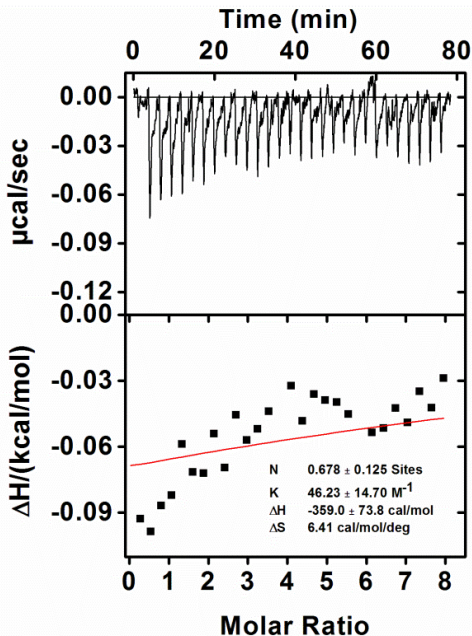


Figure S14. ITC curves obtained at 298 K from titration of NINP prepared with 1.0 equiv. of 4 with glucose in HEPES buffer (10 mM, pH 7.4). The data correspond to entry 11 in Table 1.

Table S1. Binding of Oligosaccharides by MNPs determined by Isothermal titration calorimetry (ITC).^a

Entry	MNP	Oligosaccharides	$K_a (10^3 \text{ M}^{-1})$	$\Delta G (\text{kcal/mol})$	N^b
1	MINP(<i>p</i> -G1+7h)	maltose	7.99 ± 0.56	-5.32	1.27 ± 0.04
2	MINP(<i>p</i> -G1+7h)	cellobiose	1.88 ± 0.11	-4.46	0.99 ± 0.16
3	MINP(<i>p</i> -G1+7h)	sucrose	1.83 ± 0.11	-4.45	1.75 ± 0.13
4	MINP(<i>p</i> -G1+7h)	maltulose	2.99 ± 1.29	-4.74	0.97 ± 0.42
5	MINP(<i>p</i> -G1+7h)	lactose	0.20 ± 0.04	-3.12	1.89 ± 0.61
6	MINP(<i>p</i> -G1+7h)	xylobiose	<0.05	-- ^c	-- ^c
7	MINP(<i>p</i> -G1+7h)	maltotriose	5.62 ± 0.57	-5.11	1.29 ± 0.08
8	MINP(<i>p</i> -G2+7h)	maltotriose	11.50 ± 0.50	-5.54	1.44 ± 0.01
9	MINP(<i>p</i> -G1+7h)	cellotriose	2.62 ± 0.31	-4.66	1.88 ± 0.14
10	MINP(<i>p</i> -G2+7h)	cellotriose	3.64 ± 0.34	-4.85	0.64 ± 0.11

^a The FM/template ratio in the MNP synthesis was 1:1. The cross-linkable surfactants were a 3:2 mixture of **1b** and **2**. The titrations were performed in water at 298 K. ^b N is the average number of binding site per nanoparticle measured by ITC curve fitting. ^c Binding was extremely weak. Because the binding constant was estimated from ITC, -ΔG and N are not listed.

ITC titration curves:

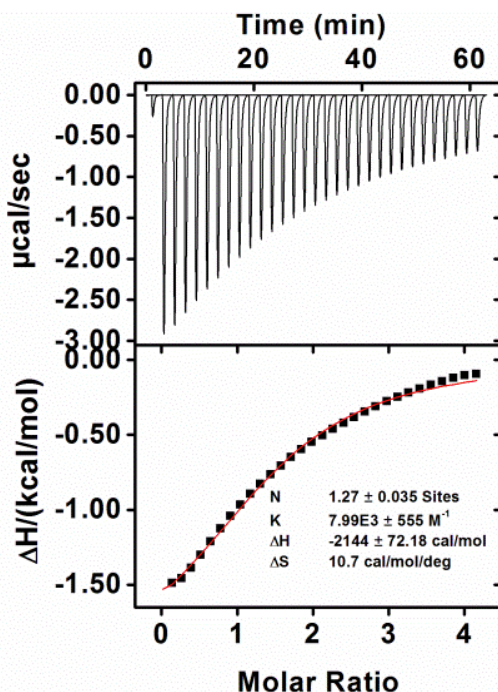


Figure S15. ITC curves obtained at 298 K from titration of MINP(*p*-G1+7h) with maltose in water. The data correspond to entry 1 in Table S1.

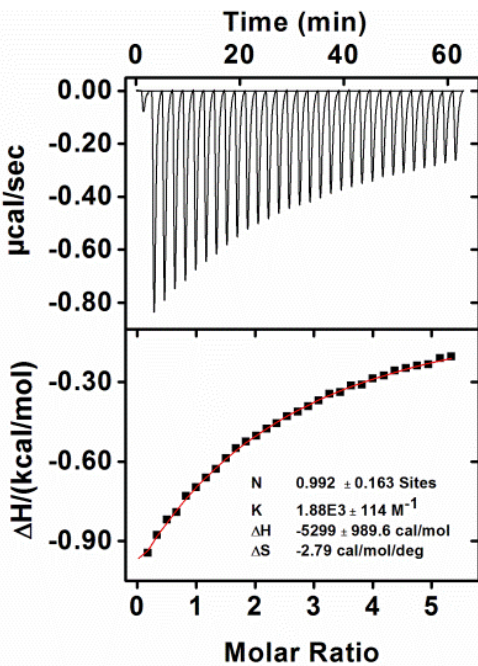


Figure S16. ITC curves obtained at 298 K from titration of MINP(*p*-G1+7h) with cellobiose in water. The data correspond to entry 2 in Table S1.

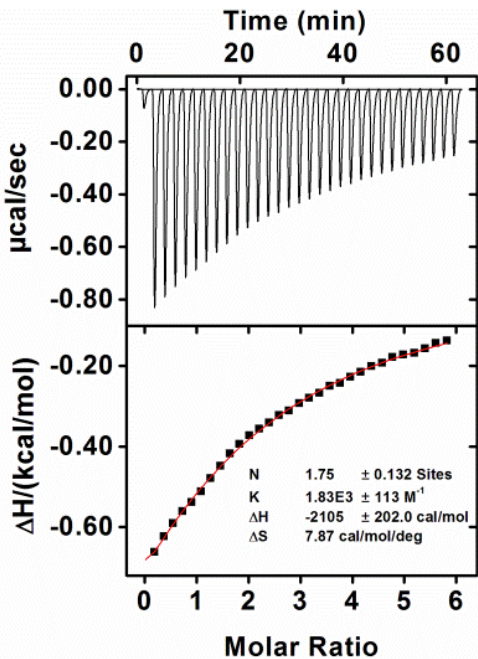


Figure S17. ITC curves obtained at 298 K from titration of MINP(*p*-G1+7h) with sucrose in water. The data correspond to entry 3 in Table S1.

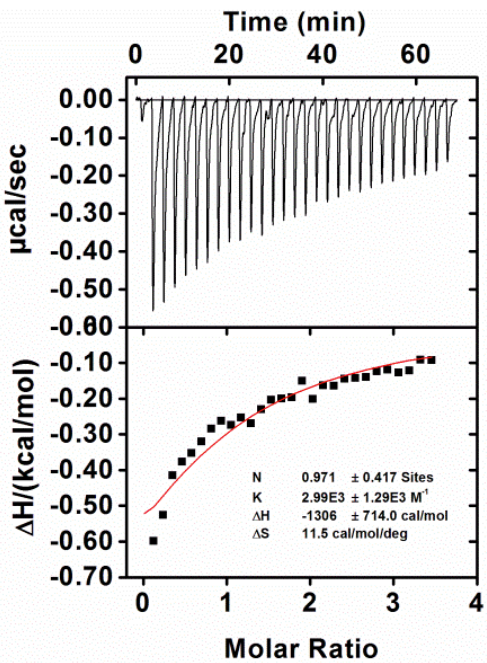


Figure S18. ITC curves obtained at 298 K from titration of MINP(*p*-G1+7h) with maltulose in water. The data correspond to entry 4 in Table S1.

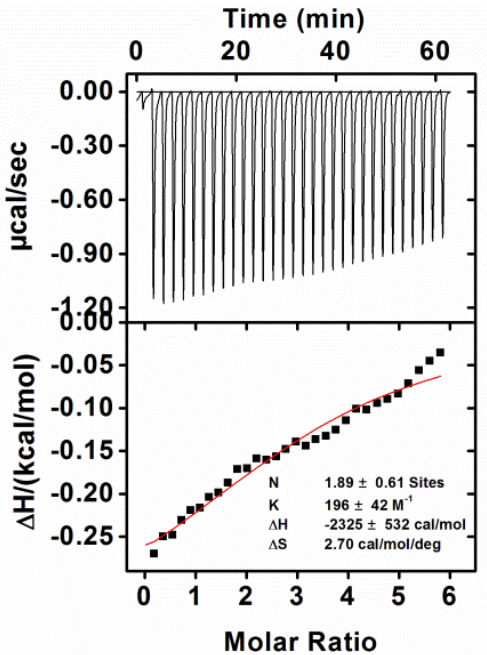


Figure S19. ITC curves obtained at 298 K from titration of MINP(*p*-G1+7h) with lactose in water. The data correspond to entry 5 in Table S1.

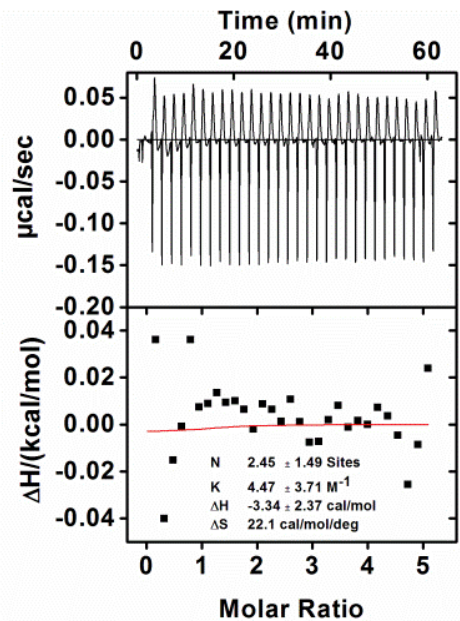


Figure S20. ITC curves obtained at 298 K from titration of MINP(*p*-G1+7h) with xylobiose in water. The data correspond to entry 6 in Table S1.

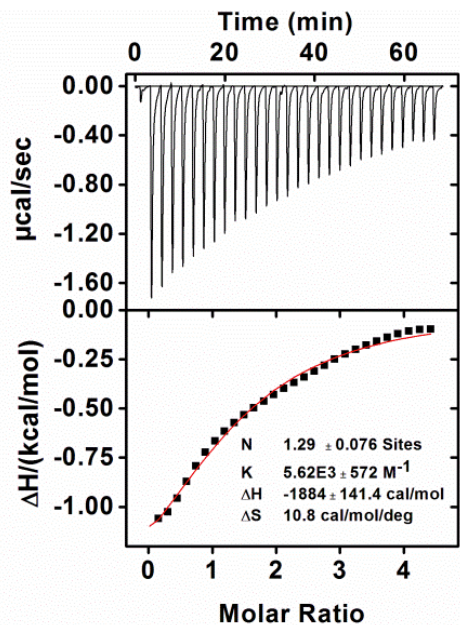


Figure S21. ITC curves obtained at 298 K from titration of MINP(*p*-G1+7h) with maltotriose in water. The data correspond to entry 7 in Table S1.

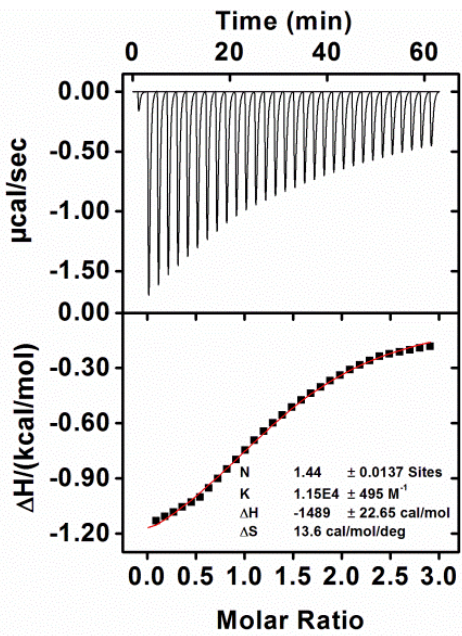


Figure S22. ITC curves obtained at 298 K from titration of MINP(*p*-G2+7h) with maltotriose in water. The data correspond to entry 8 in Table S1.

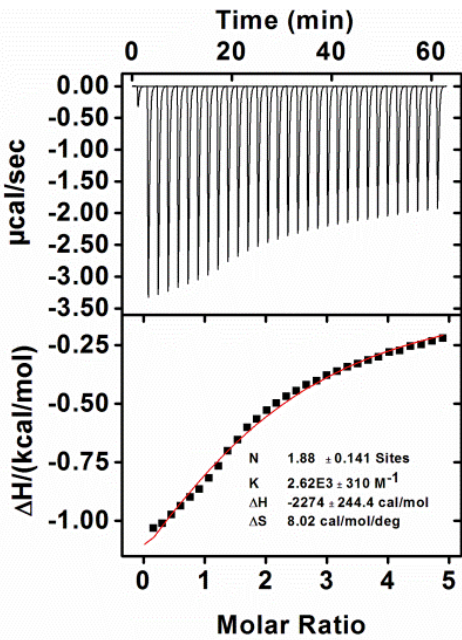


Figure S23. ITC curves obtained at 298 K from titration of MINP(*p*-G1+7h) with cellotriose in water. The data correspond to entry 9 in Table S1.

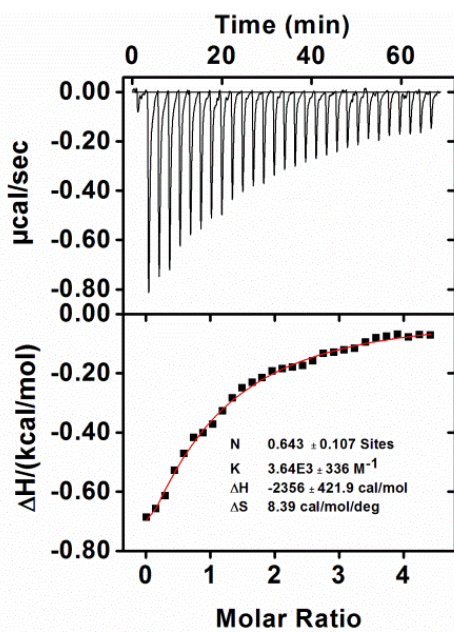


Figure S24. ITC curves obtained at 298 K from titration of MINP(*p*-G2+7h) with cellobiose in water. The data correspond to entry 10 in Table S1.

Catalytic Hydrolysis of Oligosaccharide by MINPs

Analysis of catalytic hydrolysis reactions using LC/MS

Hydrolysis of maltose and maltohexaose was monitored by LC-MS analysis using an Agilent 1200 Series Binary VWD system with an Agilent 6540 UHD Accurate Mass Q-TOF mass detector. Separation of the products was performed on a Thermo Scientific HILIC-LC column (4.6 mm, 150 mm) at 60 °C. For quantitative analysis, injection volumes were adjusted for the signal intensity to stay within the linear range of the calibration curve. All samples were centrifuged at 20,000 RPM before analysis to remove the MINP particles (to avoid column blockage over extended usage). Comparison with non-centrifuged samples showed no change in glycan concentration during the centrifugation step. The mobile phase was a mixture of acetonitrile and water, with 0.1% formic acid. Product peaks were identified by a high-resolution mass detector in the negative ion mode.

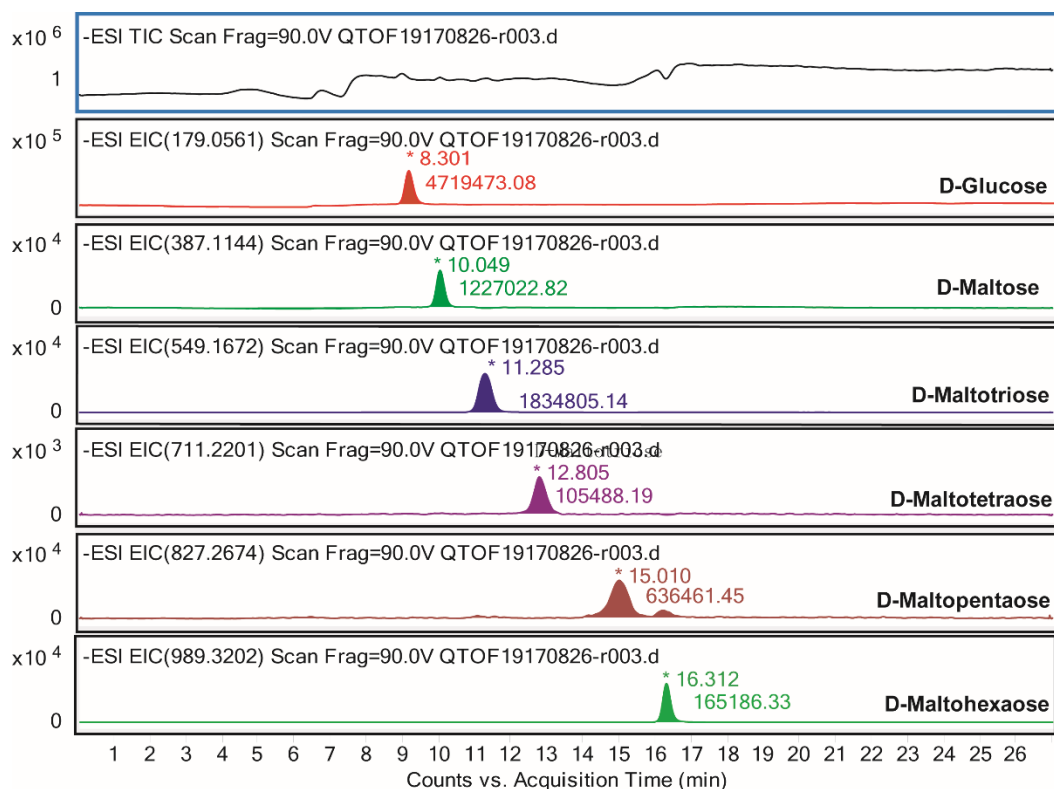


Figure S25. LC-MS analysis of a glycan mixture, with the extracted ion chromatography (EIC) spectra showing the glucose peak (red) at 8.30 min, maltose (green) at 10.05 min, maltotriose (blue) at 11.28 min, maltotetraose (purple) at 12.80 min, malopentaose (brown) at 15.01 min, and malohexaose (light green) at 16.31 min.

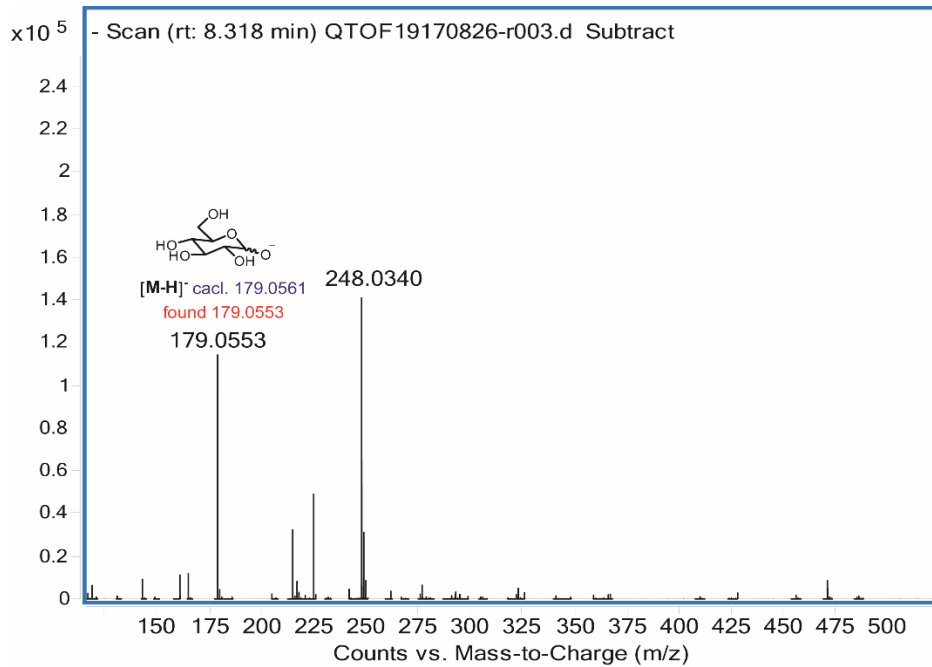


Figure S26. HR-MS spectrum of D-glucose at 8.3 min.

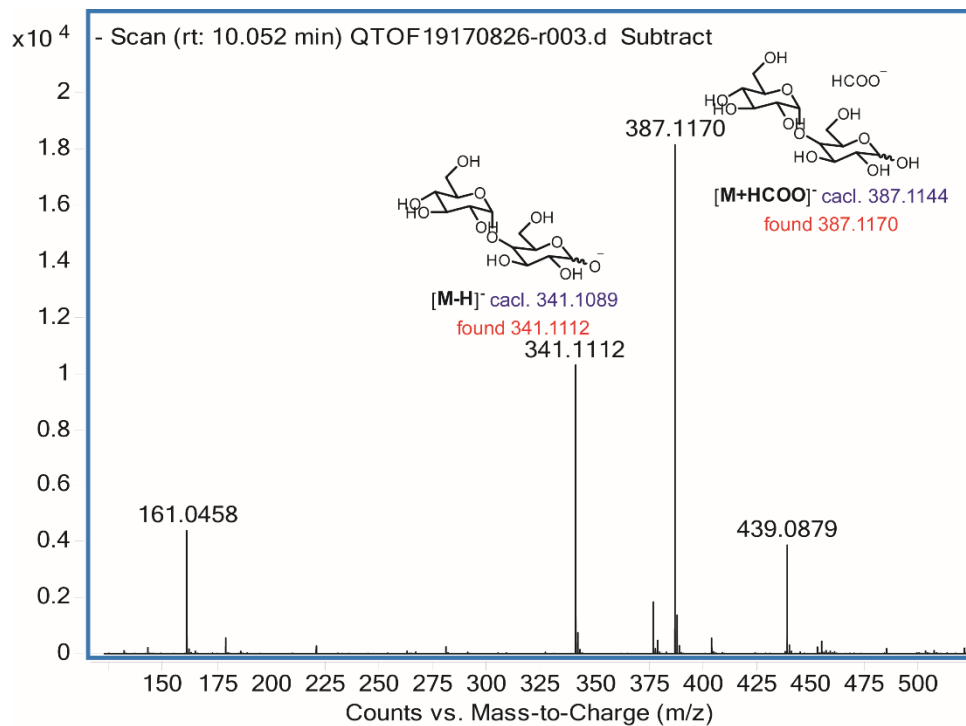


Figure S27. HR-MS spectrum of D-maltose at 10.0 min.

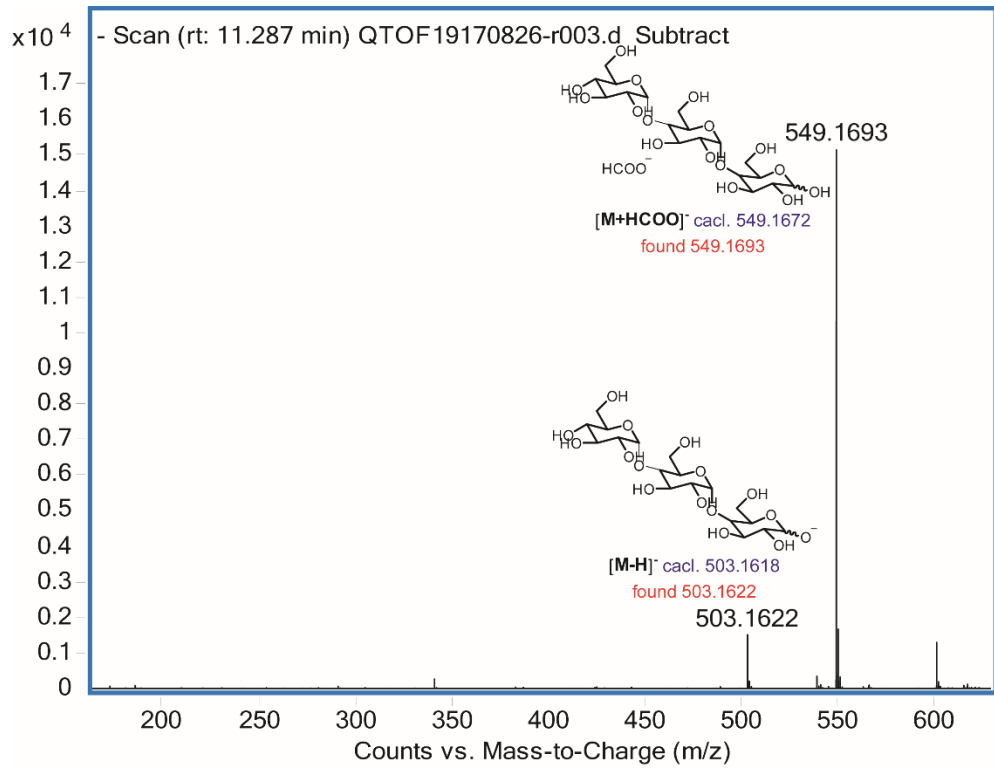


Figure S28. HR-MS spectrum of D-maltotriose at 11.3 min.

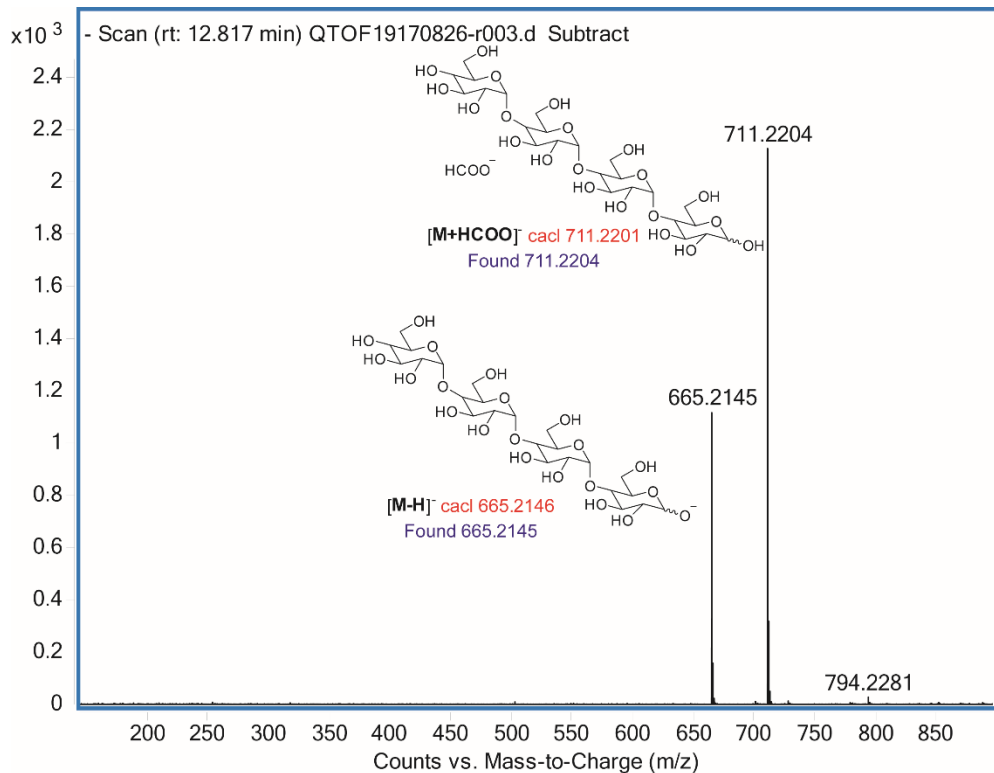


Figure S29. HR-MS spectrum of D-maltotetraose at 12.8 min.

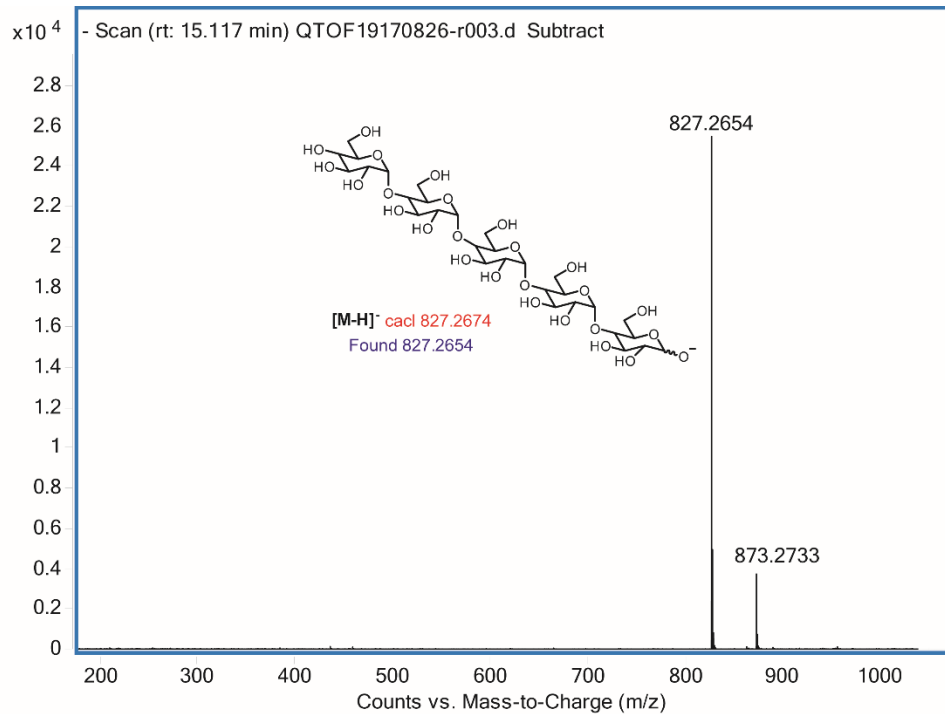


Figure S30. HR-MS spectrum of D-maltopentaose at 15.1 min.

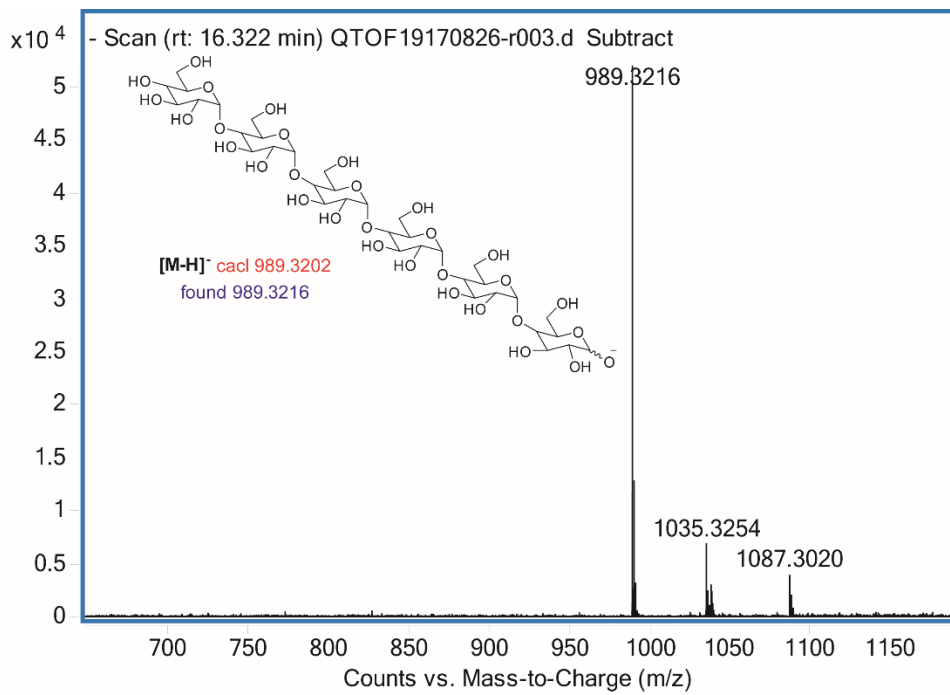


Figure S31. HR-MS spectrum of D-maltohexaose at 16.3 min.

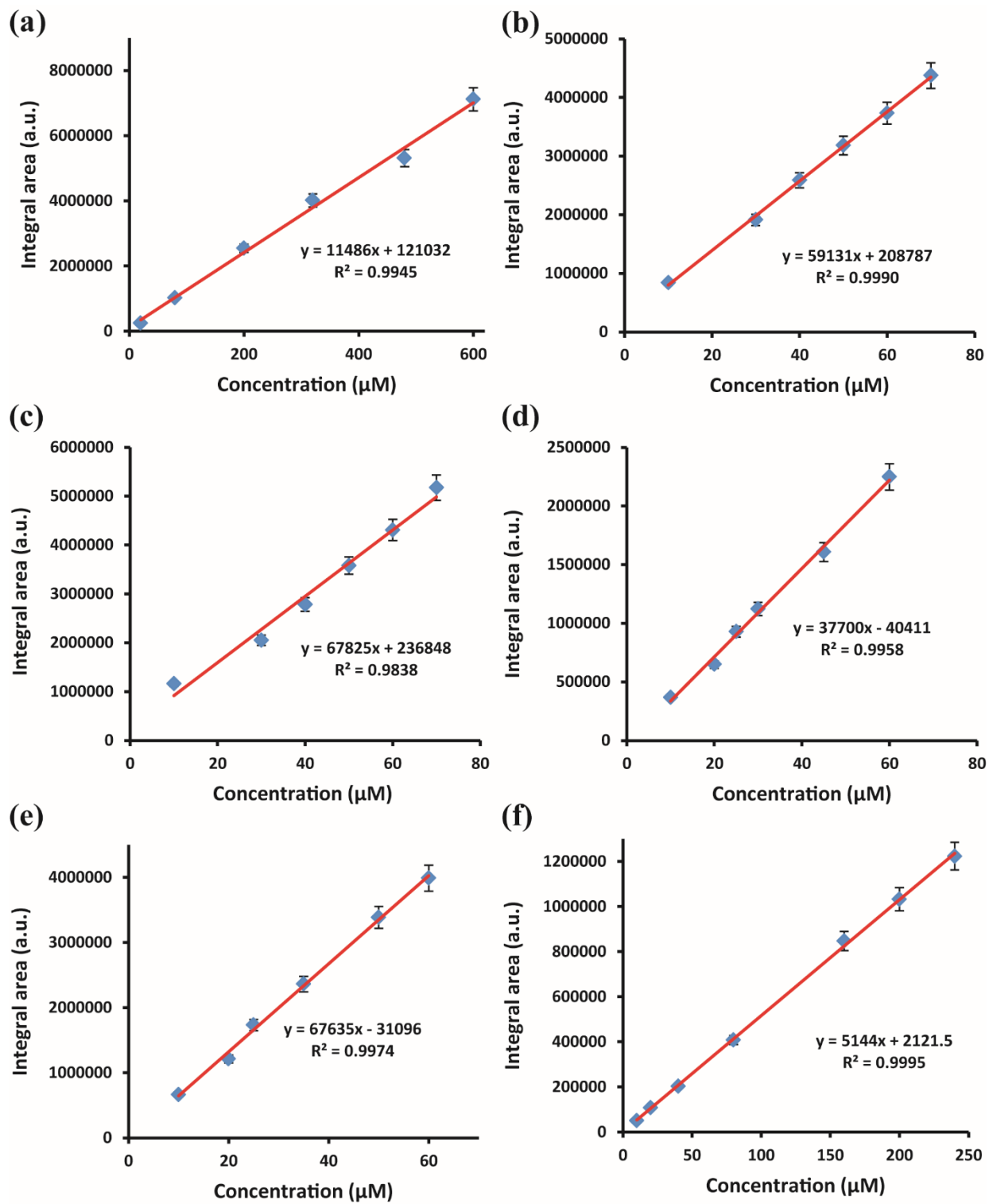


Figure S32. Calibration curves of (a) D-glucose, (b) D-maltose, (c) D-maltotriose (d) D-maltotetraose, (e) D-maltopentaose and (f) D-maltohexaose generated from LCMS analysis by using gallic acid as the internal standard.

pH Effect of Maltohexaose Hydrolysis

Table S2. Hydrolysis of maltohexaose (**G6**) catalyzed by MINPs at different pH. ^a

Entry	MINP ^c	Temp. (°C) & Time (h)	pH	Product Concentration (μM)		
				G1	G2	G3
1	MINP(<i>p</i> - G2+p-7h)	60 / 24	Water	6 ± 2	144 ± 17	7 ± 2
2	MINP(<i>p</i> - G2+p-7h)	60 / 24	7.5 ^b	n.d.	n.d.	n.d.
3	MINP(<i>p</i> - G2+p-7h)	60 / 24	7.0 ^b	trace ^d	79 ± 8	2 ± 1
4	MINP(<i>p</i> - G2+p-7h)	60 / 24	6.5 ^c	5 ± 2	122 ± 14	2 ± 1
5	MINP(<i>p</i> - G2+p-7h)	60 / 24	6.0 ^c	trace ^d	157 ± 23	7 ± 4
6	MINP(<i>p</i> - G2+p-7h)	60 / 24	5.5 ^c	13 ± 4	139 ± 16	11 ± 2

^a MINPs were prepared with surfactants **1b** and **2**. Reactions were performed in duplicates with 0.1 mM maltohexaose (**G6**) and 20 μM MINP in 1.0 mL water or buffer. Yields were determined by LC-MS using calibration curves generated from authentic samples (Figure S32). ^b HEPES buffer was used for the hydrolysis. ^c MES buffer was used for the hydrolysis. ^d The product concentration <1 μM. n.d. = not detected by MS.

Full Characterization of the Hydrolyzed Products in the Maltohexaose (G6**) Hydrolysis**

Table S3. Hydrolysis of maltohexaose (**G6**) in water catalyzed by MINPs.^a

Entry	MINP ^c	Temp. (°C)	Time (h)	Product Concentration (μM) ^b					
				G1	G2	G3	G4	G5	G6
1	MINP(<i>p</i> -G1+ <i>p</i> -7h)	60	24	253 ± 41	12 ± 4	42 ± 8	trace ^b	trace ^b	57 ± 11
2	MINP(<i>p</i> -G1+ <i>p</i> -7h)	90	48	421 ± 78	17 ± 6	24 ± 5	trace ^b	10 ± 3	32 ± 7
3	MINP(<i>p</i> -G2+ <i>p</i> -7h)	60	24	11 ± 4	117 ± 21	14 ± 3	11 ± 2	trace ^b	62 ± 12
4	MINP(<i>p</i> -G2+ <i>p</i> -7h)	90	48	15 ± 4	158 ± 28	13 ± 4	21 ± 4	trace	47 ± 10
5	MINP(<i>p</i> -G3+ <i>p</i> -7h)	60	24	14 ± 6	17 ± 5	98 ± 17	trace ^b	trace ^b	53 ± 11
6	MINP(<i>p</i> -G3+ <i>p</i> -7h)	90	48	21 ± 7	14 ± 4	133 ± 24	trace ^b	trace ^b	34 ± 8

^a MINPs were prepared with surfactants **1b** and **2**. Reactions were performed in duplicates at 0.1 mM maltohexaose (**G6**) and 20 μM MINP in 1.0 mL water. Yields were determined by LC-MS using calibration curves generated from authentic samples (Figure S32). Typically, estimated errors of product concentration were ± 20%. ^b The product concentration <1 μM.

Table S4. Hydrolysis of maltohexaose (**G6**) in MES buffer (pH = 6.0) catalyzed by MINPs.^a

Entry	MINP ^c	Temp. (°C)	Time (h)	Product Concentration (μM) ^b					
				G1	G2	G3	G4	G5	G6
1	MINP(<i>p</i> -G1+ <i>p</i> -7h)	60	24	271 ± 45	25 ± 11	24 ± 8	10 ± 4	14 ± 3	49 ± 11
2	MINP(<i>p</i> -G1+ <i>p</i> -7h)	90	48	462 ± 82	17 ± 4	29 ± 9	14 ± 4	10 ± 4	25 ± 7
3	MINP(<i>p</i> -G1+ <i>p</i> -7h)	90	96	518 ± 91	trace ^b	14 ± 4	trace ^b	7 ± 4	13 ± 4
4	MINP(<i>p</i> -G2+ <i>p</i> -7h)	60	24	trace ^b	157 ± 23	7 ± 4	31 ± 11	trace ^b	55 ± 14
5	MINP(<i>p</i> -G2+ <i>p</i> -7h)	90	48	trace ^b	245 ± 34	12 ± 4	18 ± 4	trace ^b	21 ± 9
6	MINP(<i>p</i> -G3+ <i>p</i> -7h)	60	24	14 ± 5	17 ± 4	98 ± 31	trace ^b	trace ^b	48 ± 16
7	MINP(<i>p</i> -G3+ <i>p</i> -7h)	90	48	35 ± 8	45 ± 10	175 ± 24	trace ^b	trace ^b	13 ± 7

^a MINPs were prepared with surfactants **1b** and **2**. Reactions were performed in duplicates at 0.1 mM maltohexaose (**G6**) and 20 μM MINP in 1.0 mL buffer. Yields were determined by LC-MS using calibration curves generated from authentic samples (Figure S32). Typically, estimated errors of product concentration were ± 20%. ^b The product concentration <1 μM.

Table S5. Hydrolysis of maltohexaose (**G6**) in water catalyzed by MINPs.^a

Entry	MINP ^c	Dialysis tubing	Product Concentration (μM) ^b					
			G1	G2	G3	G4	G5	G6
1	MINP(<i>p</i> - G1 + <i>p</i> - 7h)	No	253±41	12±4	42±8	trace ^c	trace ^c	57±11
2	MINP(<i>p</i> - G1+<i>p</i>-7h)	Yes	521±38	14±6	21±5	n.d. ^b	6±2	7±2
3	MINP(<i>p</i> - G2+<i>p</i>-7h)	No	11±4	117±21	14±3	11±2	trace ^c	62±12
4	MINP(<i>p</i> - G2+<i>p</i>-7h)	Yes	n.d. ^b	268±31	n.d. ^b	8±2	n.d. ^b	5±1
5	MINP(<i>p</i> - G3+<i>p</i>-7h)	No	14±6	17±5	98±17	trace ^c	trace ^c	53±11
6	MINP(<i>p</i> - G3+<i>p</i>-7h)	Yes	26±12	24±9	144±17	n.d. ^b	n.d. ^b	19±8

^a MINPs were prepared with surfactants **1b** and **2**. Reactions were performed in duplicates at 0.1 mM maltohexaose (**G6**) and 20 μM MINP in 1.0 mL water at 60 °C for 24 h. Yields were determined by LC-MS using calibration curves generated from authentic samples (Figure S32). ^b n.d. = not detected. ^c Trace is the oligosaccharide concentration was <1 μM.

Michaelis–Menten Kinetics

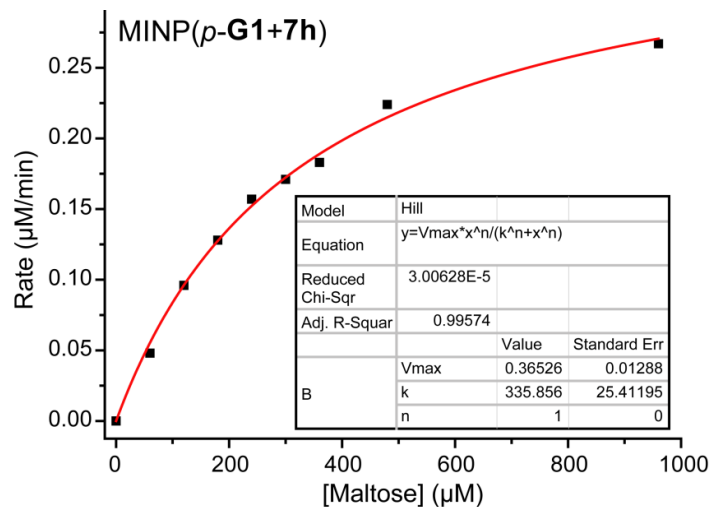


Figure S33. Michaelis–Menten plots of maltose hydrolysis catalyzed by MINP(*p*-G1+7h) at 60 °C in H₂O. The data corresponds to entry 1 in Table 4.

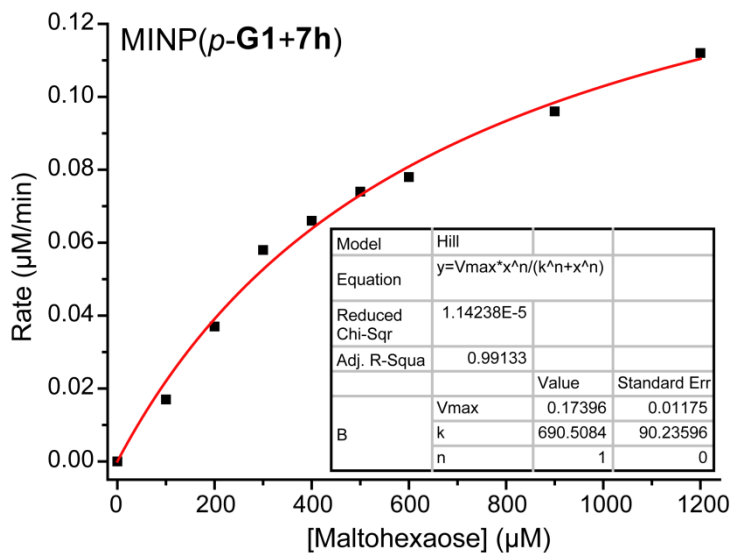


Figure S34. Michaelis–Menten plots of maltohexaose hydrolysis catalyzed by MINP(*p*-G1+7h) at 60 °C in H₂O. The data corresponds to entry 2 in Table 4.

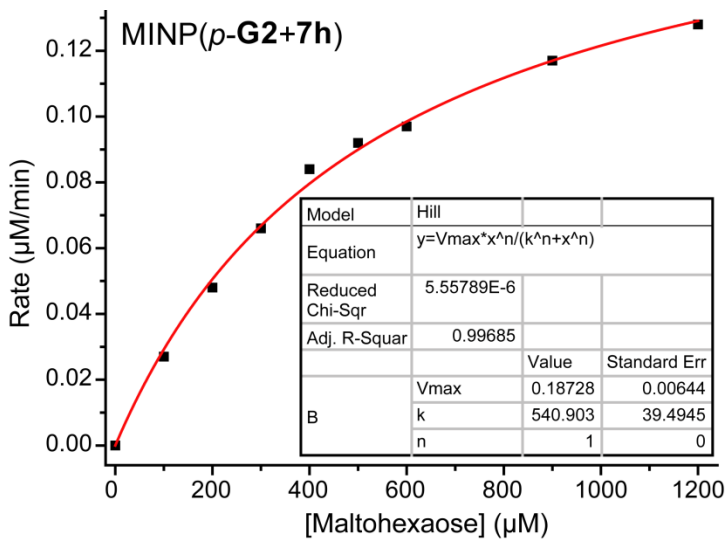


Figure S35. Michaelis–Menten plots of maltohexaose hydrolysis catalyzed by MINP(*p*-G2+7h) at 60 °C in H₂O. The data corresponds to entry 3 in Table 4.

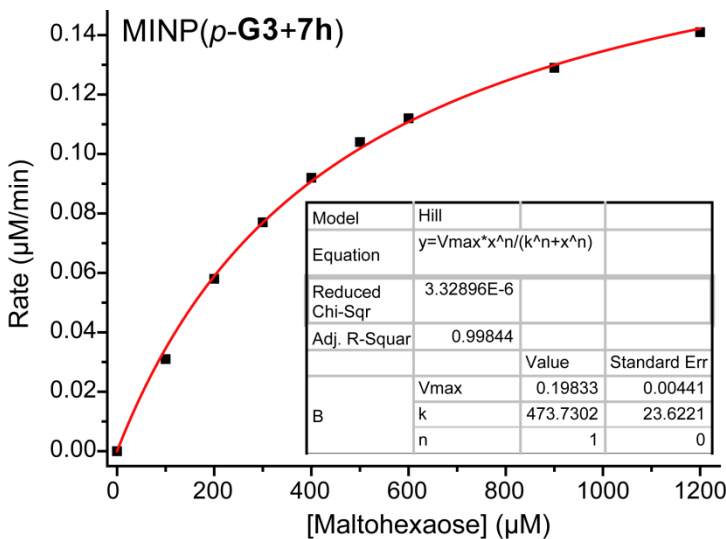


Figure S36. Michaelis–Menten plots of maltohexaose hydrolysis catalyzed by MINP(*p*-G3+7h) at 60 °C in H₂O. The data corresponds to entry 4 in Table 4.

Product Inhibition Study

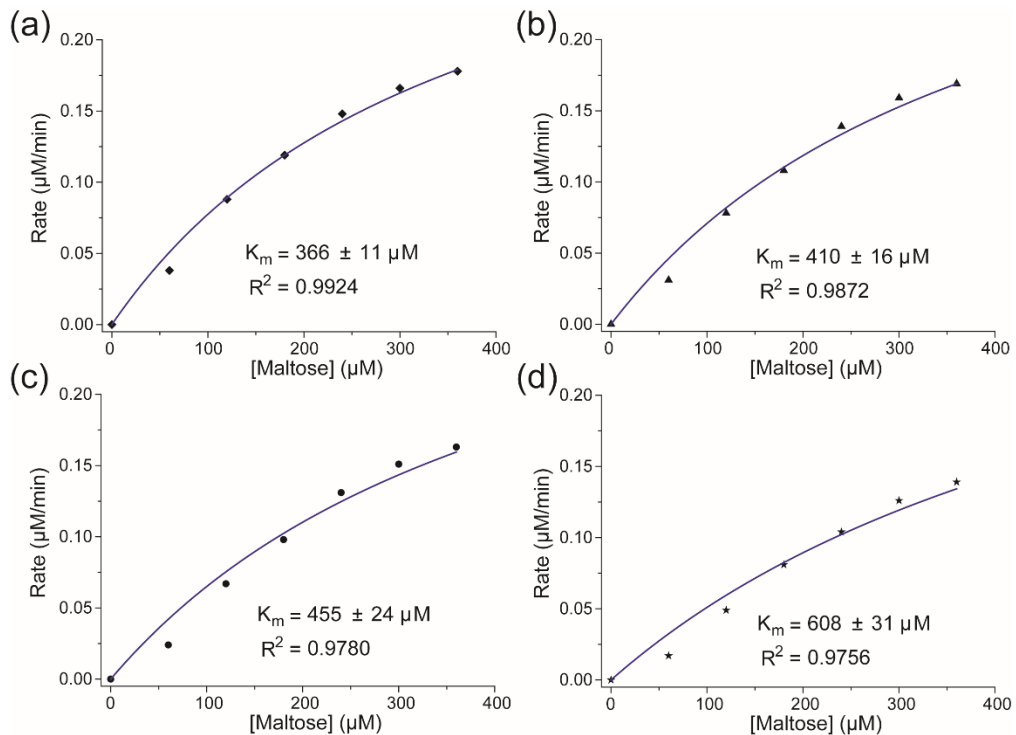


Figure S37. Michaelis–Menten curves for MINP(*p*-G1+7h) (20 μM) in maltose hydrolysis in the presence of (a) 20 μM , (b) 40 μM , (c) 80 μM , and (d) 160 μM glucose at 60 $^\circ\text{C}$ in H_2O .

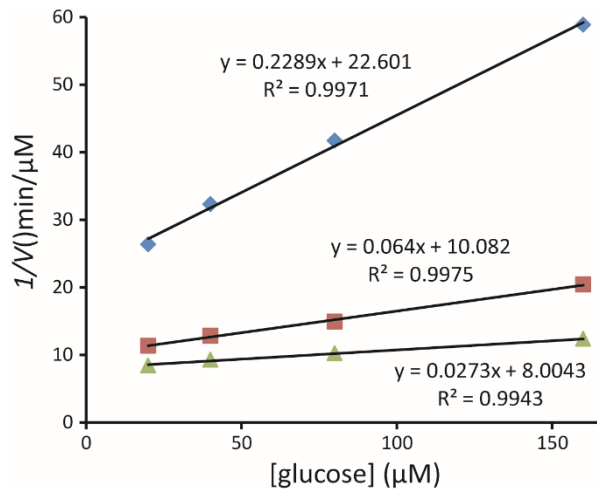


Figure S38. The linear curve fitting of $1/V$ against [glucose] in MINP(*p*-G1+7h)-catalyzed maltose hydrolysis in the presence of 20–160 μM glucose at 60 $^\circ\text{C}$ in H_2O . The average K_i is calculated to be 68.30 μM .

Substrate Selectivity Study of MINP Catalysts

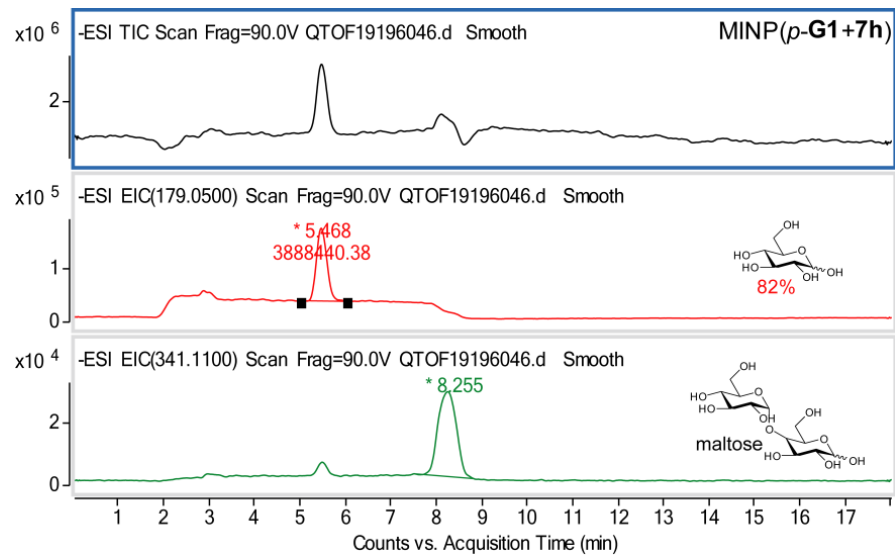


Figure S39. LC-MS analysis of maltose hydrolysis catalyzed by MINP(*p*-G1+7h) at 60 °C in water for 24 h. TIC, total ion chromatography. EIC, extracted ion chromatography. The concentration of product was calculated by using glucose calibration curve (Figure S32) generated from authentic samples.

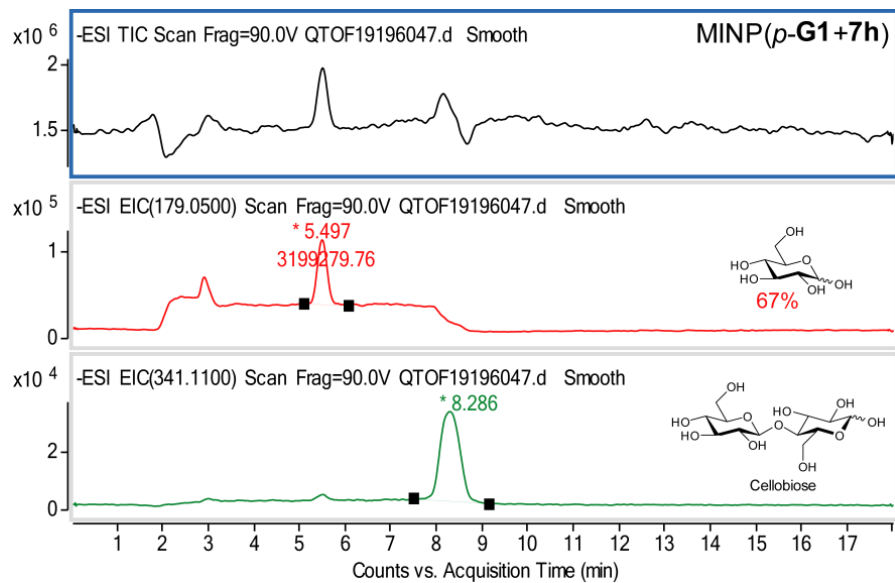


Figure S40. LC-MS analysis of cellobiose hydrolysis catalyzed by MINP(*p*-G1+7h) at 60 °C in water for 24 h. TIC, total ion chromatography. EIC, extracted ion chromatography. The concentration of product was calculated by using glucose calibration curve (Figure S32) generated from authentic samples.

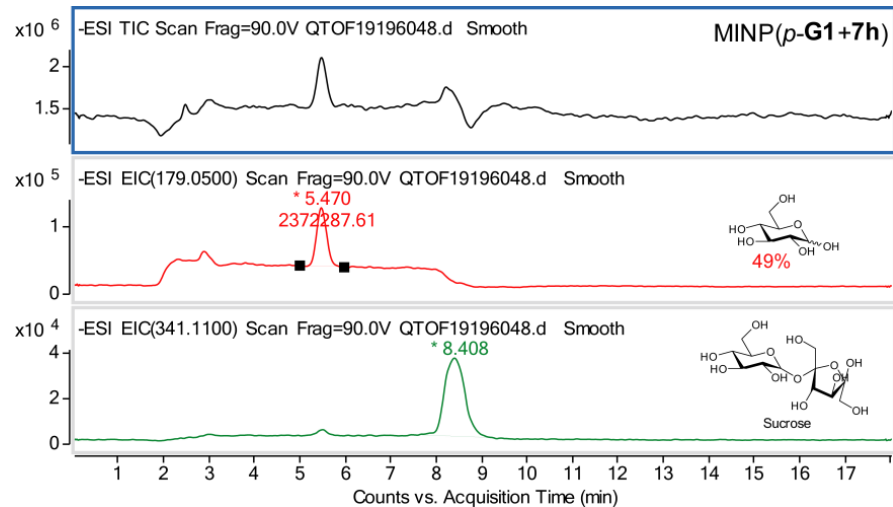


Figure S41. LC-MS analysis of sucrose hydrolysis catalyzed by MINP(*p*-G1+7h) at 60 °C in water for 24 h. TIC, total ion chromatography. EIC, extracted ion chromatography. The concentration of product was calculated by using glucose calibration curve (Figure S32) generated from authentic samples.

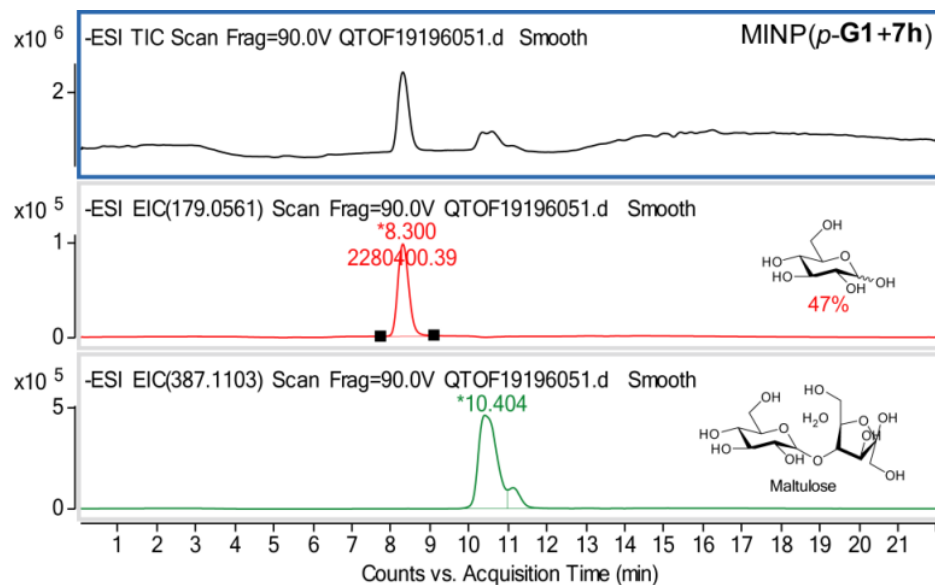


Figure S42. LC-MS analysis of maltulose hydrolysis catalyzed by MINP(*p*-G1+7h) at 60 °C in water for 24 h. TIC, total ion chromatography. EIC, extracted ion chromatography. The concentration of product was calculated by using glucose calibration curve (Figure S32) generated from authentic samples.

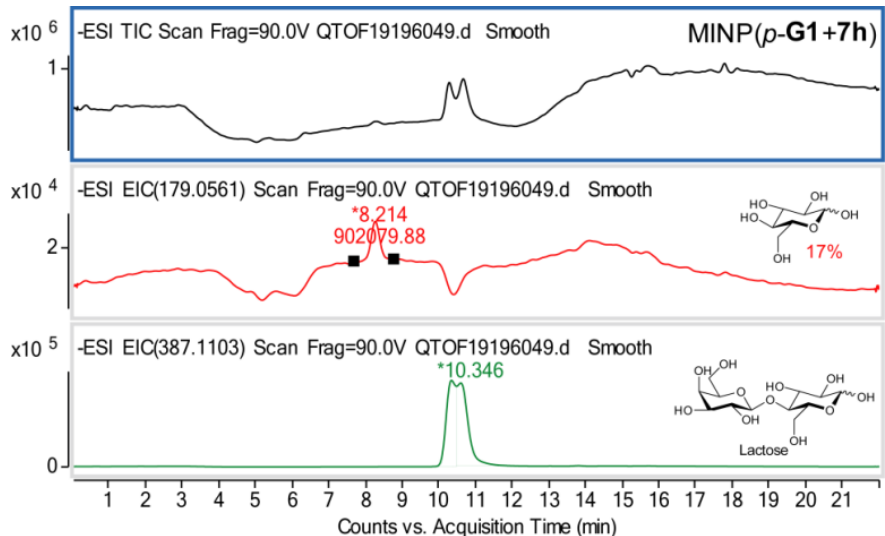


Figure S43. LC-MS analysis of lactose hydrolysis catalyzed by MINP(*p*-G1+7h) at 60 °C in water for 24 h. TIC, total ion chromatography. EIC, extracted ion chromatography. The concentration of product was calculated by using glucose calibration curve (Figure S32) generated from authentic samples.

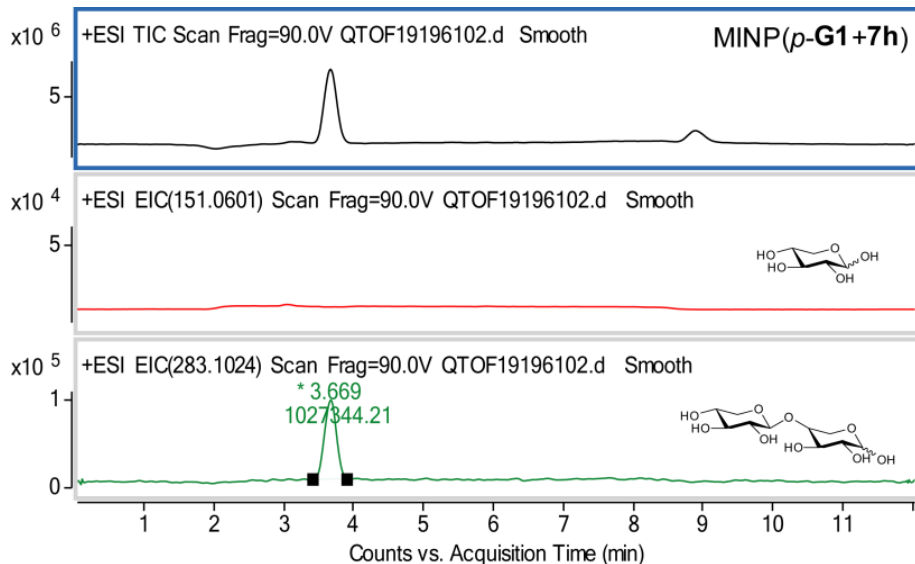


Figure S44. LC-MS analysis of xylobiose hydrolysis catalyzed by MINP(*p*-G1+7h) at 60 °C in water for 24 h. TIC, total ion chromatography. EIC, extracted ion chromatography. Product could not be detected.

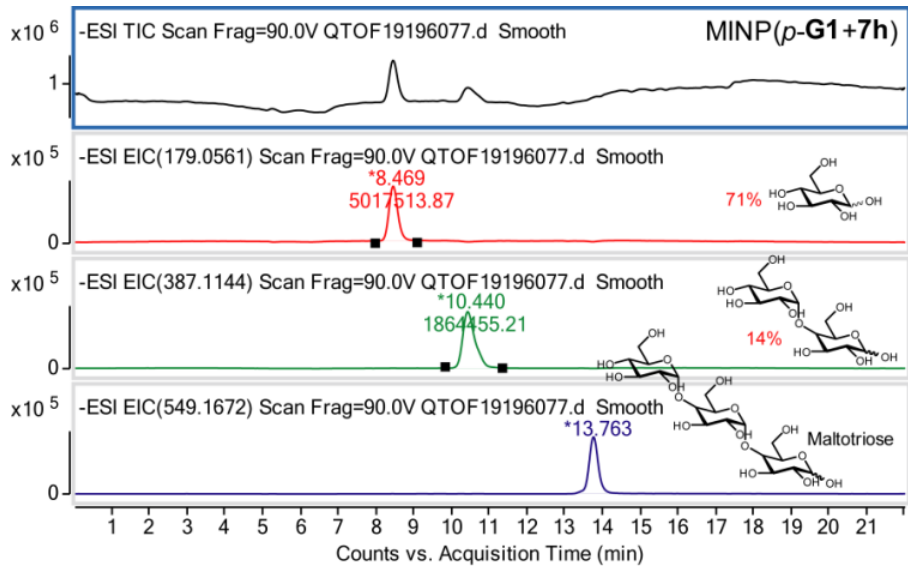


Figure S45. LC-MS analysis of maltotriose hydrolysis catalyzed by MINP(*p*-G1+7h) at 60 °C in water for 24 h. TIC, total ion chromatography. EIC, extracted ion chromatography. The concentration of product was calculated by using glucose calibration curve (Figure S32) generated from authentic samples.

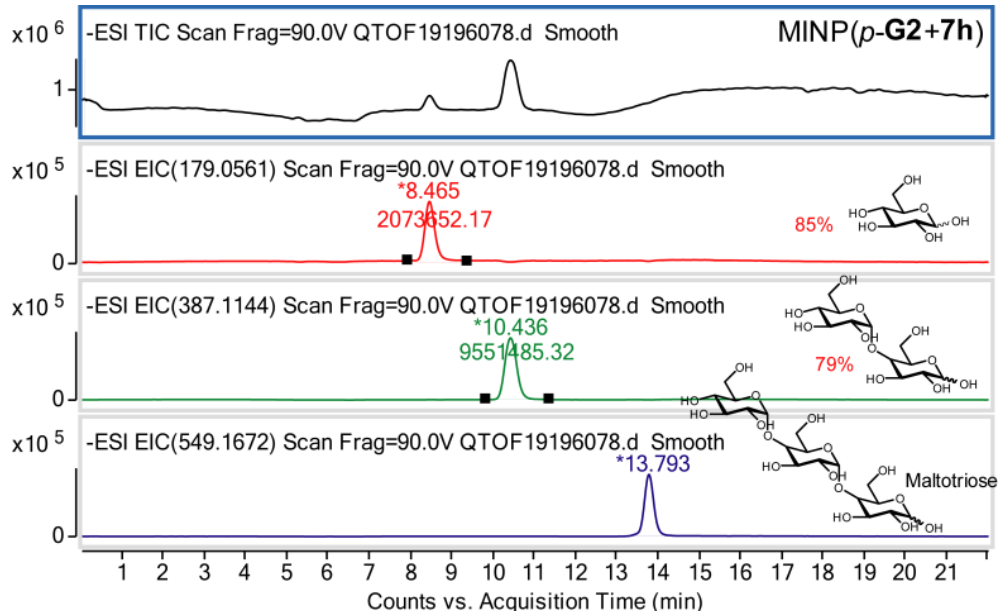


Figure S46. LC-MS analysis of maltotriose hydrolysis catalyzed by MINP(*p*-G2+7h) at 60 °C in water for 24 h. TIC, total ion chromatography. EIC, extracted ion chromatography. The concentration of product was calculated by using glucose calibration curve (Figure S32) generated from authentic samples.

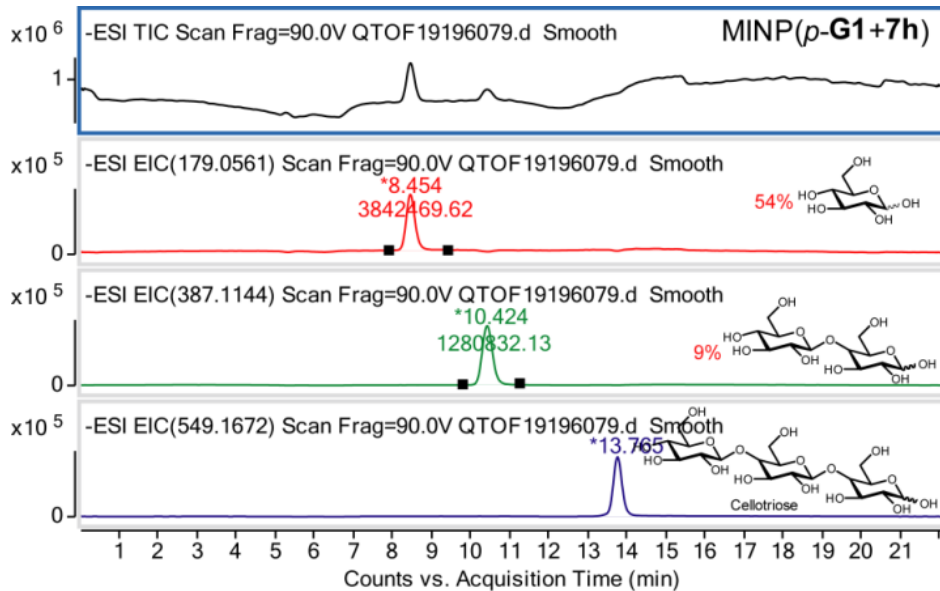


Figure S47. LC-MS analysis of cellobiose hydrolysis catalyzed by MINP(*p*-G1+7h) at 60 °C in water for 24 h. TIC, total ion chromatography. EIC, extracted ion chromatography. The concentration of product was calculated by using glucose calibration curve (Figure S32) generated from authentic samples.

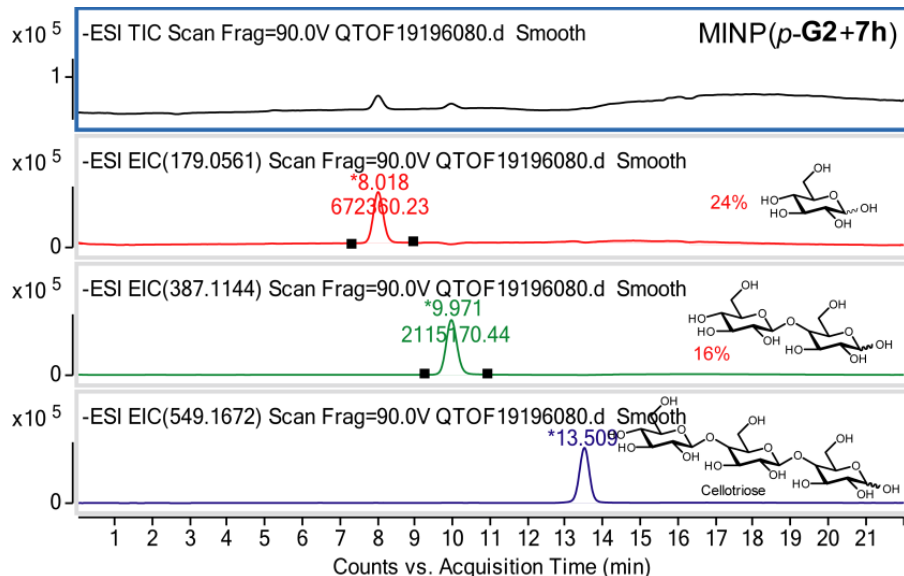
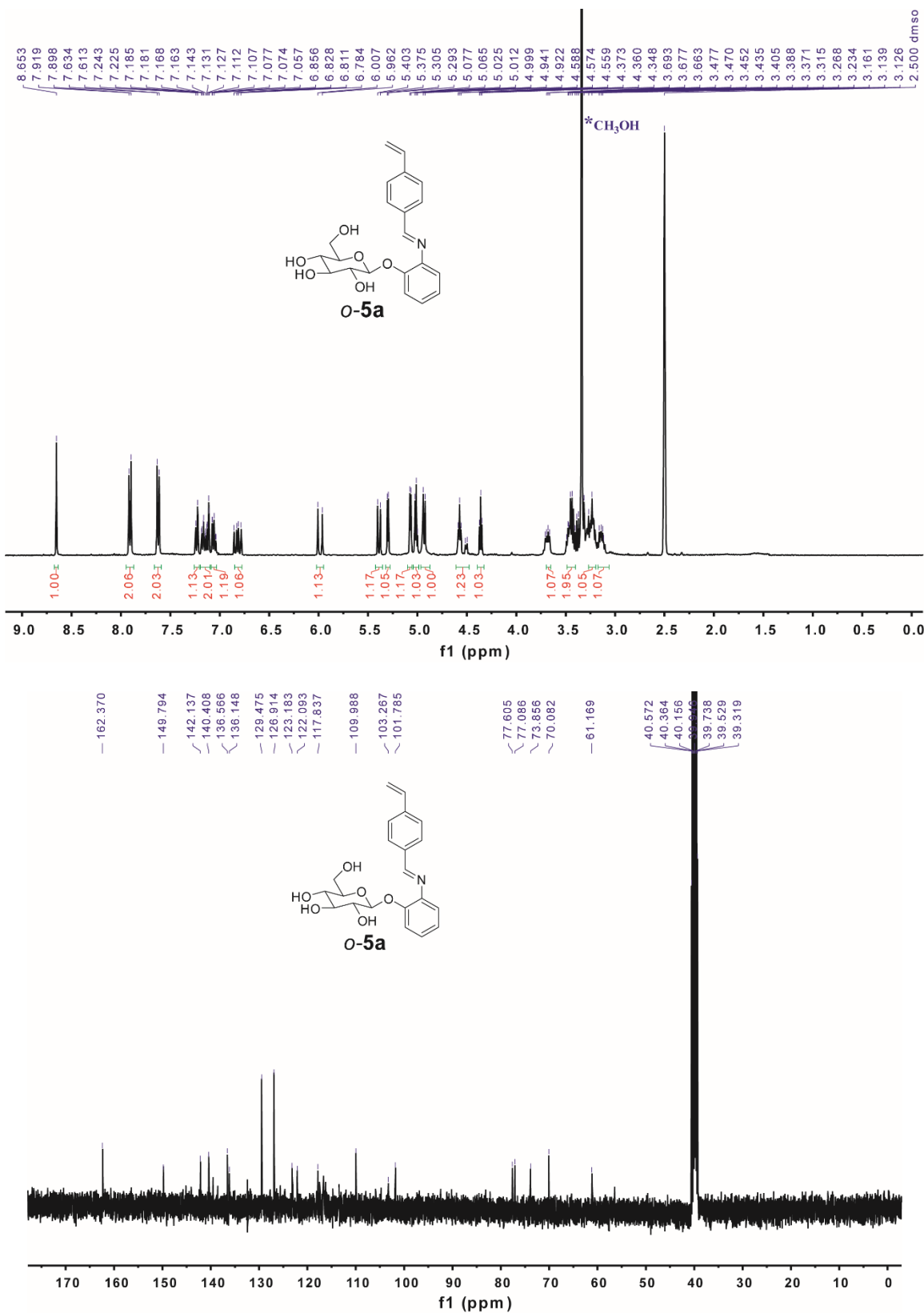
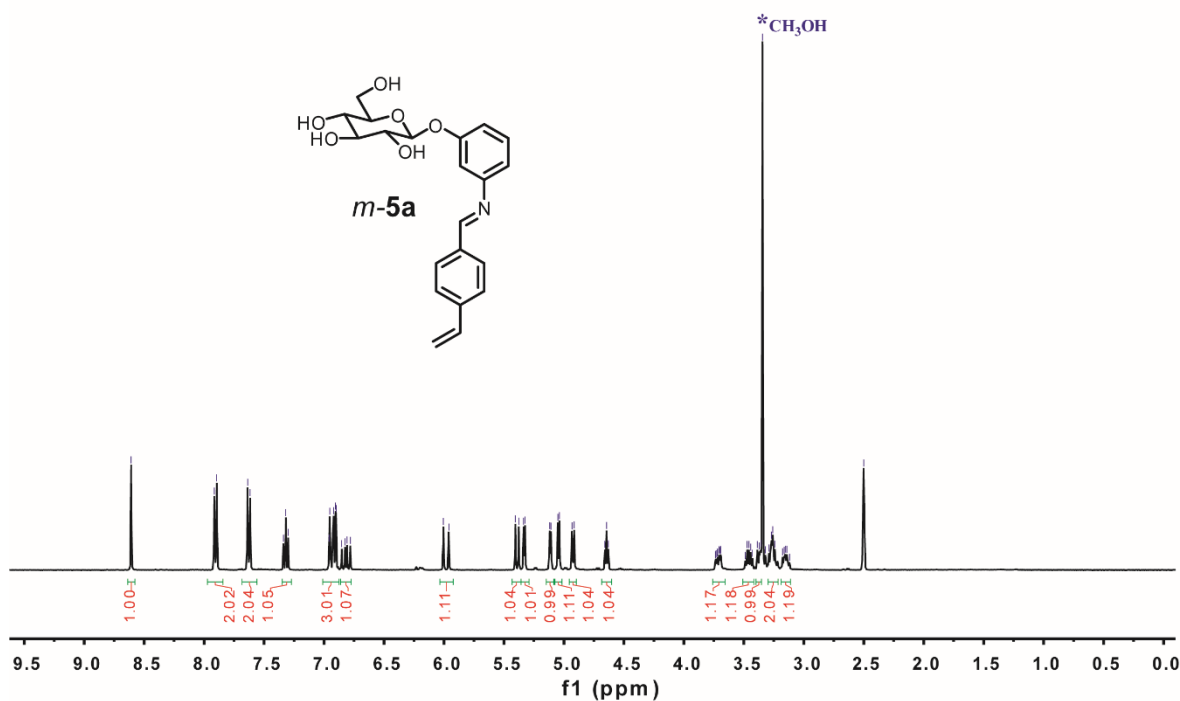
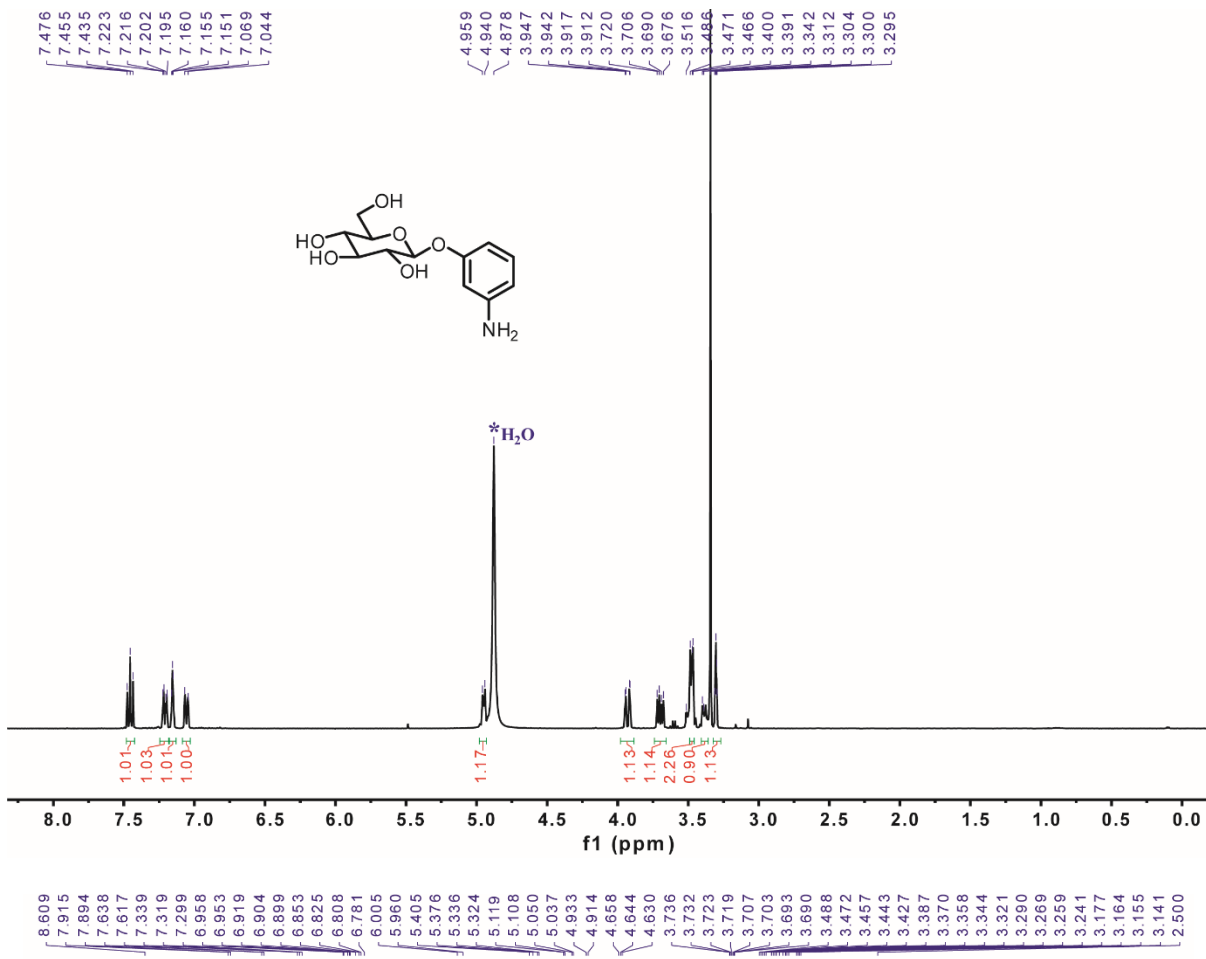
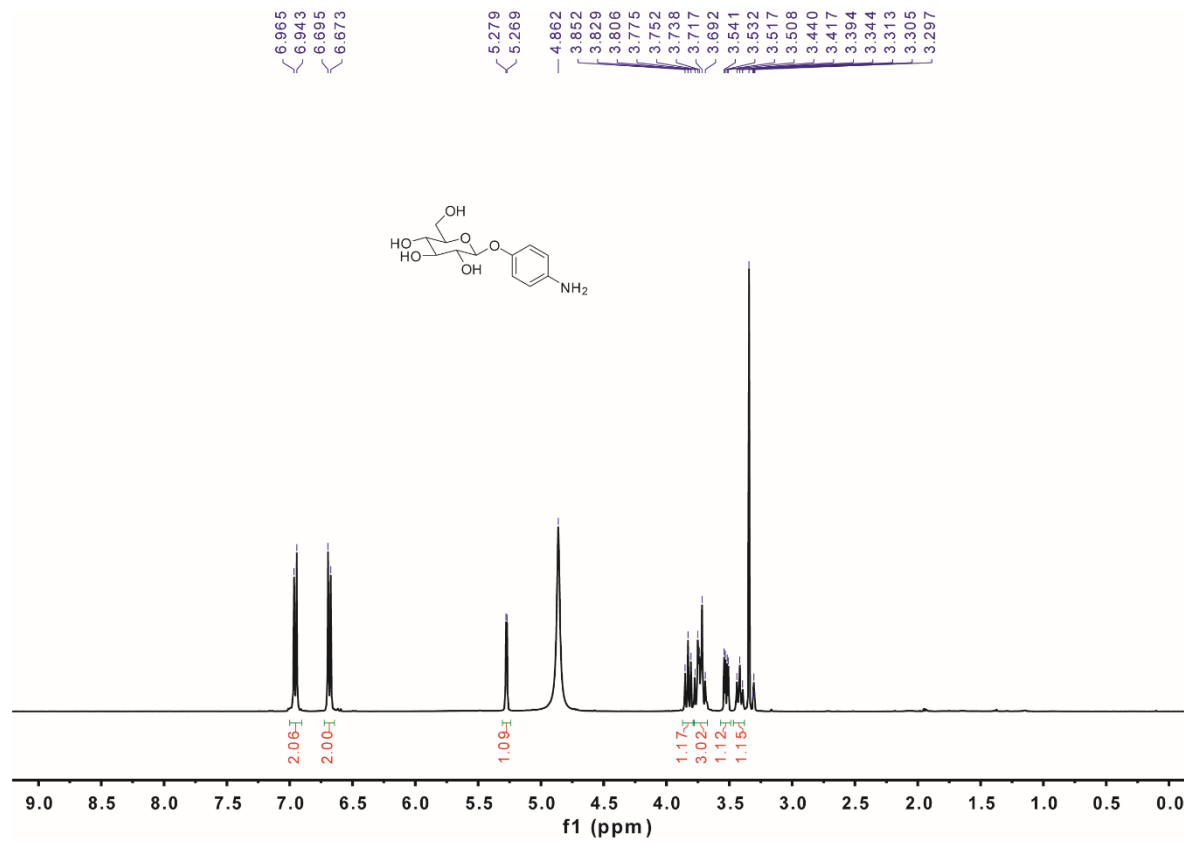
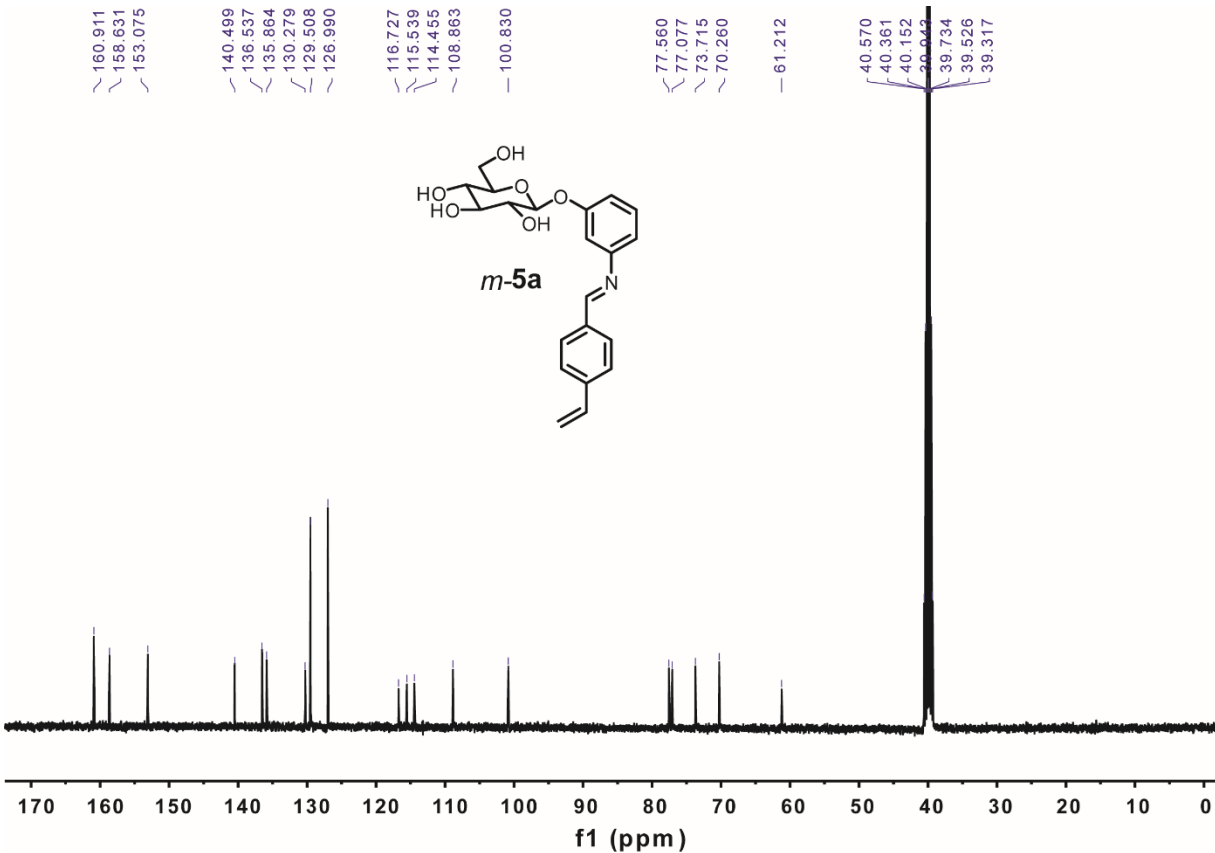


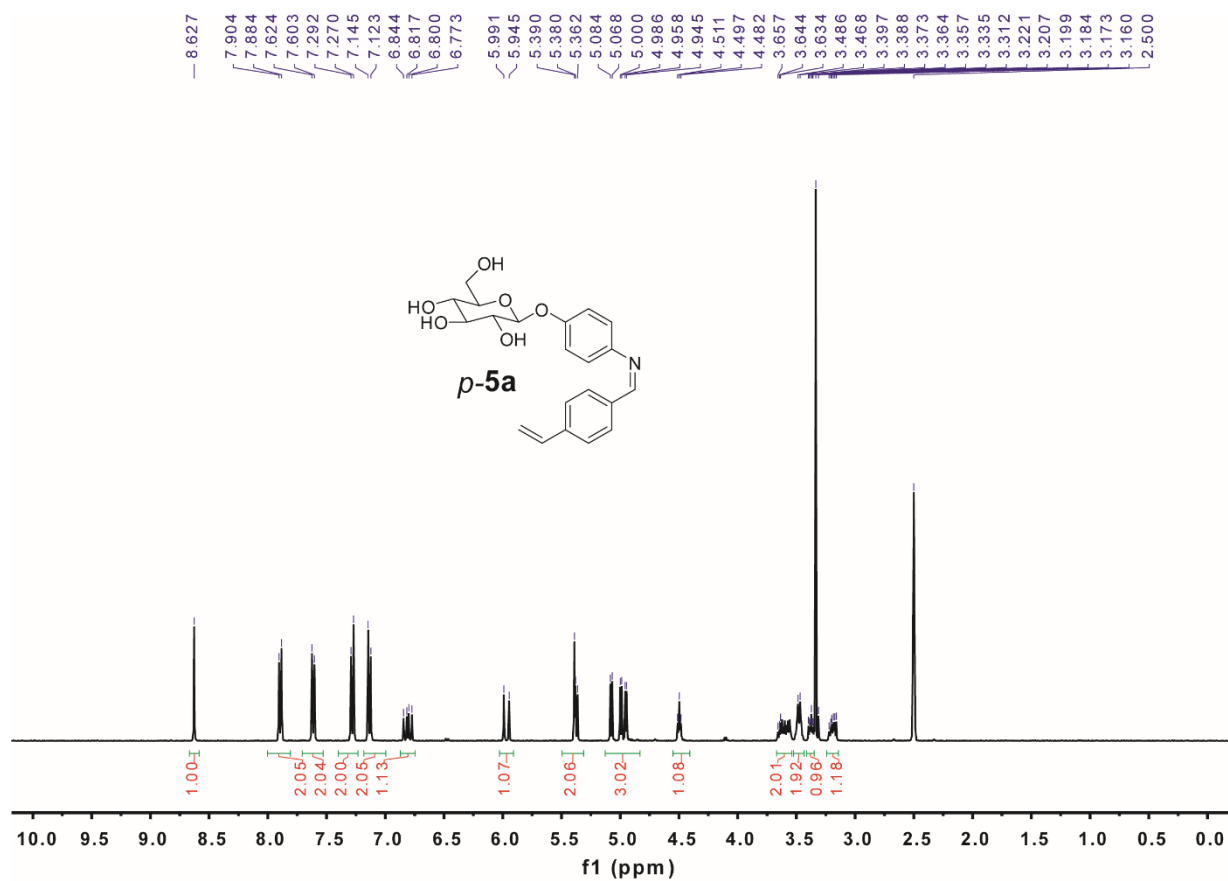
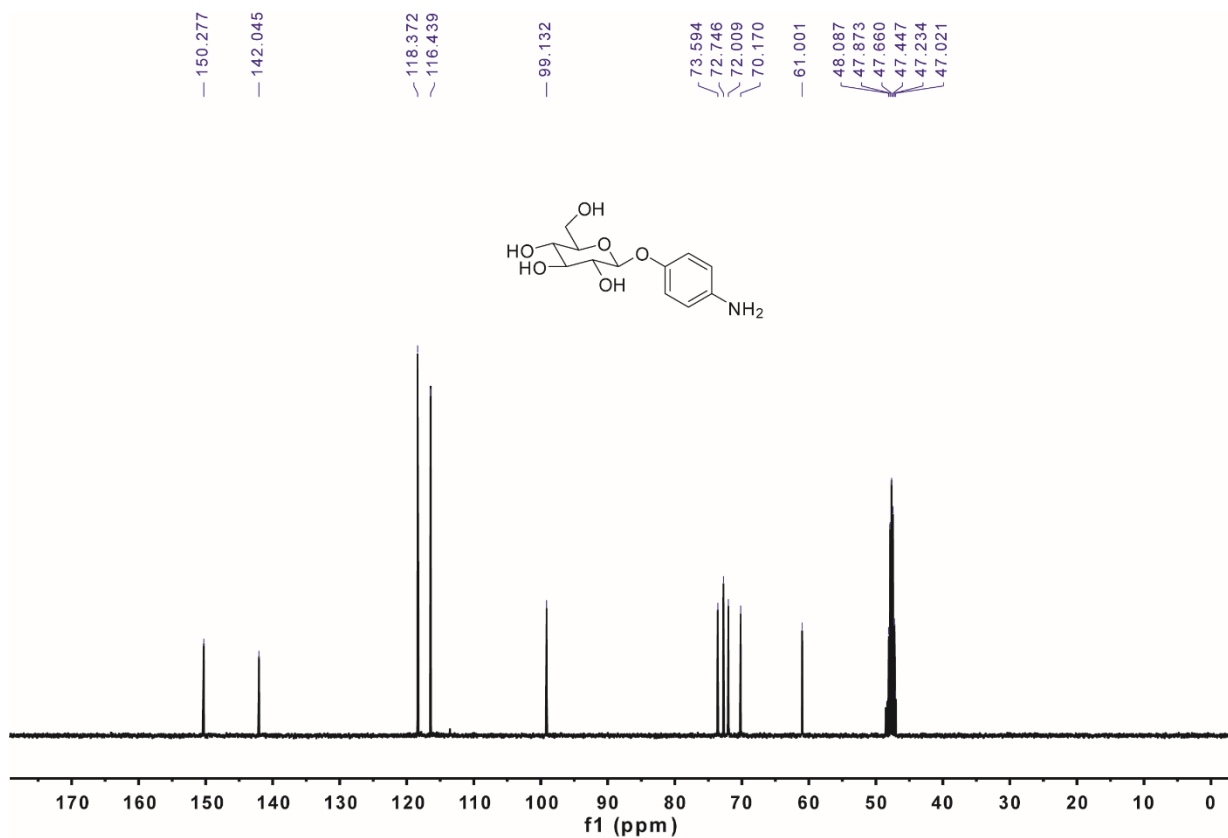
Figure S48. LC-MS analysis of cellobiose hydrolysis catalyzed by MINP(*p*-G2+7h) at 60 °C in water for 24 h. TIC, total ion chromatography. EIC, extracted ion chromatography. The concentration of product was calculated by using glucose calibration curve (Figure S32) generated from authentic samples.

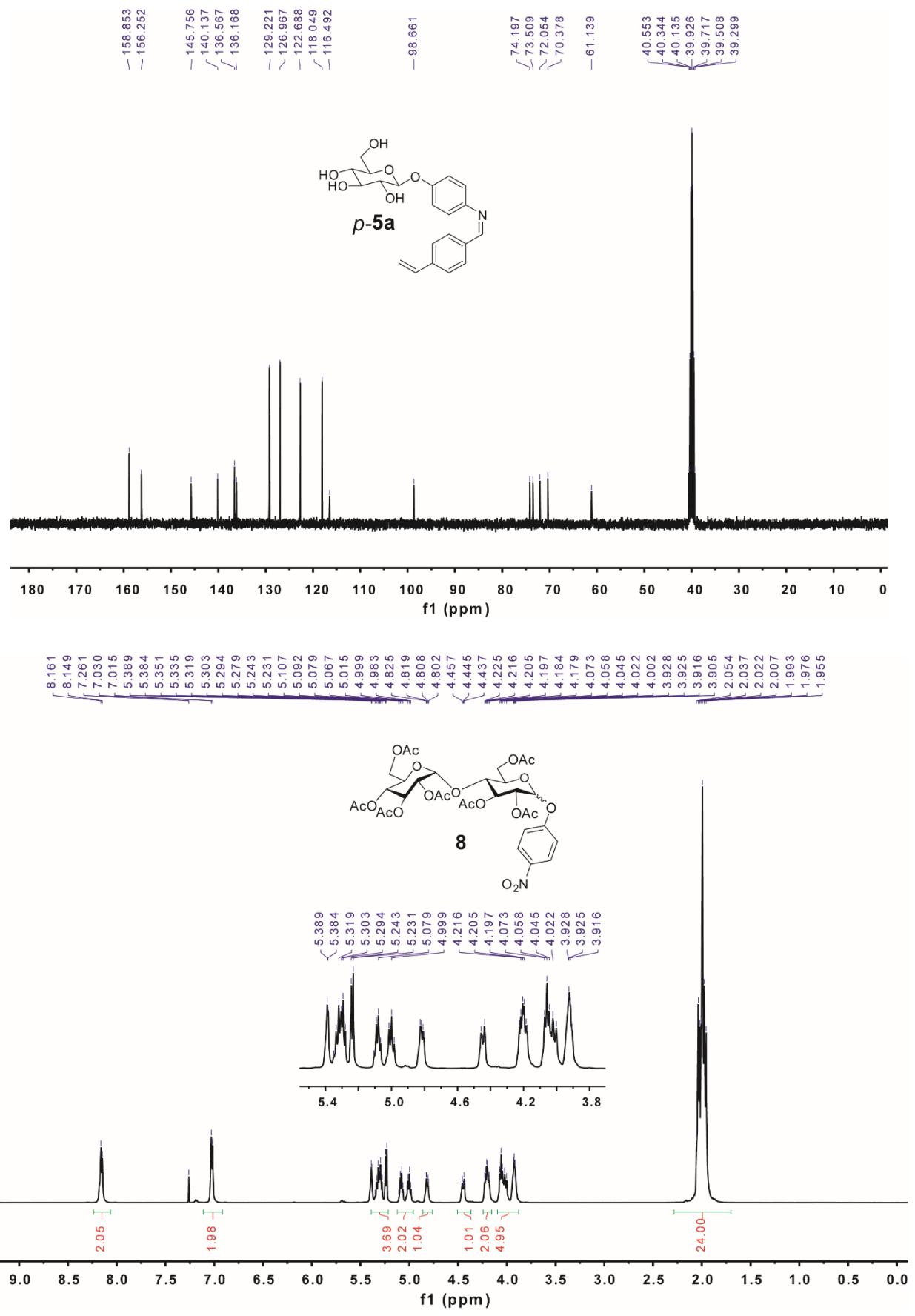
¹H & ¹³C NMR Spectra

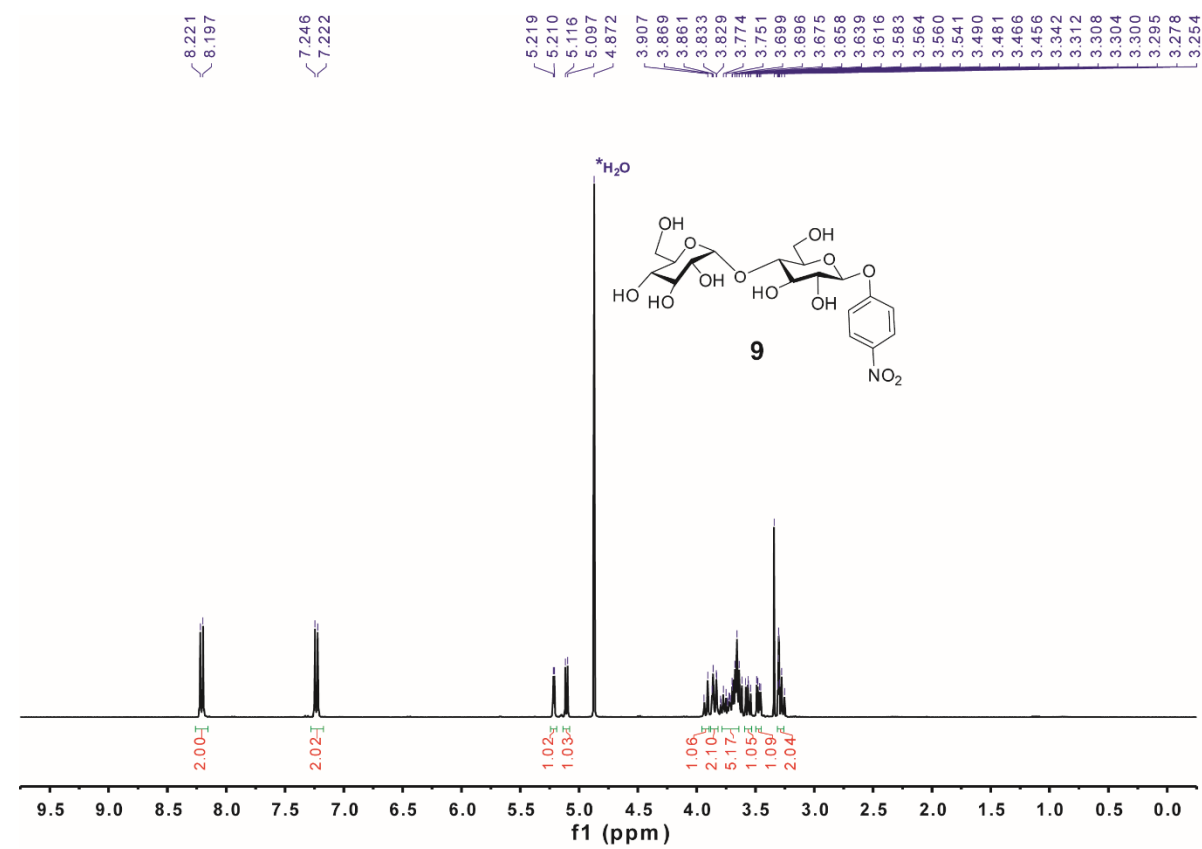
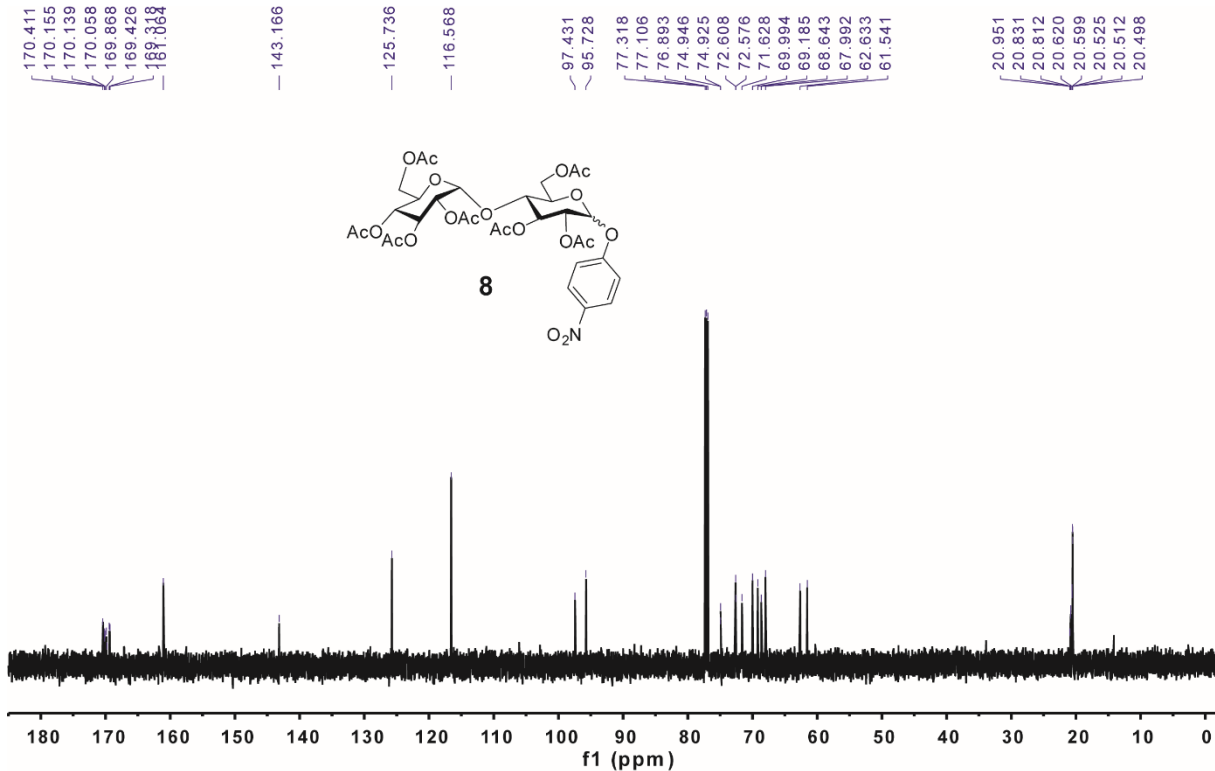


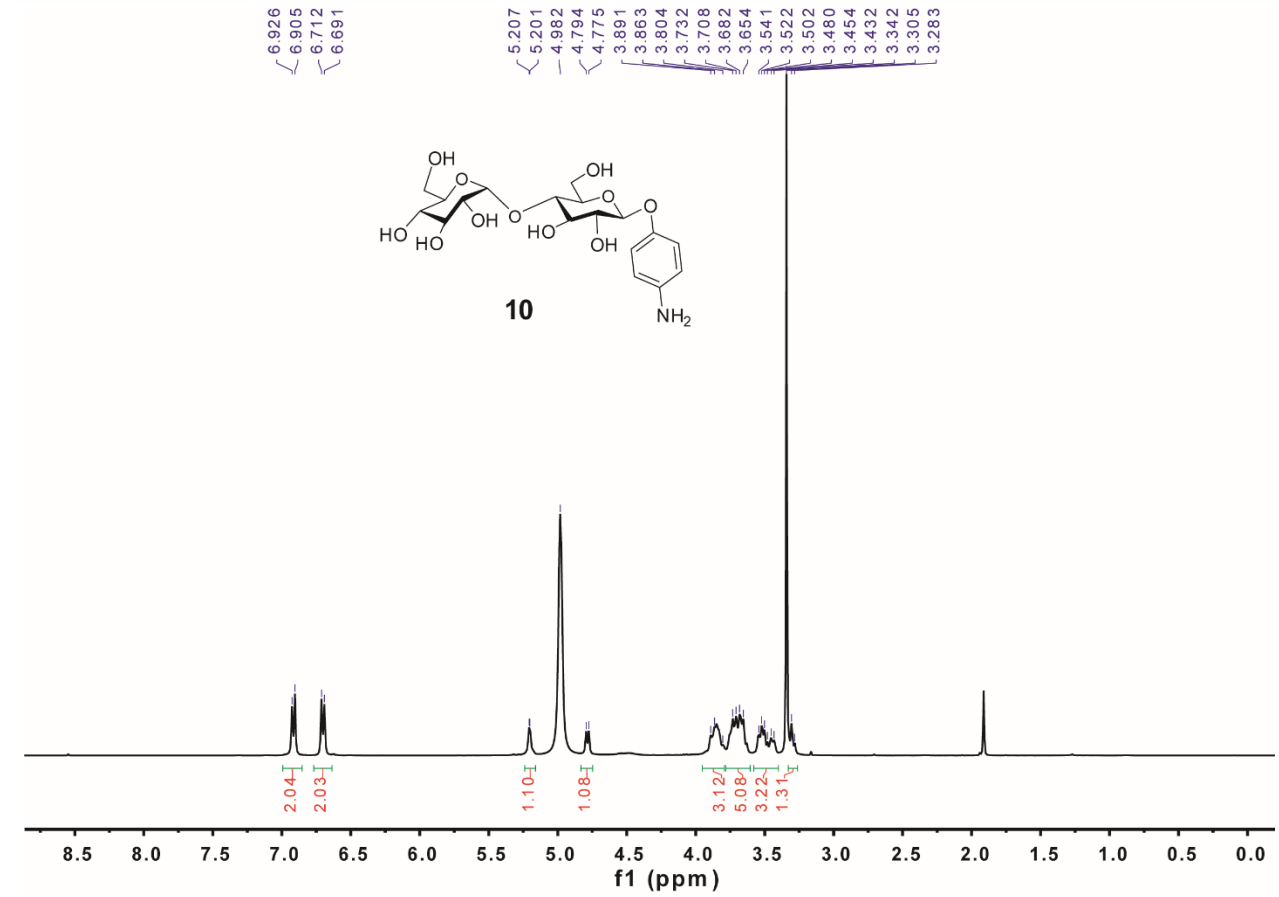
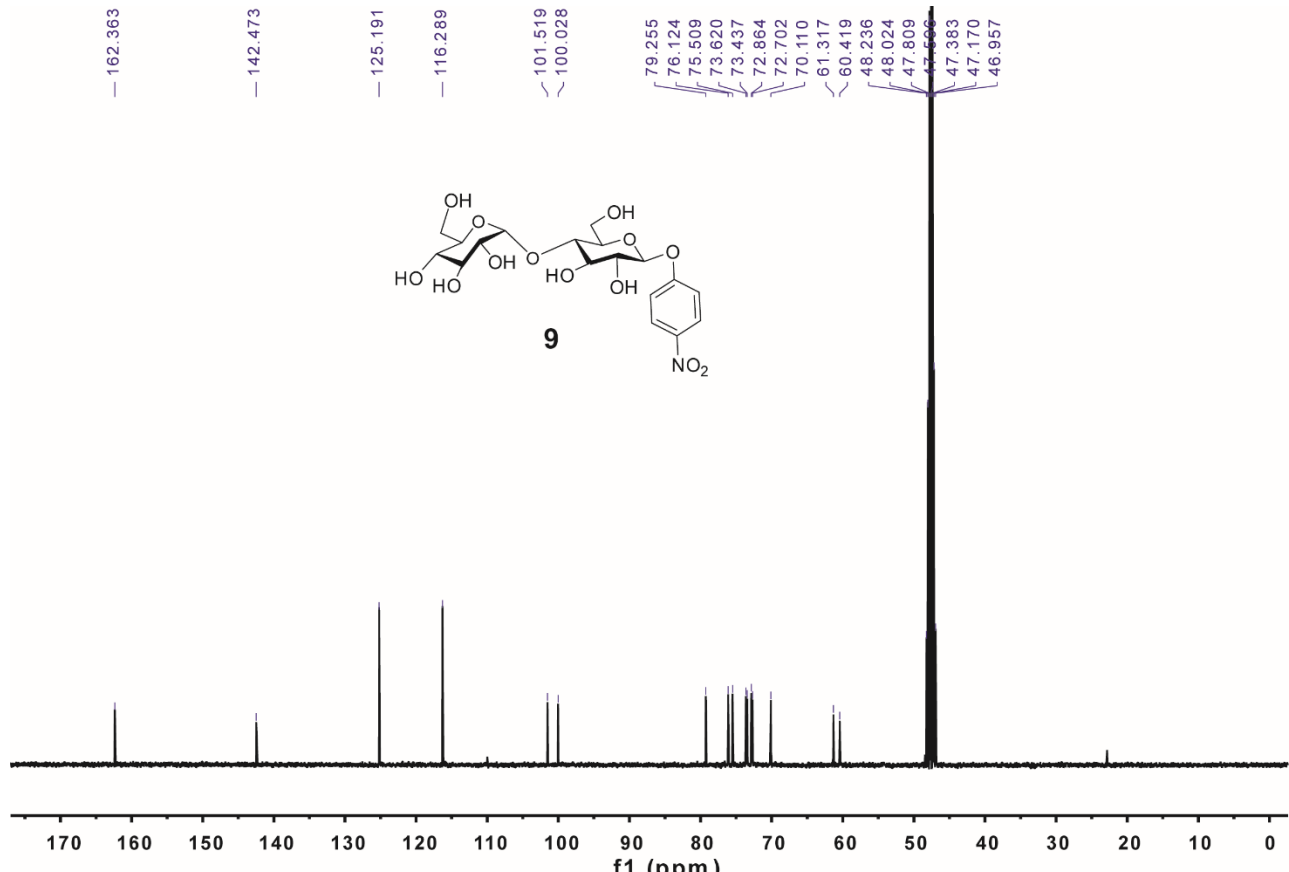


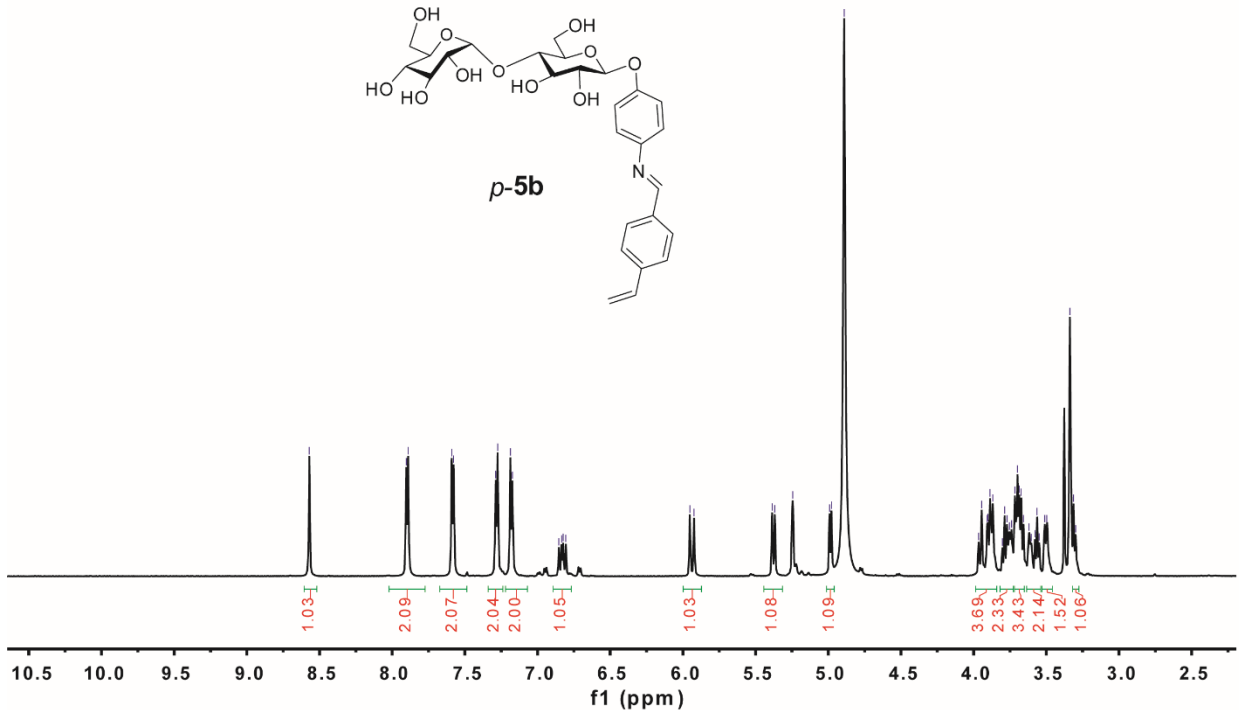
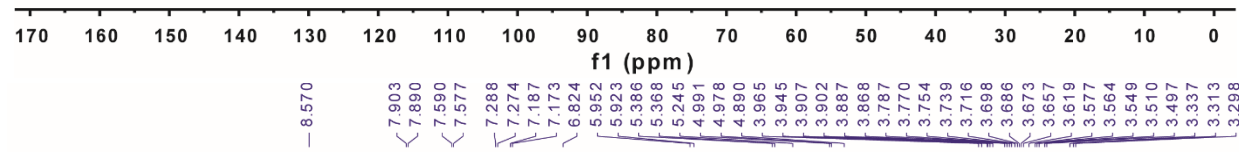
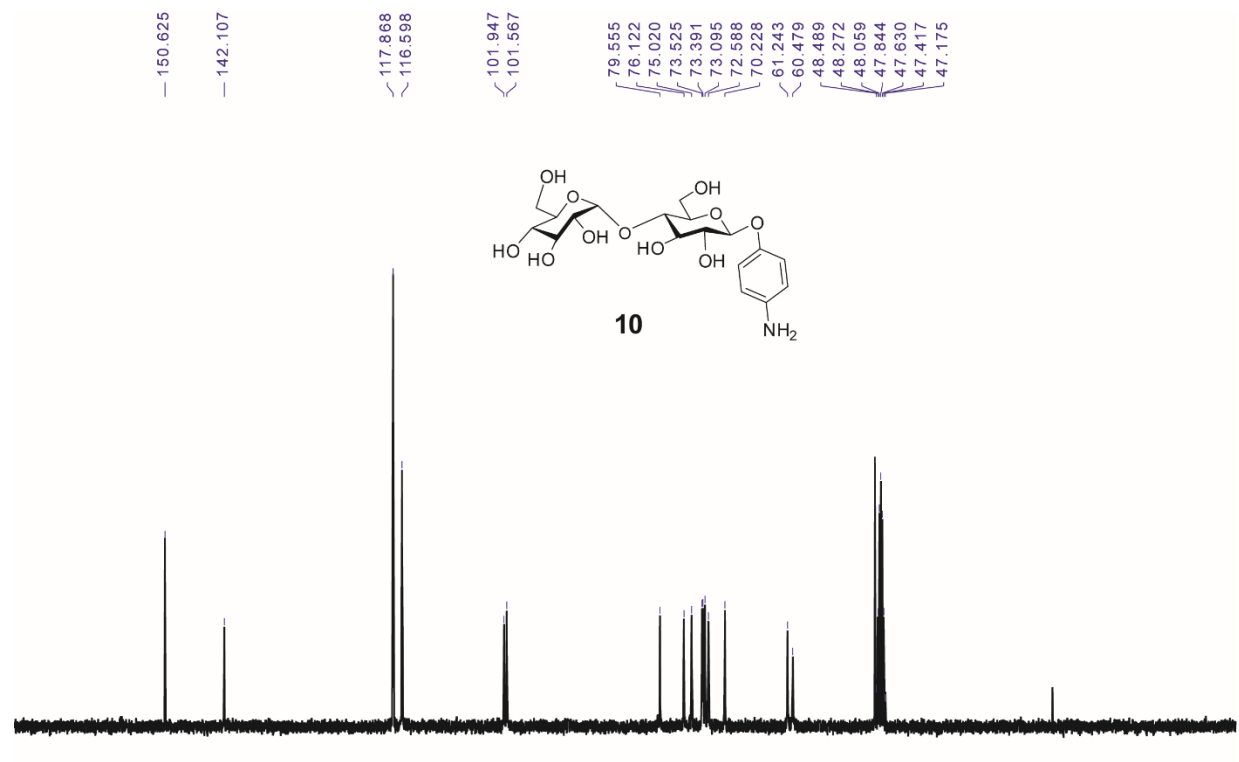


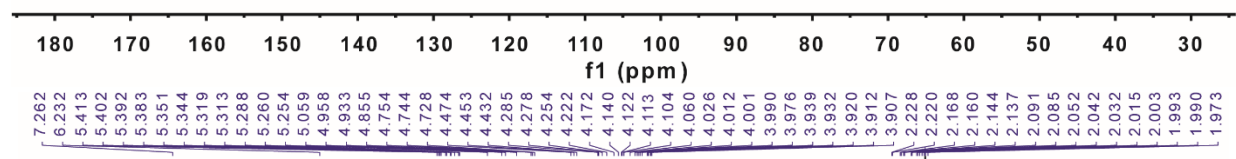
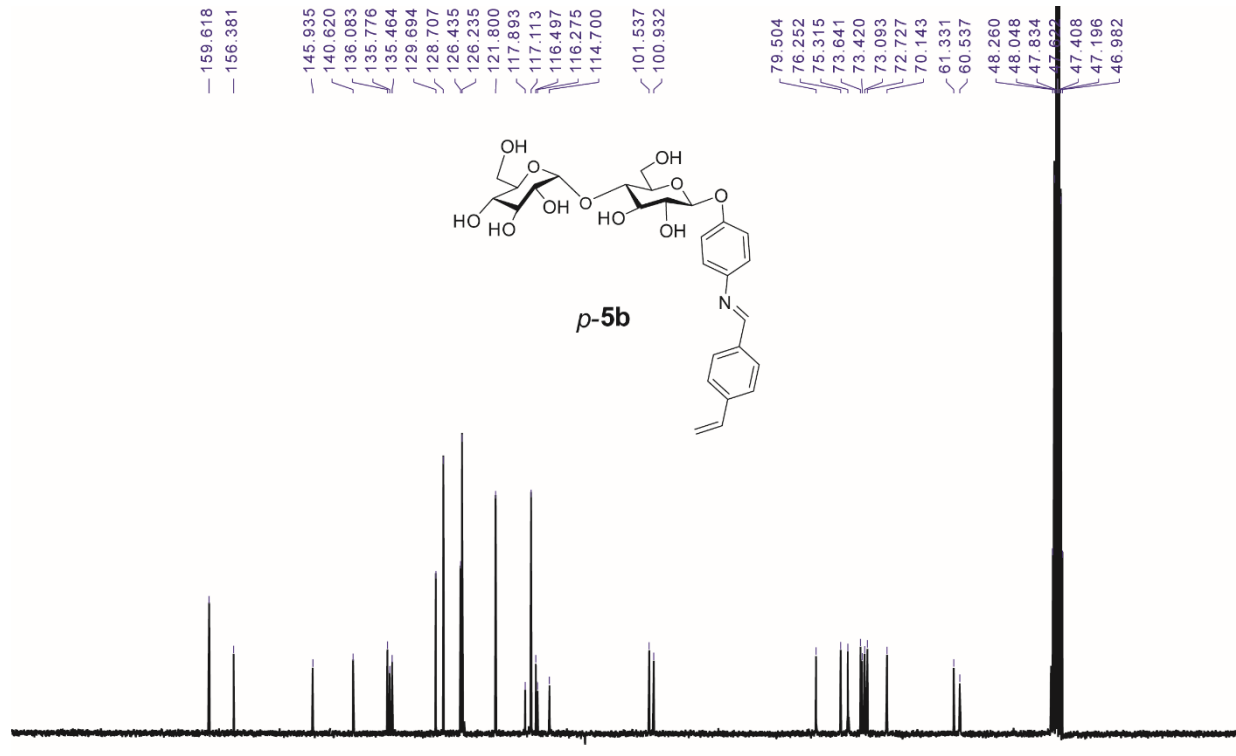


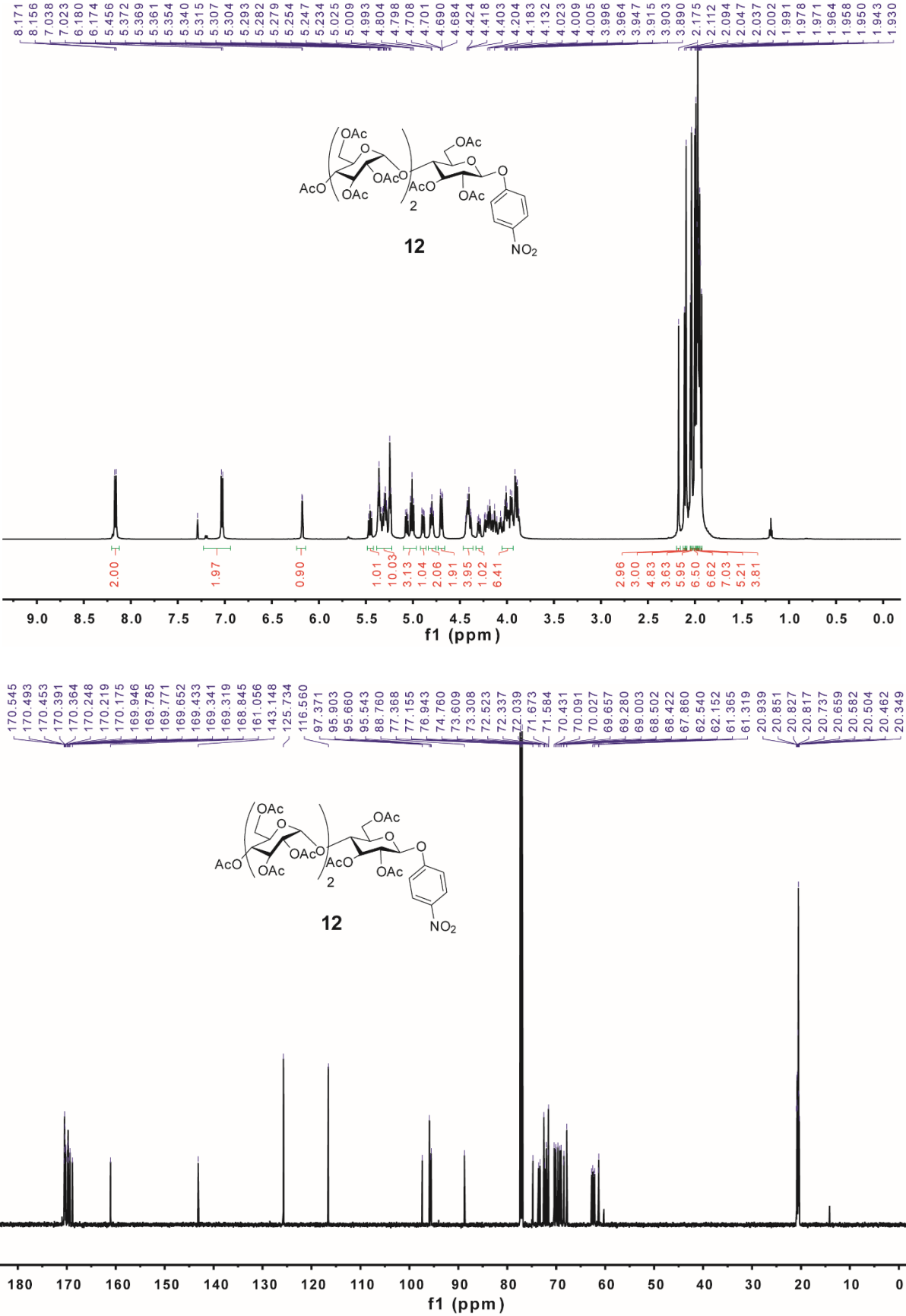


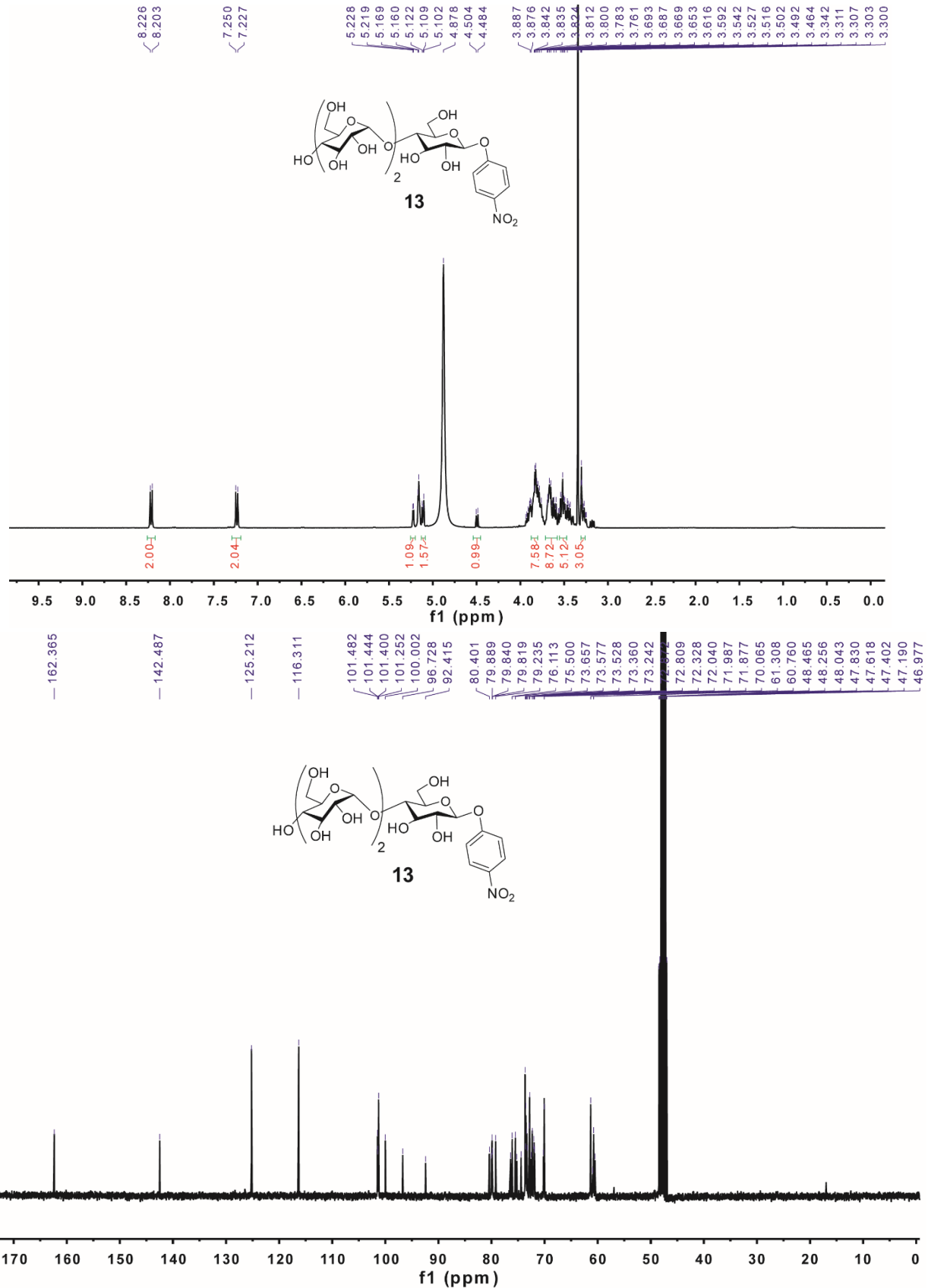


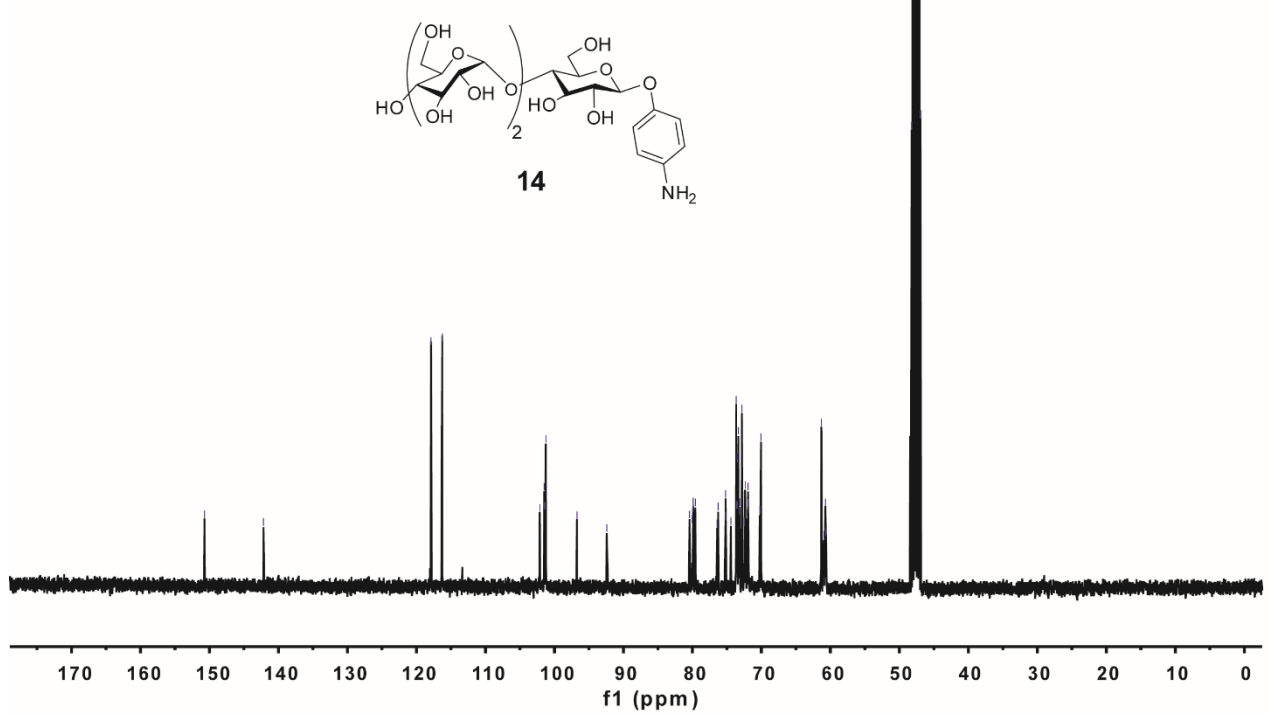
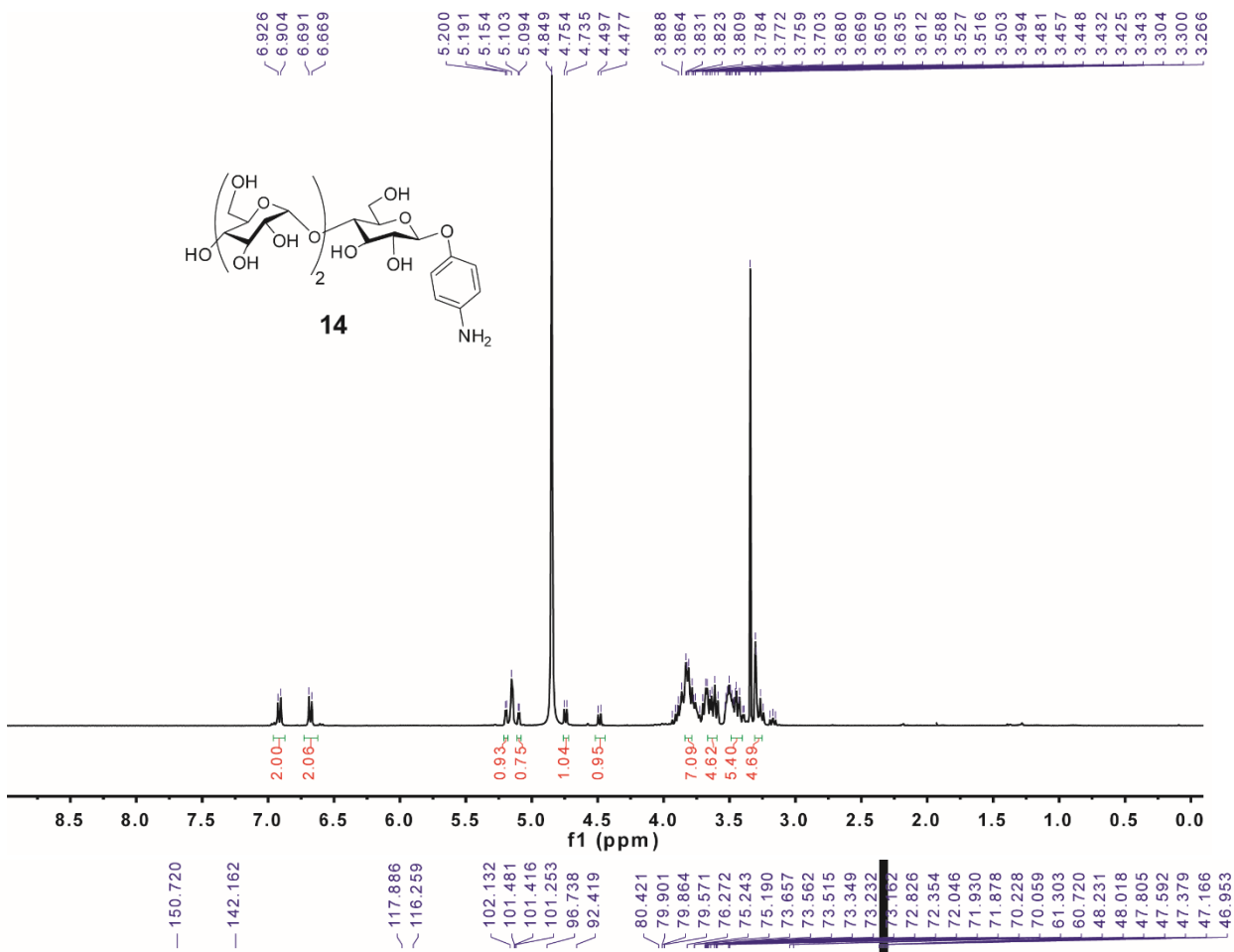


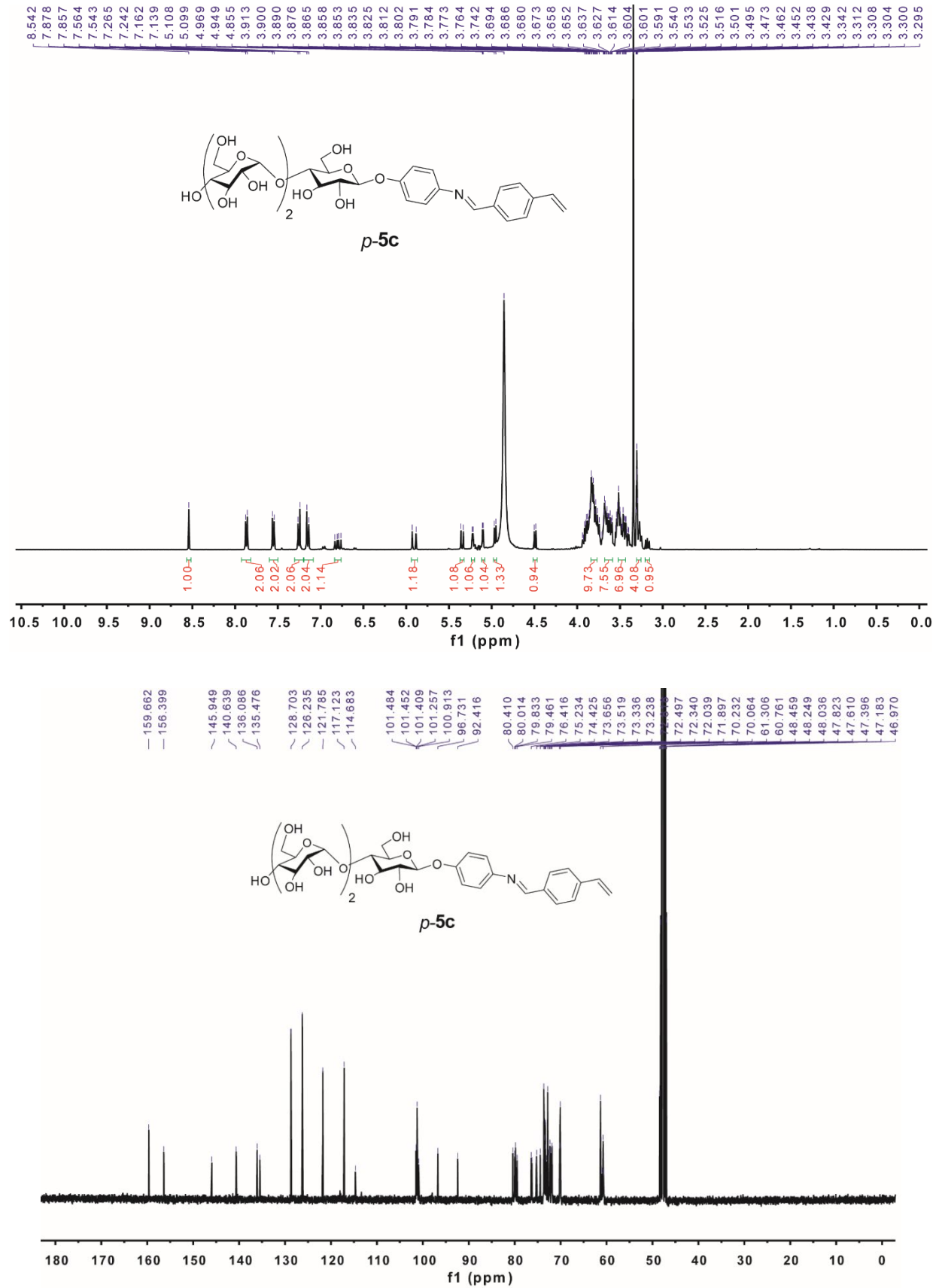




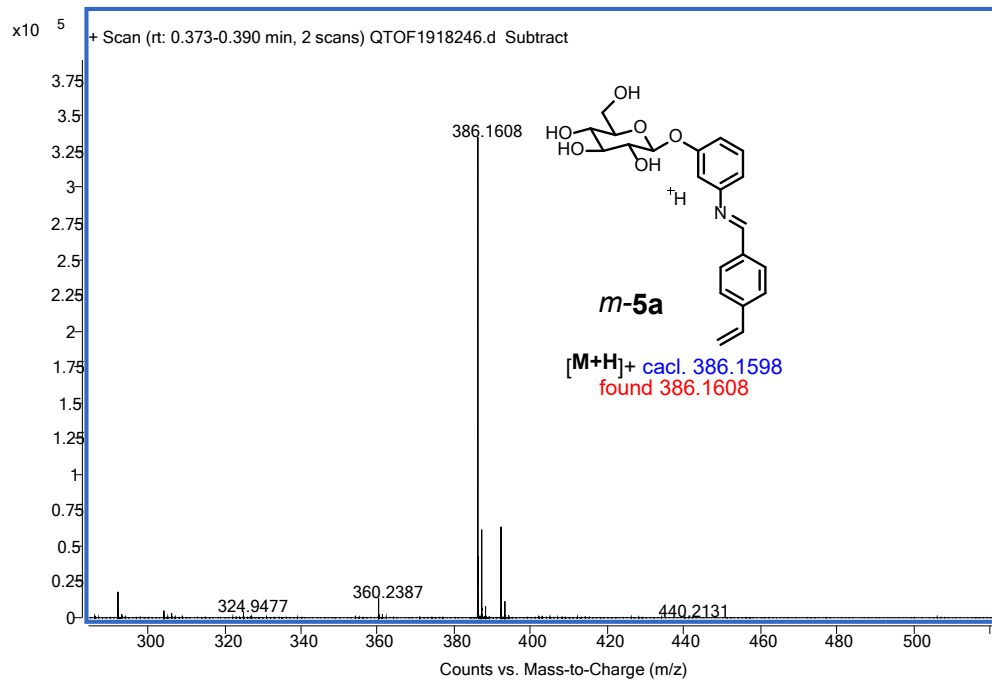
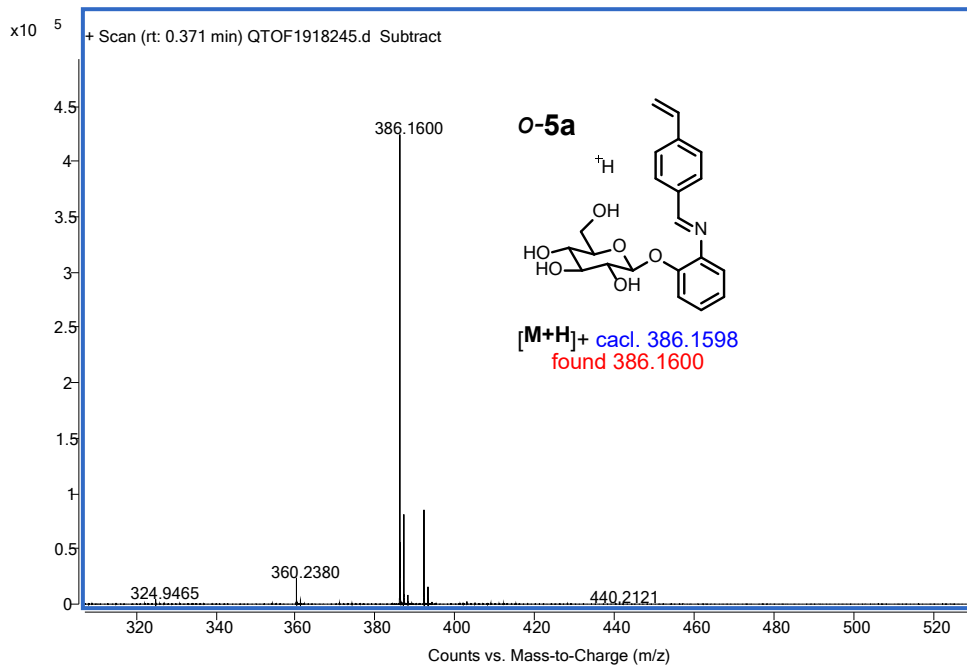


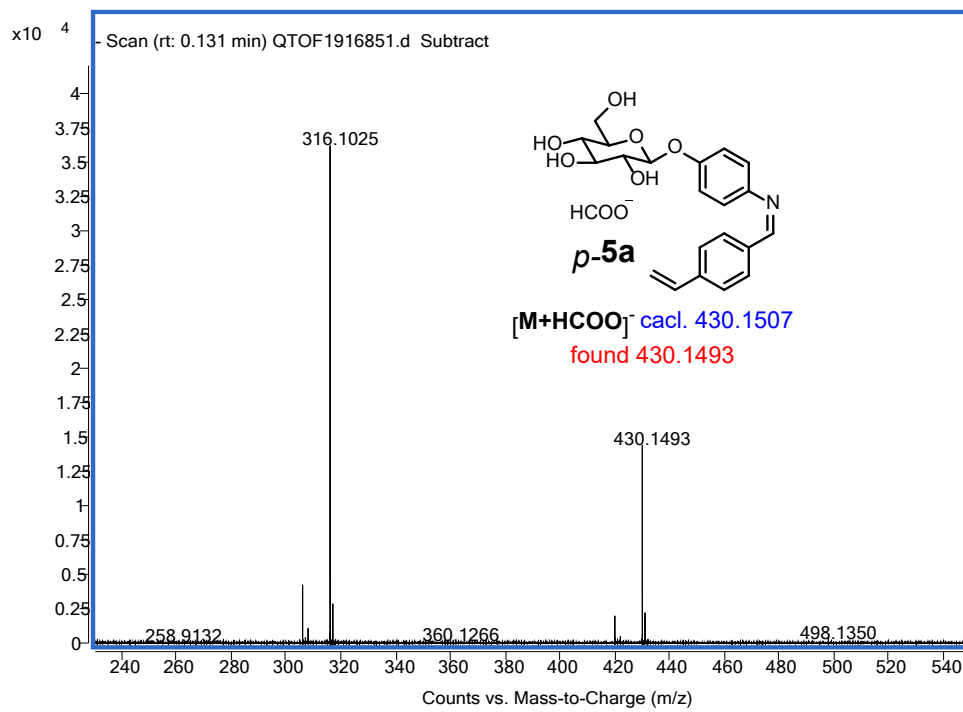
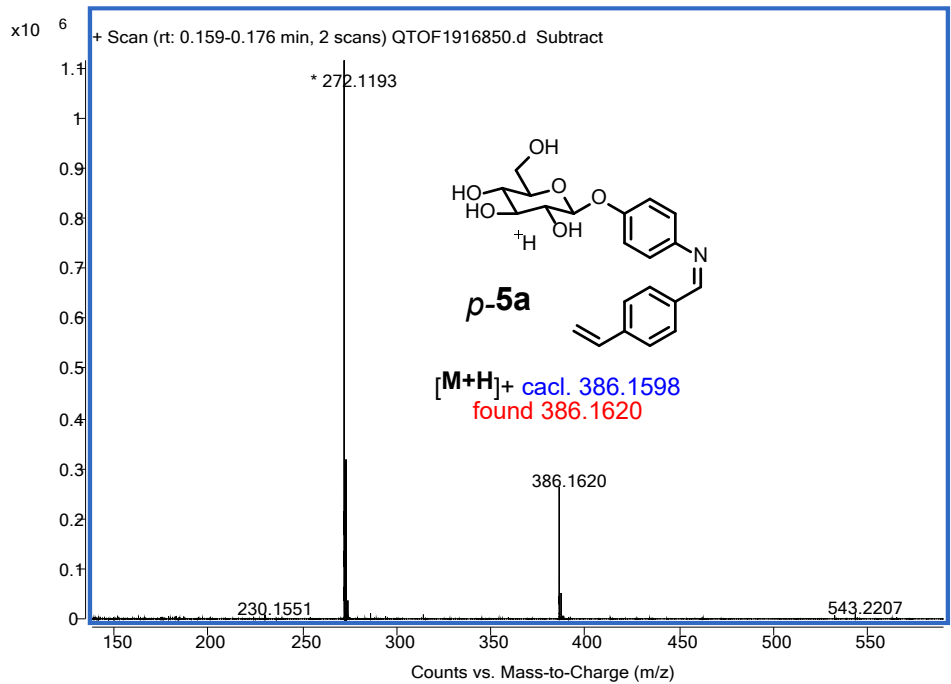


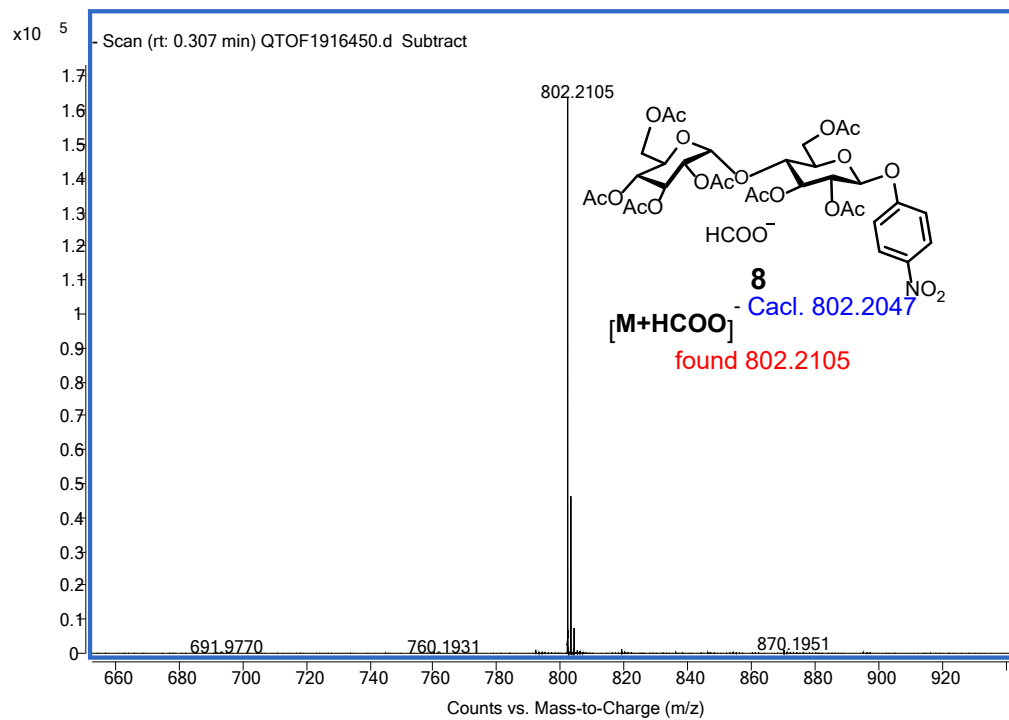
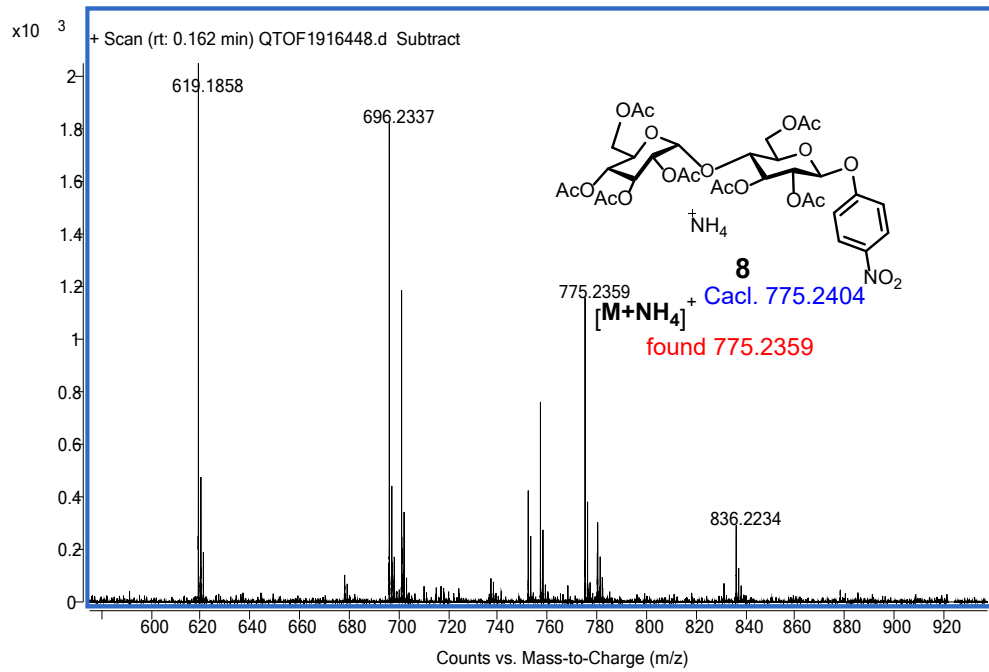


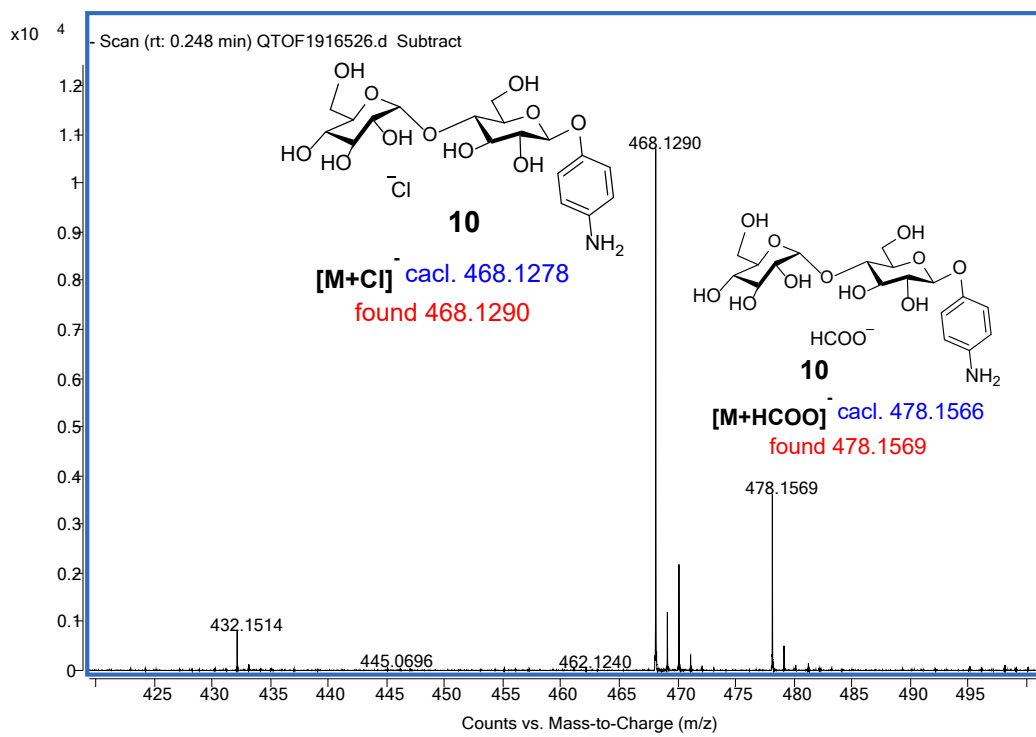
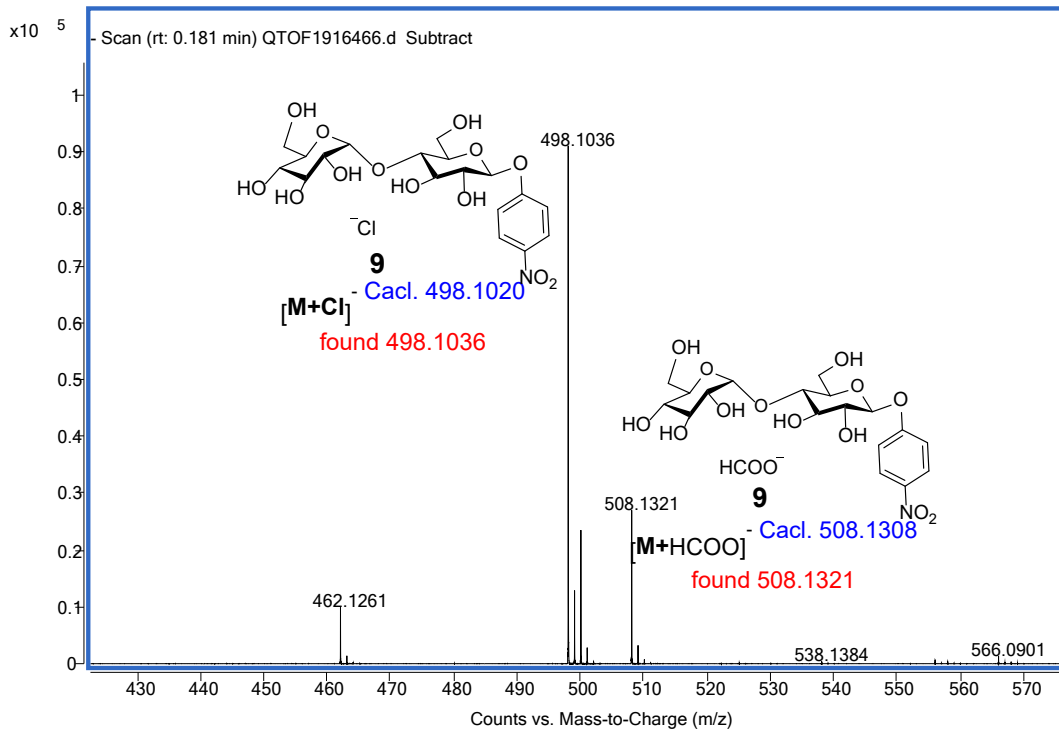


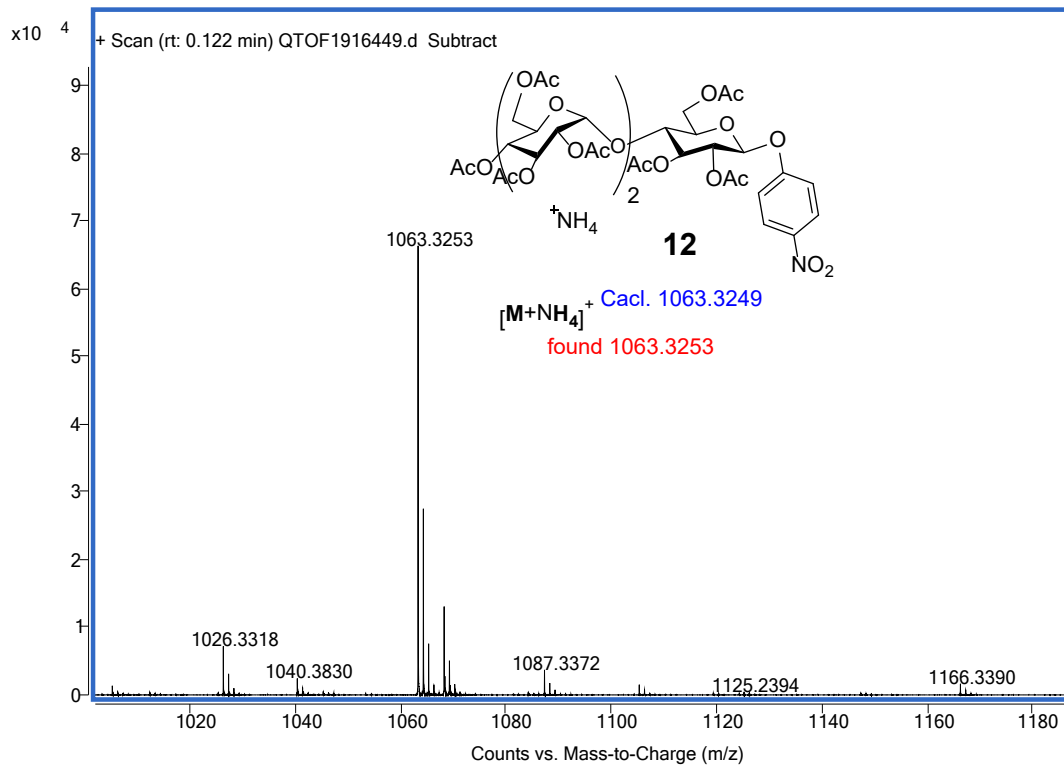
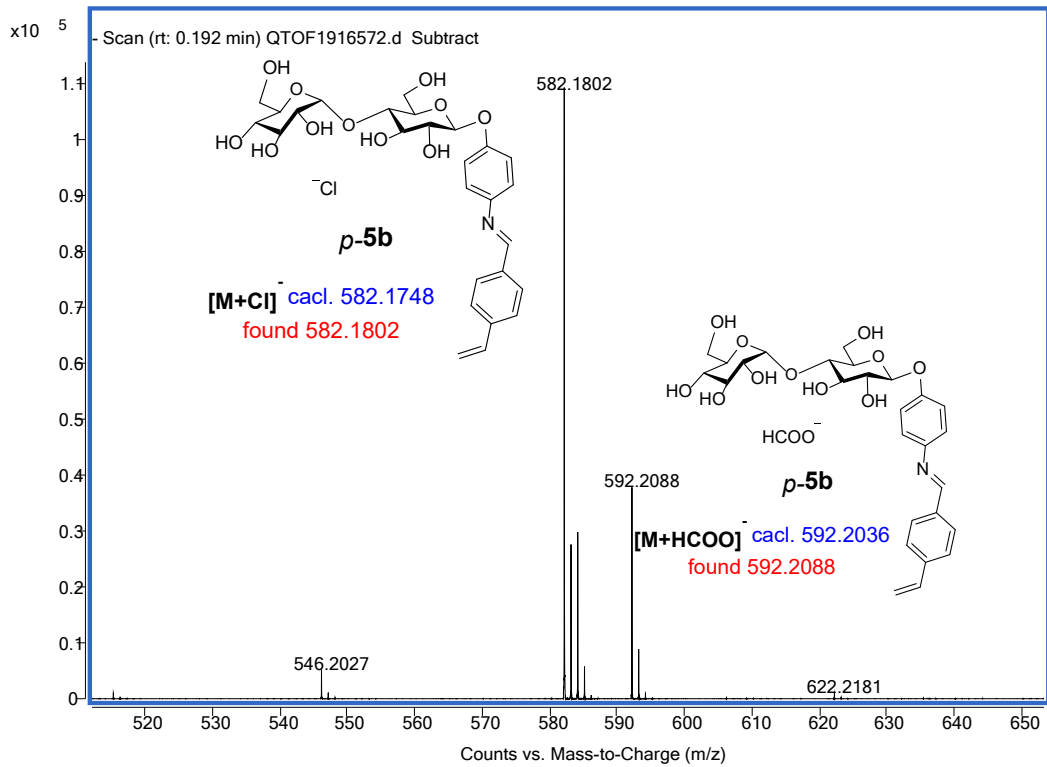
ESI-MS Spectra

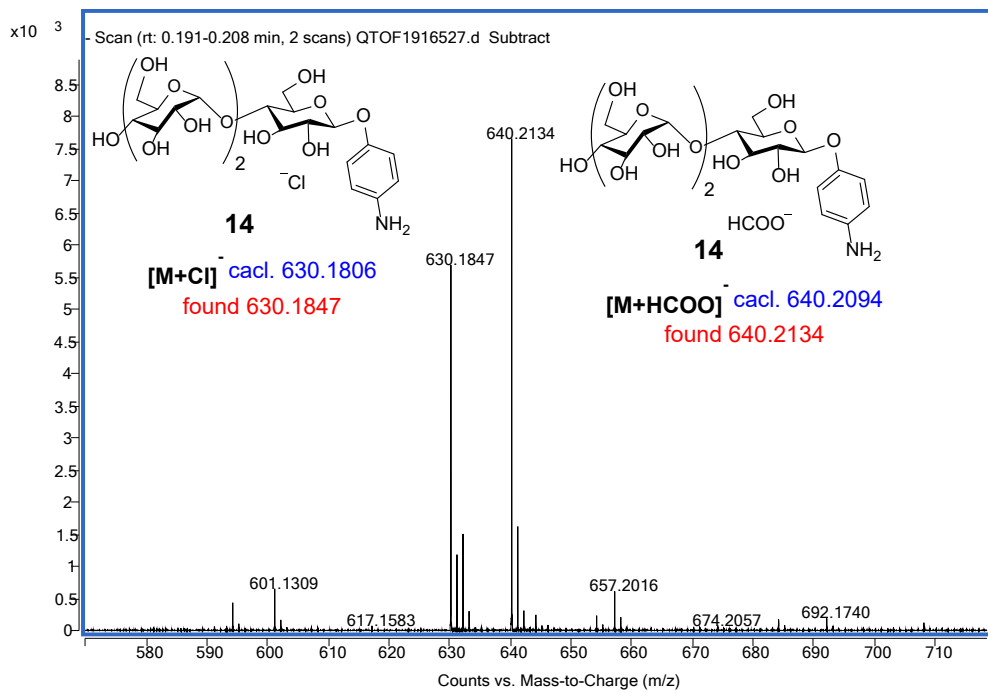
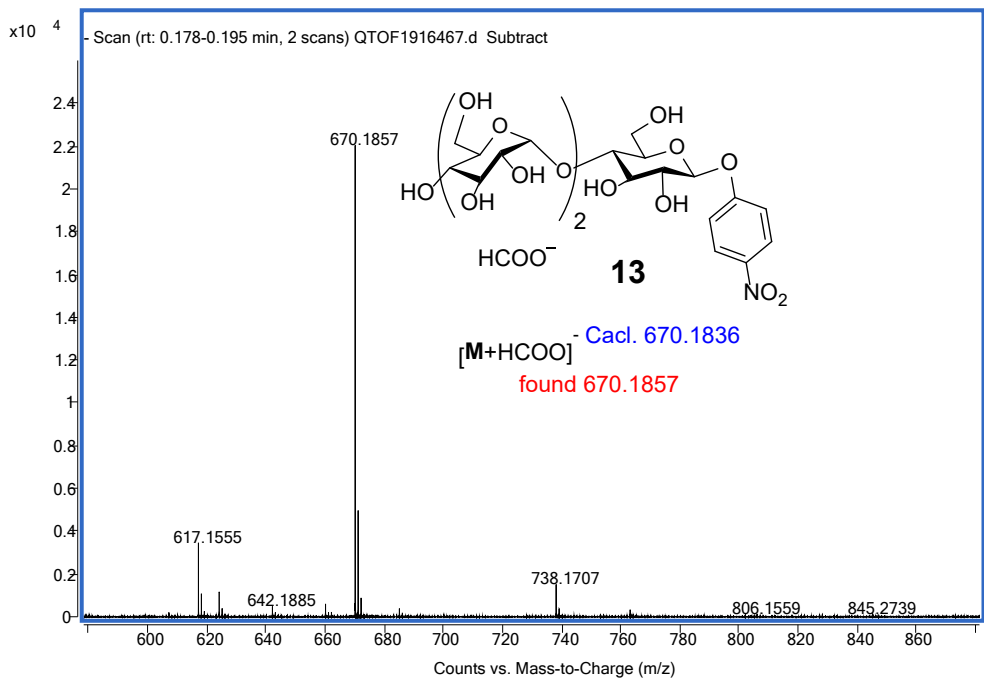


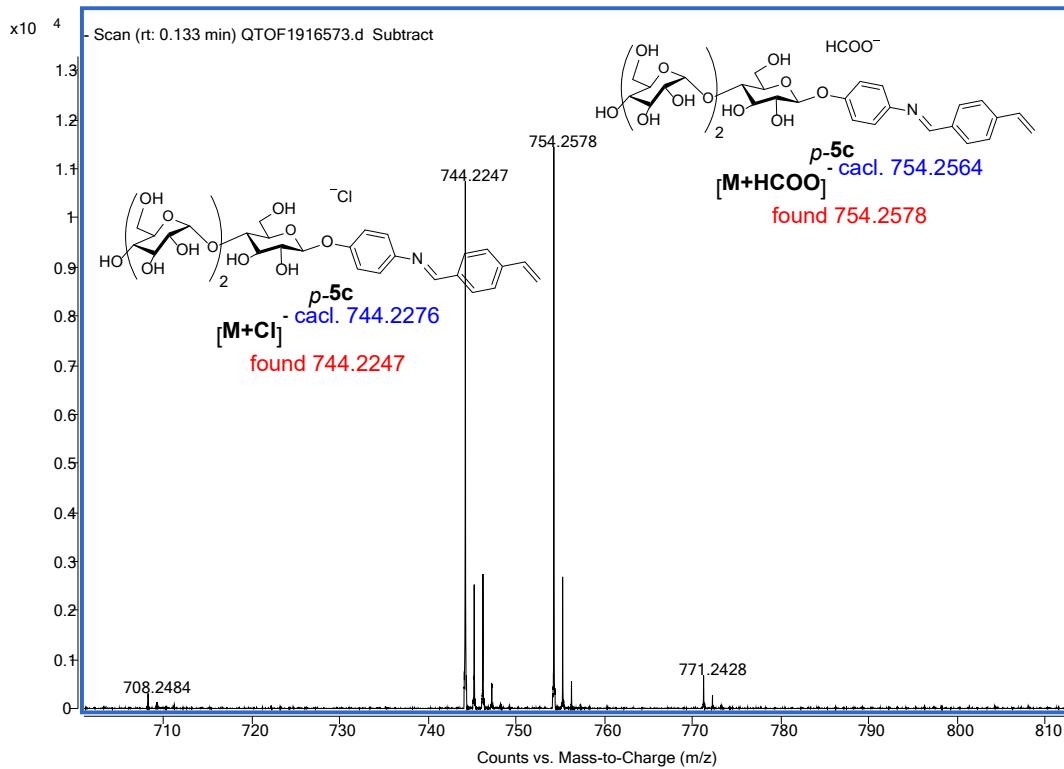












References

- [1] Awino, J. K.; Zhao, Y. *J. Am. Chem. Soc.* **2013**, *135*, 12552.
- [2] Arifuzzaman, M. D.; Zhao, Y. *J. Org. Chem.* **2016**, *81*, 7518.
- [3] Gunasekara, R. W.; Zhao, Y. *J. Am. Chem. Soc.* **2017**, *139*, 829.
- [4] Burke, H. M.; Gunnlaugsson, T.; Scanlan, E. M. *Org. Biomol. Chem.* **2016**, *14*, 9133.
- [5] Erickson, H. P., Size and shape of protein molecules at the nanometer level determined by sedimentation, gel filtration, and electron microscopy. *Biol. Proced. Online* **2009**, *11*, 32-51.
- [6] Wiseman, T.; Williston, S.; Brandts, J. F.; Lin, L. N. *Anal. Biochem.* **1989**, *179*, 131-137.
- [7] Jelesarov, I.; Bosshard, H. R. *J. Mol. Recognit.* **1999**, *12*, 3-18.
- [8] Velazquez-Campoy, A.; Leavitt, S. A.; Freire, E. *Methods Mol. Biol.* **2004**, *261*, 35-54.